National Library of Canada

Acquisitions and Bibliographic Services Branch

395 Wellington Street
Ottawa, Ontario
K1A 0N4

Bibliothèque nationale du Canada

Direction des acquisitions et des services bibliographiques

395, rue Wellington
Ottawa (Ontario)
K1A 0N4

Your file Votre référence

Our file Notre référence

NOTICE

The quality of this microform is heavily dependent upon the quality of the original thesis submitted for microfilming. Every effort has been made to ensure the highest quality of reproduction possible.

If pages are missing, contact the university which granted the degree.

Some pages may have indistinct print especially if the original pages were typed with a poor typewriter ribbon or if the university sent us an inferior photocopy.

AVIS

La qualité de cette microforme dépend grandement de la qualité de la thèse soumise au microfilmage. Nous avons tout fait pour assurer une qualité supérieure de reproduction.

S'il manque des pages, veuillez communiquer avec l'université qui a conféré le grade.

La qualité d'impression de certaines pages peut laisser à désirer, surtout si les pages originales ont été dactylographiées à l'aide d'un ruban usé ou si l'université nous a fait parvenir une photocopie de qualité inférieure.

Canada

Study of Hybrid Permutation Frequency Phase Modulation

by

Wensheng Li, B.Eng.

A thesis submitted to
the School of Graduate Studies and Research
in partial fulfillment of
the requirements for the degree of

Master of Applied Science

Ottawa-Carleton Institute for Electrical Engineering
Faculty of Engineering
Department of Electrical Engineering
University of Ottawa
Ottawa, Ontario, Canada, K1N 6N5

December,1995

ISBN 0-612-11574-7

Canada

UNIVERSITÉ D'OTTAWA
UNIVERSITY OF OTTAWA

Abstract

In future communication applications, it is desirable to provide good system performance and more services to a number of users using the minimum resources. These expectations pose challenges in the design of modulation and coding. This thesis presents and studies the hybrid permutation frequency phase modulation (HPM) communication systems.

By combining FSK and PSK, the signal energy per symbol is increased. Applying this type of signals to permutation modulation, the concept of HPM is presented and its signal properties have been mathematically analyzed. The expression for bandwidth efficiency is derived. The performance of transmission systems is related with channel characteristics. The behavior of HPM is appraised in the case of AWGN and frequency selective fading channels. The coherent and noncoherent detection have been considered respectively. Our performance analysis are based on the measures of bit error performance and bandwidth efficiency.

It is shown that a large set of waveforms can be easily obtained in HPM. For uncoded HPM, most of the possible waveforms are used, and the system power and bandwidth efficiency can be greatly improved in AWGN channels. The nature of permutation modulation indicates an implicit diversity in frequency selective fading channels. By using a small portion of waveforms, which leads to coded HPM, the effective diversity increases. The rule of selecting waveforms is worth of studying. We propose t-designs as the candidate. The results show that coded HPM is a power efficient scheme and is robust in fading environments.

I hereby declare that I am the sole author of this thesis.

I authorize the University of Ottawa to lend this thesis to other institutions or individuals for the purpose of scholarly research.

Wensheng Li

I further authorize the University of Ottawa to reproduce this thesis by photocopy or by other means, in total or in parts, at the request of other institutions or individuals for the purpose of scholarly research.

Wensheng Li

Acknowledgments

I would like to express my sincere gratitude to my thesis supervisor, Dr. A. Yongaçoğlu, for his constructive suggestions, valuable guidance and financial support throughout my graduate study. Also many thanks to him for his useful advice, comments and corrections in the progress of this thesis.

I would also like to thank my wife and parents. Their affection and various supports are always beside me in this whole period.

Contents

List of Figures

List of Tables

List of Acronyms

ASK	Amplitude Shift Keying
AWGN	Additive White Gaussian Noise
BIBD	Balanced incomplete block design
BER	Bit Error Rate
CDMA	Code Division Multiple Access
DPSK	Differential Phase Shift Keying
FPSK	A combined frequency and phase shift keying modulation scheme ($v = w = 2$) proposed in [21].
FSRF	Frequency selective Rayleigh fading channel
FSK	Frequency Shift Keying
HPM	Hybrid Permutation Frequency-Phase Modulation
ISI	Inter-symbol Interference
JFPM	Joint Frequency Phase Modulation
MCM	Multicarrier modulation
MFSK	M-ary Frequency Shift Keying
MSK	Minimum Shift Keying
MT-FSK	Multiple Tone FSK
PAM	Pulse Amplitude Modulation, or ASK
PDF	Probability density function
PFSK	Permutation FSK
PSK	Phase Shift Keying
QAM	Quadrature Amplitude Modulation
SNR	Signal to Noise Ratio

List of Symbols

α	The amplitude attenuation; the roll-off factor
$\delta(\cdot)$	Impulse function
γ_b	Bit energy to noise spectral density ratio
$\bar{\gamma}_b$	Average bit energy to noise spectral density ratio
γ_c	The received SNR per subcarrier
$\bar{\gamma}_c$	The average received SNR per subcarrier
γ_s	Signal energy per symbol to noise spectral density ratio
ϕ	The phase shift introduced by the transmission channel
φ_{mn}	The initial phase introduced by modulator
$\theta^{(k)}$	The phase shift in the k-th symbol interval
θ_{jr}	The phase shift generated by the input data in any symbol interval
$\triangle f$	The frequency separation between frequency subcarriers
η	Bandwidth efficiency in bps/Hz
ρ	Correlation coefficient of the HPM waveforms
$\rho^{'}$	Correlation coefficient of the HPM component signals
λ	The number of blocks containing a certain t-subset of elements in t-designs
σ^2	The average scattered power due to multipath in fading channel
a_{in}	The element of the frequency signaling matrix
A	The frequency signaling matrix of HPM
B	The amplitude of a waveform
$B(\cdot)$	Beta function
b	The total number of blocks in a t-design
C_v^w	A notation of combination
d	Hamming distance between codewords
d_{min}	The minimum Hamming distance
E_b	Bit energy
E_s	Symbol energy
f_c	Central carrier frequency
$H(n,k)$	A Hadamard code with length n

h	modulation index of CPFSK
$h(\tau;t)$	The channel impulse response
$I_0()$	The zero order modified Bessel function
k_s	The total number of bits per symbol
k_f	The number of bits which are mapped into frequency signals per symbol
k_p	The number of bits which are mapped into phase signals per symbol
L	The number of diversity branch
M	The total number of symbols
M'	The total number of available symbol signals
M_f	The total number of frequency arrangements
M_p	The total number of phases in HPM
N_0	One-sided thermal noise power spectral density
n	The length of a Hadamard code
P_2	Pairwise probability of error
P_b	Probability of bit error
P_{b1}	Bit error probability for the frequency detection part of noncoherent HPM receiver
P_{b2}	Bit error probability for the phase detection part of noncoherent HPM receiver
P'_{b2}	Bit error probability for the first stage of noncoherent HPM receiver in the condition of correct frequency detection
$P_{DPSK\|PFSK}$	The probability of an incorrect detection on the phase given the correct detection in noncoherent PFSK stage
P_e	Error probability for a single MDPSK receiver
P^w	The probability that at least w of the noise samples exceed the value of the largest w signal plus noise samples in detection of MT-FSK signals
P_{MTFSK}	Symbol error probability of noncoherent MT-FSK detection
$P_{PFSK}(v,w)$	Symbol error probability of noncoherent PFSK detection
$P_s(v,w,M_p)$	Symbol error probability of HPM
$p(\alpha_i)$	PDF of amplitude attenuation
$Q(\cdot)$	Q-function
$Q(\cdot,\cdot)$	The generalized Q-function
R_b	Information transmission bit rate
r	The number of blocks containing a certain element in t-designs
$r(t)$	The received signal
$u_p(t)$	One of the HPM component signals in the p-th subset from a total of v subsets
$S_m(t)$	The m-th symbol signal in HPM
$S(t,w,v)$	A Steiner system
t	Time variable; a notation used in t-designs

T_b	Bit duration
T_s	Symbol duration
v	The total number of orthogonal frequency tones
w	The number of active frequency tones in HPM or permutation FSK
x_i	The number of codewords containing i common elements to a given codeword
W	Required channel bandwidth
$z(t)$	A zero mean white Gaussian noise process
Component signal:	One of the orthogonal frequency-phase modulated signals which constitute a HPM waveform
Frequency tone:	One of the orthogonal frequency carriers
Signaling frame:	One symbol interval
Signaling set:	The entire signal class from which the arrangements of signal waveforms are selected to represent symbols
Subset signals:	One subclass of signaling set with the same frequency subcarrier and distinct phase shifts
Waveform:	A certain combination of frequency-phase modulated signals representing a given symbol in HPM scheme

Chapter 1

Introduction

1.1 Motivation

The selection of an appropriate modulation technique for a specific communication application is of great importance and related with the factors such as channel characteristics, performance requirements, bandwidth efficiency and implementation complexity. Since these factors vary from case to case, there is no single modulation scheme which outperforms others in all aspects. In future mobile communication systems, such as land mobile satellite (LMS) communication systems and personal communication system (PCS), more new services need to be provided or more users need to be supported. There are constraints imposed by the available transmission bandwidth. Selecting a modulation technique which can make use of the limited bandwidth efficiently, and can combat channel impairments is crucial for a good design. These expectations pose challenges to the design.

Most mobile communication channels are characterized as multipath fading channels. Unless the symbol duration is much larger than the multipath spread, intersymbol interference (ISI) usually appears due to multipath. This imposes a limit on the transmission rate unless ISI removing techniques are employed. Multicarrier Modulation (MCM) has been proposed [2] to combat channel impairments, such as fading, impulse noise, non-linear distortions, and especially ISI. The main idea of

MCM is to divide the channel into several orthogonal subchannels in the frequency domain. The data is sent in parallel on a number of narrowband ISI free subchannels. In strict sense, MCM uses all the subchannels or carriers for transmission in each symbol interval. If we extend this concept and use only part of available carriers for transmission in any signaling interval, this embodies the concept of permutation modulation. For convenience, we use a generic name, multiple carrier modulation to refer to all these schemes.

In permutation modulation, a codeword set is formed by permuting the order of an initial code with length n and weight w (we only deal with the special case in which the code set contains only two values: 0 or 1). Without loss of generality, we assume that the initial code is in ascending order. Based on this principle, permutation FSK (PFSK), which is an extension of M-ary FSK, is obtained by applying the code set to frequency modulation when selecting the active tones. By assigning each codeword to v orthogonal frequency tones, each carrier corresponds to one element in the permuting code. But only w carriers are active in any waveform. Symbols are identified by the different combinations of w carriers. In this respect, "1" in any code indicates the corresponding carrier is active. The modulator evenly divides the symbol energy into $w > 1$ frequency tones. Any one of the arrangements of these v frequency tones with w active elements may correspond to a unique input symbol. Thus in every symbol interval, w tones are transmitted simultaneously to convey as many as $\log_2 \begin{pmatrix} v \\ w \end{pmatrix}$ bits of information in special conditions. MFSK is a special case of PFSK with $w = 1$. The advantage of PFSK lies in the fact that with the same total number of symbols $M_f = \begin{pmatrix} v \\ w \end{pmatrix}$, less tones are needed, i.e., $M_f > v$ if $w > 1$ and $M_f = v$ if $w = 1$. This implies the reduction of the total number of orthogonal frequency tones required in the signaling set. Therefore permutation modulation demonstrates itself to be more bandwidth efficient than M-ary FSK. Moreover, since $w > 1$, we see it as a form of multiple carrier transmission technique.

Depending on the number of simultaneously active carriers, the modulation scheme

can be classified as single carrier and multiple carrier modulation. Most of the conventional modulation schemes, such as M-ary FSK, MPSK, can be categorized as single carrier modulations, in which only one carrier is active at any time.

On the other hand, in terms of the information carrying parameters, modulation schemes can be classified as frequency, phase, or amplitude keying, or as combined modulation. In most schemes, the transmitted signals are modulated by single type modulation. However, combined modulation is desired to achieve the hybrid advantages. It possesses the properties of both of its component parts. For example, the widely used quadrature amplitude modulation, or QAM, is actually a combination of ASK and PSK. It outperforms both ASK and PSK if given the same available spectrum resources.

Using the above definitions, conventional multiple phase shift keying (MPSK) can be seen as single carrier phase modulation, and permutation FSK can be seen as multiple carrier frequency modulation. It is known that MPSK has the remarkable advantage of high bandwidth efficiency. The Euclidean distance between signal points reduces to accommodate more signals in a 2-dimensional signal space, which causes the error performance degradation. This is, in fact, a method which sacrifices power efficiency to achieve bandwidth efficiency and the spectral efficiency is proportional to the number of phases. On the contrary, the error rate performance of conventional orthogonal M-ary FSK improves as the number of transmitted tones M increases. This is because higher symbol energy is obtained as M increases but all the signal points keep the same Euclidean distance with each other in the signaling constellation, which gives rise to larger signal to noise ratio at the receiver under the same channel conditions. In this case, the signals come from an M dimensional signal space. Thus power efficiency is accomplished at the expense of bandwidth efficiency and the bandwidth required is in proportion to M.

We plan to present a new modulation scheme which can utilize better the available bandwidth and power under certain conditions. To this end, we focus our attention

on a combination of permutation FSK and phase modulation scheme. We denote this novel scheme as hybrid permutation frequency phase modulation (HPM). This scheme brings the major advantages of multiple carrier transmission, such as inherent diversity in frequency selective fading channels, and it provides the flexible ways of selecting waveforms for different applications with different bandwidth and power efficiency requirements.

1.2 Related Researches

After Slepian proposed permutation modulation [8], most efforts have been directed to PFSK which employs frequency modulated signals. The expression of symbol error probability for noncoherent detection of PFSK has been developed in [9], while Brookner [10] conducted the evaluation with the same system configuration in both the frequency selective and nonselective fading channels. The error performance of PFSK is further improved by expurgating some of the codewords rather than using all the permuting arrangements of the source code. The aim is to reduce the number of the possible frequency arrangements or codewords in a given alphabet to trade off bandwidth for power efficiency. This modified version can be seen as PFSK employing channel coding and is denoted as multiple tone FSK (MT-FSK). MT-FSK employing Steiner system for nonflat fading channel was proposed in [13]. The implicit diversity has been exploited by modifying the receiver structure. The concept has also been applied to a DS-CDMA system[14]. A combined modulation and multiple access scheme was proposed in [15]. The issues pertaining to its implementation has also been addressed.

In the aspect of combined schemes, the combination of MFSK and MPSK modulation yields the joint frequency-phase modulation (JFPM) [20]. This hybrid scheme embodies both the features of FSK and PSK. In other words, it can be both power efficient and bandwidth efficient. Extensive studies have been done in this aspect [18]-[23]. In the initial work [18], the error rate expression for coherent detection of

this hybrid scheme under a different notation "N-orthogonal phase modulated codes" in Gaussian channel was developed. Bounds on the performance of the optimum receiver and the performance of several suboptimum receiver structures for this orthogonal polyphase signaling technique were given by [19]. Both the coherent and differentially encoded signals were also investigated. In [20], the performance for noncoherent detection JFPM in AWGN and frequency-nonselective Rayleigh fading channel was evaluated. The comparisons with conventional MPSK and MFSK were demonstrated based on the exact bit error probability derived. The same signal structure was extended to multiple-tone cases in [21]. Only the performance of the system having two phase-modulated frequencies has been investigated in AWGN and fading channel. The resultant transmission signals are selected from 4-dimensional signal space. The coherent detection was assumed and the union bounds on the symbol error probability were derived. Further improvement was achieved by expurgating the complete codewords. This scheme has been applied to direct sequence [23] and frequency hopped spread spectrum system [20]. In general this modulation technique provides performance improvements with a slight increase of complexity in implementation.

In fact, HPM can be seen as a general family. When some special values applied to its parameters, it is actually a familiar conventional modulation scheme. More specifically this relation is shown in Table 1.2.

$v = 1, w = 1, M_p > 1$	M_p-DPSK
$M_p = 1$	Permutation FSK ($w = 1$,M_vFSK)
$w = 1$	JFPM

Table 1.2: Special cases of general HPM family

1.3 Contributions of the Thesis

One objective of this thesis is to present a power and bandwidth efficient modulation scheme based on the concept of multicarrier modulation. Our starting point is permutation modulation, employing combined frequency and phase modulation to obtain an extra advantage. The second objective is to investigate a systematic way of selecting waveforms from a complete HPM waveform set for the purpose of achieving diversity gain, especially in fading channel environment. In this respect, we restrict our attention to t-designs.

The concept of employing combined modulation schemes is proposed. By employing permutation and combined modulation, for a given bit energy, more symbol energy is obtained in the resultant HPM system. This will yield a better error performance. In other aspect, given the same symbol energy, less bandwidth is required for transmission.

A mathematical expression for HPM waveforms is presented and the correlation coefficient is obtained. The bandwidth efficiency based on minimum frequency separation is given.

Since the system performance also depends on channel characteristics and employed detection strategy. Our goal is to study HPM in AWGN and frequency selective fading channels. The system model on the basis of coherent and noncoherent detection is presented respectively. The probability of error for HPM signals is analyzed and the expression for bit error probability is developed.

Results show that uncoded HPM can provide large transmission capacity and performs very well in AWGN channels. To overcome the inefficiency in fading channels, coded HPM is employed and discussed. We consider Steiner system and Hadamard code as the candidates to replace the permutation code in uncoded HPM case. The bit error performance of coded system is analyzed. Results show that diversity gain is obtained in the case of fading channel and coding gain is obtained in the case of

AWGN channel.

1.4 Thesis Organization

The remainder of this thesis is organized as follows.

In chapter 2, the signal properties, correlation coefficient and bandwidth efficiency are analyzed and derived. The system configuration is presented. Based on coherent detection, the error rate performance of HPM signals over AWGN channels is discussed. Then a frequency selective Rayleigh fading (RSRF) channel model is described. The analytical performance is provided and a modification on waveform selection for performance improvement under the considered channel model is given and examined.

Chapter 3 presents a receiver structure employing noncoherent detection for the frequency part of HPM signals and differential detection for the phase part of HPM signals. The expression for bit error probability is developed. The performance, which is in terms of bit error rate and bandwidth efficiency, is analyzed under the condition of AWGN and FSRF channels. Numerical results are obtained and comparisons are made with some other comparable schemes.

Chapter 4 is devoted to the methods to optimally select waveforms to mitigate the impairments in fading channels. Our studies are concentrated on t-designs and its concept is reviewed. Two types of codes, namely, Steiner system and Hadamard codes are considered for waveform mapping. The bit error performance of coded HPM over AWGN and FSRF channels are evaluated. A computer simulation is carried out to verify the bound expression used. Note that uncoded system has poor performance, and coherent reception is not practical. In this respect, the results obtained from chapter 2 and chapter 3 do not offer much contributions, but they provide completeness for the thesis.

In chapter 5, summaries are made and suggestions for further research are given.

The discussion of HPM applied in binary and nonbinary transmission system is put in Appendix A. The examples for the approximations of bit error probability of permutation FSK are given in Appendix B. Appendix C includes the correlation coefficient results of some HPM formats. The detailed background information on t-designs can be found in Appendix D, where some of the derivations for the equations are also included.

Chapter 2

Uncoded Coherent Hybrid Permutation Modulation Systems

2.1 Introduction

Future applications of digital communications are expected to provide the desired quality of service using the minimum resources, i.e., power, bandwidth and complexity. In general, we can use bit error rate P_b as a measure of performance, energy per bit to noise power density ratio E_b/N_0 required for a given P_b as a measure of power usage, and information bit rate transmitted per bandwidth unit R_b/W as a measure of bandwidth efficiency. The system is also related to the channel characteristics. When passing through the channel, the transmitted signals usually face the channel impairments such as noise, fading, and intersymbol interference (ISI) in the case of high speed transmission. All these factors are related to each other and this forces the system designer to consider them thoroughly. The aim is to design a modulation system requiring less E_b/N_0, more R/W for a given data error rate and with moderate complexity.

Most of conventional modulation schemes can be categorized as single carrier modulation. In each symbol duration, only one carrier, phase or frequency modulated, is present in the transmission process. While multicarrier modulation has the features of good immunity to impulse noise and fast fades, and no need for equalization.

HPM can be seen as a form of MCM and also possesses some features of MCM. But one of main advantages of HPM is its flexibility. More dimensional signal space is provided using relatively less bandwidth so that more signals can be accommodated and more transmission capacity can be obtained. The power and bandwidth efficiency of a modulation scheme depend heavily on the signal constellation of the transmitted waveforms. Besides, some modifications are needed when HPM is applied to different channels.

This chapter is devoted to the HPM signal properties and system performance using coherent detection. In the following, i.e., section 2.2, we present a mathematical model to represent HPM signals. The transmitter and receiver structure are described in section 2.3. Based upon the analysis on bit error probability in section 2.4, the BER performance of uncoded HPM over AWGN channels is evaluated in section 2.5. In section 2.6, we analyze the system performance over frequency selective Rayleigh fading channels. A modified version of HPM is presented in section 2.7. Finally a summary is given in section 2.8.

2.2 System Structure

2.2.1 Signal Representation

HPM is specified by three parameters and is denoted as HPM(v, w, M_p), where M_p denotes the total number of phases, v and w are the total number of frequency tones and active tones receptively. There exists some basic relations among these parameters. Due to the symmetry of permutation, i.e., $\begin{pmatrix} v \\ w \end{pmatrix} = \begin{pmatrix} v \\ v-w \end{pmatrix}$, we only consider the case when $w \leq v/2$. It is easy to see that the maximum size of code set can be obtained when $w = v/2$. If the information bearing phase is independent of the active carrier, the total number of bits per symbol k_s which can be transmitted is

$$k_s = k_f + wk_p \tag{2.1}$$

where k_f is the the number of bits represented by PFSK signals and k_p corresponds to the number of bits represented by phase signals carried by each active frequency tone.

From a practical point of view, k_f is set to be integer[1] and satisfies

$$k_f = \left\lfloor \log_2 \binom{v}{w} \right\rfloor \tag{2.2}$$

The total number of symbol signals is M. It is defined by

$$M = 2^{k_s} \quad \text{and} \quad M = M_f (M_p)^w,$$

where $M_f = 2^{k_f}$ indicates the number of frequency arrangements used to represent the input data and $M_p = 2^{k_p}$.

In general, we have

$$M = 2^{wk_p + \lfloor \log_2 C_v^w \rfloor} \tag{2.3}$$

where

$$C_v^w = \binom{v}{w} = \frac{v!}{(v-w)!w!}$$

From the total of v subsets of polyphase signals, w component signals are activated every symbol interval. The energy is equally divided into these w active component signals[2]. Given v orthogonal frequency tones and M_p available phases, there are total of vM_p possible waveforms.

We suppose that each of the v orthogonal frequency tones has a frequency shift from the central frequency f_c and takes one of the values

$$f_n = f_c + (2n + 1 - v)\Delta f/2 \quad n = 0, 1, \ldots, v-1 \tag{2.4}$$

where Δf is the frequency separation between adjacent tones. Besides, there is an initial phase φ_{mn} carried by each active frequency tone. The initial phases are

[1]See appendix A for a discussion for noninteger k_f values.

[2]In practical systems, we usually employ the system with equal signal energy to ease the implementation and also to simplify the analytical evaluation. Otherwise some modifications have to be made on the receiver to compensate for the unequal energy. In this thesis, we consider the equal energy case.

introduced by the frequency synthesizers and it may switch to a new value only at the start of every symbol interval.

The phase of each frequency tone is independent of others since it is generated by a different input random sequence. For coherent HPM, the phase in the k-th signaling interval takes one of the values of

$$\theta^{(k)} = \theta_{j_r} = \frac{2\pi j_r}{M_p} \qquad r = 0, 1, \ldots, w-1, \quad j_r = 0, 1, \ldots, M_p - 1 \tag{2.5}$$

Based on these concepts, the m-th signal from a set of M signals for HPM in the k-th signaling interval is expressed as

$$S_m(t) = B \sum_{n=0}^{v-1} a_{in} \cos(2\pi f_n t + \theta^{(k)} + \varphi_{mn}) \quad kT_s \le t \le (k+1)T_s, \quad m = 0, 1, \ldots, M-1, \;\; a_{in} = 0 \text{ or } 1 \tag{2.6}$$

where

$$m = iwM_p + \sum_{r=0}^{w-1} (w - r) M_p j_r$$

$$i = 0, 1, \ldots, M_f - 1, \quad j_r = 0, 1, \ldots, M_p - 1, \quad r = 0, 1, \ldots, w-1$$

$\theta^{(k)}$ is given by (2.5) and j_r indicates the phase index corresponding to the phase shift of the r-th active frequency tone. B is the amplitude of the waveform and we assume equal amplitude waveforms. φ_{mn} is the initial phase introduced by the modulator. For simplicity we assume that the initial phases introduced are identical for all the subcarriers at the start of each symbol interval. Therefore $\varphi_{mn} = \varphi_m$ and it is independent of n. In addition, a_{in} is the element of frequency signaling matrix A in which the rows are the complete w permutations out of v. Thus the matrix could be up to $\begin{pmatrix} v \\ w \end{pmatrix}$ rows and v columns. There are w "1"s per row and the other elements are "0". An example of a typical HPM system is given in Section 2.2.2.

There is a special version of HPM in which all the active frequency tones have the same information-bearing phase. In this case, $k_s = k_f + k_p$ and only one phase corresponding to the input data modulates all the subcarriers without the consideration of

the value w. It also means that j_r is independent of r and has one value during signaling interval. This modified scheme implies that the same information-bearing phase signals corresponding to the k_p bits input sequence are transmitted over w channels. In AWGN channel, unless the perfect carrier and phase information are available at the receiver, i.e., in the optimum coherent detection case, this version of HPM would result in a loss in performance. On the other hand, in fading channels, sometimes the signals in one or more channels severely fade and higher error rates occur. In this situation, a diversity technique is desired. We observe that the modified version of HPM has the implicit diversity nature with diversity order of w if all the subcarriers are transmitted in independent fading channels. Thus it is suitable for applications in fading channels. The bandwidth efficiency decreases in this scheme and we find that there is a tradeoff between bandwidth efficiency and the attainable performance. We will discuss this in more detail later in fading channel conditions.

The way of mapping symbols into waveforms is not confined by the method above. There is a more general way to perform the mapping process. In HPM, each waveform is composed of a combination of a few phase-frequency modulated signals and corresponds to a unique symbol. Since the total number of available waveforms can be up to

$$M' = w2^{k_p} \begin{pmatrix} v \\ w \end{pmatrix},$$

and the number of symbols is given by (2.3), we have $2M > M' \geq M$ so that some possible waveforms are not used. The criterion of selection of the signal waveforms to represent the signal set is to minimize the maximum correlation between any pair of symbol signals , i.e., choose the ones with the maximum distance in the signal constellation. In this way, the mapping from symbols to signals may not necessarily follow a regular pattern, i.e., the same frequency arrangement corresponds to the same k_f bits stream. This means that the mapping can't be performed separately between PFSK and PSK parts. For implementation, we need an integrated mapping unit without bit stream splitter and combiner at the transmitter and receiver. An

example of this approach is also given in Section 2.2.2.

2.2.2 Correlation Coefficient

In HPM, the whole signaling set has v subsets of polyphase signals. In each symbol period, w component signals are selected from v subsets and each subset can provide only one waveform at most. The signals in each subset are orthogonal to the signals in other subsets. We know that the multiple phase signals constitute a 2-dimensional signal space. This is also the case for signals in each subset. In fact, given the v orthogonal signal subsets and if $M_p > 2$, the whole signal set forms an overall $2v$-dimensional signal space. But each signal can only take values on $2w$ dimensions. In HPM with $M_p = 1$ or 2, there are only v dimensions in the signal space. When $M_p = 2$ or 4, the signal constellation is formed by a set of biorthogonal signals. In order to meet the requirement of orthogonality, the frequency separation between adjacent tones must exceed a minimum value. To derive the conditions for obtaining orthogonality between component signals, we must find the signal correlation coefficient.

From (2.6), we know the expression for one of the component signals in the i-th subset (from a set of v subsets) is

$$u_i(t) = B\cos(2\pi f_i t + \theta_q)$$
$$p = 0, 1, \ldots, v-1, \quad q = 0, 1, \ldots, M_p - 1 \tag{2.7}$$

The correlation coefficient of the component signals, with the phases of θ_{q_1} and θ_{q_2} respectively, between the i-th and j-th subsets is defined as

$$\rho' = \frac{1}{E_t}\int_0^{T_s} u_i(t)u_j(t)dt \tag{2.8}$$

where $E_t = B^2T_s/2$ is the tone energy and it is related to the symbol energy E_s as

$$E_s = wE_t.$$

Recall from (2.4) that $f_n = f_c + (2n + 1 - v)\Delta f/2$, substituting (2.7) into (2.8), the expression can be written as

$$\begin{aligned} \rho' &= \frac{2}{T_s}\int_0^{T_s} \cos(2\pi f_i t + \theta_{q_1})\cos(2\pi f_j t + \theta_{q_2})dt \\ &= \frac{\sin[\pi\Delta f T_s(i-j)]}{\pi\Delta f T_s(i-j)}\cos[\pi\Delta f T_s(i-j) + (\theta_{q_1} - \theta_{q_2})] \end{aligned} \tag{2.9}$$

When $\rho' = 0$, the component signals satisfy the orthogonality condition. In coherent detection, the phases θ_{q_1} and θ_{q_2} are known at the receiver. To make ρ' in (2.9) be equal to zero, either of the following must be satisfied:

$$\Delta f T_s = k_1,$$

$$\Delta f T_s = k_2/2,$$

where k_1, k_2 are any two integers. It is obvious that the minimum frequency separation is $\Delta f = 1/2T_s$.

In noncoherent detection, the receiver does not need the carrier phase information. ρ' equals to zero if the sine term is zero, which gives

$$\Delta f T_s = k \qquad \text{for any integer } k.$$

The minimum frequency separation satisfying the above expression is $\Delta f = 1/T_s$. Therefore the minimum Δf is related to the detection technique adopted. It is concluded that

$$\Delta f = \begin{cases} 1/2T_s & \text{coherent detection} \\ 1/T_s & \text{noncoherent detection.} \end{cases} \tag{2.10}$$

In our studies, we assume that all the tone frequencies are much larger than $1/T_s$ so that the scheme can still be analyzed as a narrowband system. In the following, we study the signal energy of HPM waveforms. Without loss of generality, we use $w = 3$ and assume that the three active tones are consecutive in the frequency band. The energy of symbol S_m $(m = 0, 1, \ldots, M-1)$ can be defined by

$$E_s = \int_0^{T_s} S_m^2(t)dt$$

$$\approx B^2T_s\left(\frac{w}{2}+\frac{\sin(\pi\triangle fT_s)}{\pi\triangle f}\cos(\pi\triangle fT_s+\triangle\theta_{12})+\frac{\sin(\pi\triangle fT_s)}{\pi\triangle f}\right.$$
$$\left.\cos(\pi\triangle fT_s+\triangle\theta_{23})+\frac{\sin(2\pi\triangle fT_s)}{2\pi\triangle f}\cos(2\pi\triangle fT_s+\triangle\theta_{13})\right) \quad (2.11)$$

where $\triangle\theta_{ij}$, $i \neq j$ is the information bearing phase difference between the active carriers. From this expression, to let the energy be independent of m, we must set

$$\triangle f = 1/T_s \quad (2.12)$$

or

$$\triangle f = 1/2T_s \quad \text{and } \triangle\theta_{ij} = 0 \text{ or } \pi \quad (2.13)$$

To meet the second requirement, M_p should be less or equal to 2, or all the active tones in the same signaling interval have the identical phases. In this case, all the symbol energies are equal and

$$E_s \simeq wB^2T_s/2$$

This condition can be extended to any HPM case. By combining the above two expressions with (2.10), the following condition has to be met

$$\triangle f = \begin{cases} 1/2T_s & \text{coherent detection with } M_p \leq 2, \text{ or the identical phases for all active carriers} \\ 1/T_s & \text{coherent detection with } M_p > 2 \\ 1/T_s & \text{noncoherent detection.} \end{cases} \quad (2.14)$$

The correlation coefficient between any two symbols, given the m_1-th and m_2-th symbol, is defined as

$$\rho_{m_1m_2} = \frac{1}{E_s}\int_0^{T_s} S_{m_1}(t)S_{m_2}(t)dt. \quad (2.15)$$

Considering the coherent detection, (2.6) becomes

$$S_m(t) = \sqrt{\frac{2E_s}{wT_s}}\sum_{n=0}^{v-1} a_{in}\cos(2\pi f_n t + \frac{2\pi j_r}{M_p} + \varphi_m). \quad (2.16)$$

Because φ_m is known at the receiver, we can neglect it when calculating ρ. By substituting (2.16) into (2.15) and after some manipulations, we obtain

$$\rho_{m_1m_2} \simeq \frac{1}{w}\sum_{n=0}^{v-1} a_{i_1n}a_{i_2n}\cos(2\pi(j_{r_1}-j_{r_2})/M_p) \quad (2.17)$$

We observe that the correlation coefficient is associated with the distance distribution between the signal blocks, the phase difference between the subcarriers if they are both activated.

To help understanding these concepts, we consider the HPM(4,2,2) scheme as an example. In this particular alphabet, there are a total of 4 frequency tones and only 2 tones are active per signaling frame. Each tone can take any one of 2 possible phases. The frequency signaling matrix is

$$A = \begin{pmatrix} 0 & 0 & 1 & 1 \\ 0 & 1 & 0 & 1 \\ 1 & 0 & 0 & 1 \\ 1 & 0 & 1 & 0 \\ 0 & 1 & 1 & 0 \\ 1 & 1 & 0 & 0 \end{pmatrix}$$

In the matrix, "1" stands for the active elements indicating the frequency tone is present and "0" means that the corresponding frequency tone is not present in that frequency arrangement.

It is derived that $k_f = \lfloor \log_2 C_4^2 \rfloor = 2$, $M_p = 2$ and $M_f = 2$, $M_p = 2$, $k_s = 4$. There are 6 blocks in PFSK part and 4 of them are needed to represent 2 bits. Suppose we choose (0011), (0101), (1010), (1100) as the codewords corresponding to the signaling frames. We select the codewords in such a way that anyone of the frequency tones appears the same number of times in the whole signaling set. This condition can't always be met in any given alphabet. In some alphabets, the same frequency arrangement may be used less than $M_p{}^w$ times to represent symbols. In that case, in order that the sum of all correlation coefficients between a reference symbol and any other symbols to be independent of whatever the symbol being chosen as the reference, we must select the signals in such a way that each phase value appears in equal times in the whole signaling set. If this requirement is met, the symbol error probability will be the same for any transmitted symbols.

There are total of $2 \times 2 \times 6 = 24$ possible waveforms and 16 of them are used to represent the valid symbols for input binary data. Every 4 incoming information bits

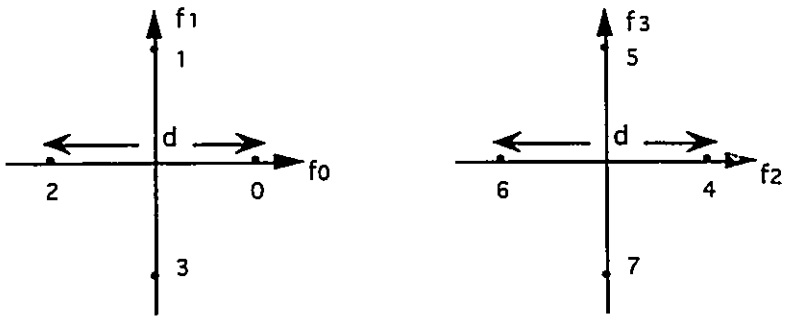

Figure 2.1: Signal constellation for HPM(4,2,2)

groups into one symbol. In each symbol interval, the first 2 bits are used to map the signal which is a specific combination of 2 frequency tones selected from the available 4 frequency tones. The third bit determines the phase of the first (lower frequency) active tone which has the lower frequency. Following the same process, the fourth bit determines the phase shift of the other active frequency tone. The signal constellation for this case is illustrated in Figure 2.1, where $d = 2\sqrt{E_w}$. There are $vM_p = 4 \times 2 = 8$ signal points which are distributed in 4-dimensional signal space, and any two points not being in the same dimension can be used to represent a symbol. Certainly we need only 16 combinations. The whole signaling set is listed in Table 2.1. The values in the slots of second to fifth columns indicate that the corresponding frequency tone is active during the transmission of the symbol in the same row. The value in each entry indicates the information-bearing phase shift carried by that particular tone. In the last column, every symbol is also specified by two integers representing the signal points. For instance, the seventh symbol S_6 is represented by f_1 with the phase being π and f_3 with the phase being 0. The corresponding signal points are 3 and 5. The symbol signal is

$$S_6(t) = B[\cos(2\pi f_1(t) + \pi + \varphi_6) + \cos(2\pi f_3(t) + \varphi_6)]$$

where $i = 1$, $j_0 = 1$, $j_1 = 0$. The correlation coefficients between S_0 and other symbols are also listed in the table. The maximum and minimum correlation between any pair of symbols is $\frac{1}{2}$ and -1 respectively.

symbol=S_m \ Phase	f_0	f_1	f_2	f_3	ρ_{0m}	
$S_0 = 0000$			0	0	-	(4,5)
$S_1 = 0001$			0	π	0	(4,7)
$S_2 = 0010$			π	0	0	(6,5)
$S_3 = 0011$			π	π	-1	(6,7)
$S_4 = 0100$		0		0	0.5	(1,5)
$S_5 = 0101$		0		π	-0.5	(1,7)
$S_6 = 0110$		π		0	0.5	(3,5)
$S_7 = 0111$		π		π	-0.5	(3,7)
$S_8 = 1000$	0		0		0.5	(0,4)
$S_9 = 1001$	0		π		-0.5	(0,6)
$S_{10} = 1010$	π		0		0.5	(2,4)
$S_{11} = 1011$	π		π		-0.5	(2,6)
$S_{12} = 1100$	0	0			0	(0,1)
$S_{13} = 1101$	0	π			0	(0,3)
$S_{14} = 1110$	π	0			0	(2,1)
$S_{15} = 1111$	π	π			0	(2,3)

Table 2.1: The signaling set for HPM(4,2,2).

Another more general way of mapping symbols into signal waveforms is shown in Table 2.2. In this way, all the six possible frequency tone combinations are used. The aim is to make the Euclidean distance among symbols in signal space as large as possible, and more importantly, to make fewer bit errors when a symbol error occurs. In the table, the correlation coefficients between S_0 and other symbols are calculated. The closest four signals related to S_0 are assigned to S_1, S_2, S_4 and S_8 respectively. Since they differ with S_0 only in one bit. This will result in lower bit error rate when making an erroneous decision if S_0 is transmitted. However, this is not true for all the symbols. Some symbols have worse correlation properties and it implies that error performance may vary from symbol to symbol. But generally the system created in this approach may have better error performance, especially BER performance than

the previous one. Therefore it is attractive in practice. On the other hand, not having a regular pattern to describe how to perform the mapping results in the difficulty of deriving the exact expression for bit error probability. In this thesis, we mainly focus on the HPM system constructed in the previous method, which gives the worst case performance. We may expect better performance if employing optimum mapping between symbols and waveforms.

symbol=S_m \ Phase	f_0	f_1	f_2	f_3	ρ_{0m}
$S_0 = 0000$			0	0	-
$S_1 = 0001$		0		0	0.5
$S_2 = 0010$	0		0		0.5
$S_3 = 0011$	0	0			0
$S_4 = 0100$	π			0	0.5
$S_5 = 0101$		0	π		-0.5
$S_6 = 0110$			π	π	-1
$S_7 = 0111$			π	0	0
$S_8 = 1000$		π	0		0.5
$S_9 = 1001$	π	0			0
$S_{10} = 1010$			0	π	0
$S_{11} = 1011$	0			π	-0.5
$S_{12} = 1100$	π	π			0
$S_{13} = 1101$	π		π		-0.5
$S_{14} = 1110$		π		π	-0.5
$S_{15} = 1111$	0	π			0

Table 2.2: Another signaling set for HPM(4,2,2).

The correlation coefficient and the Euclidean distance in signal space are two parameters for characterizing the similarity or dissimilarity of the signals. Their relation can be specified as (given the m-th and n-th symbol)

$$d_{mn}^2 = 2E_s(1 - \rho_{mn}) \tag{2.18}$$

Finally, if in some certain applications, the symbols to be transmitted comprise 24 nonbinary characters, each of the 24 signal blocks can be utilized to represent a

unique character, then the maximum transmission capacity can be reached. In this case, $M_f = C_2^4 = 10$ and $k_f = 2.585$, $k_s = 4.585$.

2.2.3 Bandwidth Efficiency

One of primary resources in digital communications is the available transmission bandwidth W. A communication system has a specific transmission rate R_b (in bits per second). The measure showing how efficiently the bandwidth resource is utilized is R_b/W, and it is interpreted as the bandwidth efficiency. In fact, for a given modulation scheme it can be defined as the allowable information bit rate transmitted per unit bandwidth while satisfying the required error performance. Thus it reflects the channel throughput. In practice, the bandwidth occupied by the transmitted signals is not uniquely defined. The most common definitions are half power bandwidth, minimum frequency separation bandwidth and null-to-null bandwidth. Therefore the bandwidth efficiency is meaningful only when the signal bandwidth definition is specified. In the following we evaluate the bandwidth efficiency of HPM scheme based on minimum frequency separation bandwidth.

Focusing on equal symbol energy case, we consider the general cases of uncoded HPM with the minimum frequency separation of $1/T_s$, which corresponds to $M_p > 2$. The transmission bandwidth required for general HPM is

$$W = v\triangle f = v/T_s$$

The transmitted bit rate is specified as

$$R_b = k_s/T_s = (k_f + wk_p)/T_s \tag{2.19}$$

Thus the bandwidth efficiency in terms of R_b/W is

$$\eta = \frac{R_b}{W} = \frac{k_f + wk_p}{v} \tag{2.20}$$

For the special cases of HPM employing coherent detection, the minimum frequency separation of $1/2T_s$ is possible. This refers to the case of $M_P \leq 2$, or HPM with the identical phases for all active tones. The corresponding expression of η is

$$\eta = \frac{2(k_f + wk_p)}{v} = \frac{2(k_f + 1)}{v} \tag{2.21}$$

2.3 System Model

2.3.1 Transmitter Model

The transmitter model for HPM is depicted in Figure 2.2. The input bit stream is grouped in symbols and each symbol consists of two parts. One part (k_f bits) of a symbol is used by the modulator to select a certain combination of frequency tones or subcarriers. This function is realized in a frequency synthesizer in which there are w subcarriers at the output depending on the input sequence. The modulator corresponding to this portion can be seen as a permutation FSK modulator. Another part of the source bits ($wk_p = w \log_2 M_p$ bits) are fed to phase selectors. Each k_p bits determines the corresponding phase shift of each subcarrier. Thus the second modulation part consists of w phase selectors and modulators which have different carrier frequencies coming from the outputs of the frequency synthesizer. Finally the resultant polyphase signals from the output of each phase modulator are combined together in the multiplexer to form the transmitted HPM signals.

A more general HPM transmitter model uses a set of frequency synthesizers and phase selectors directly. It maps the incoming symbol to a predefined signal waveform according to a mapping table. We can see that the above model is a special case of this general model.

2.3.2 Receiver Model

The optimum reception uses coherent detection but no structure based on coherent detection for permutation modulation has been proposed in the literature, because

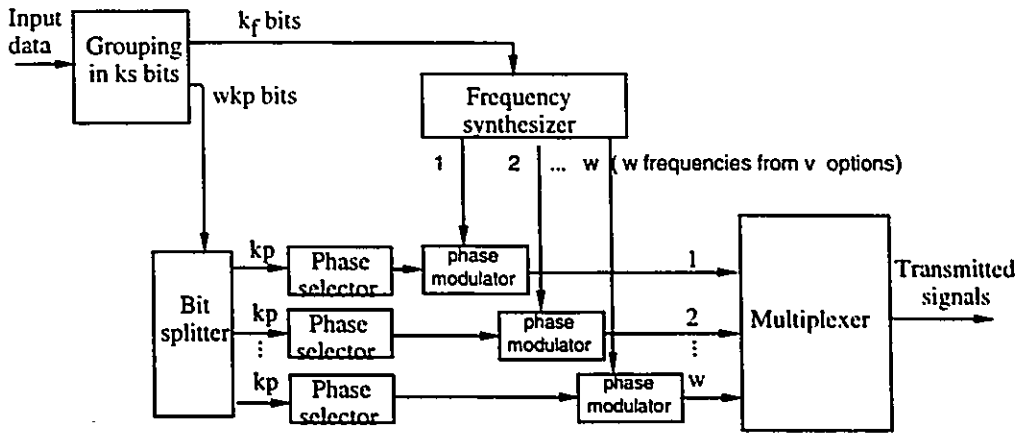

Figure 2.2: Transmitter model of HPM

noncoherent detection is attractive for this type of modulation. Although it may not practical, we consider the optimum detection to obtain a reference point for our later analysis and comparisons.

In this section, the channel model we considered is AWGN channel. Each signal waveform is assumed to be transmitted through independent AWGN channels. If the signal $S_m(t)$ is transmitted, the received signal in the k-th signaling interval can be specified as

$$r(t) = B\sum_{n=0}^{v-1}\left[\, a_{in}\cos(2\pi f_n t + \theta^{(k)} + \phi_n + \varphi_m) + z_n(t)\,\right] \qquad kT_s \le t \le (k+1)T_s \tag{2.22}$$

where $z_n(t)$, $n = 1, \ldots, v-1$, is a set of independent zero mean white Gaussian noise process with an identical two-sided power spectral density $N_0/2$. ϕ_n denotes the phase shift introduced by the channel and it is assumed to be a different constant for each frequency. This phase shift can be estimated by a time tracking loop at the receiver [25].

In coherent detection, we assume that the initial phases of the transmitted signals are perfectly known at the receiver. This is achieved by a carrier tracking mechanism. One of the possible ways of achieving a coherent system is to use a pilot signal as the

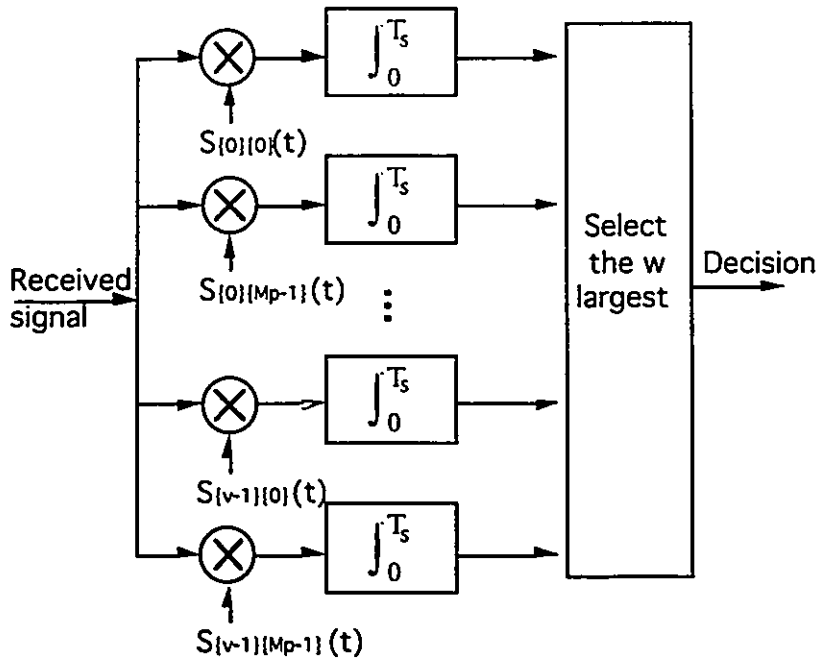

Figure 2.3: The optimum coherent detection receiver of HPM

carrier phase reference for demodulation. The subcarrier and initial phase information is extracted from this pilot signal in the detection process. In principle, the receiver correlates the received signal with all possible vM_p noiseless waveforms to form the decision variables. At the decision unit, the largest w correlator outputs are selected. The symbol corresponding to this w signal combination is the final decision. This is a maximum likelihood receiver and its structure is shown in Figure 2.3.

2.4 Bit Error Probability

The bit error probability is more meaningful than symbol error probability for performance comparisons of different modulation techniques. Usually the symbol error probability can be evaluated from an exact expression or using bounds. The conversion from symbol error to bit error probability is related to the distance property of the codewords which correspond to the waveform arrangements, the mapping between bit combinations and symbols. Usually this problem can be solved in a simple way by

assuming the symbol corresponding to all zero bits is transmitted and then one finds the probability of 1s after making a symbol error. For equally correlated signals such as orthogonal signals, it does not matter which waveform arrangement corresponds to this transmitted symbol and a constant conversion factor exists. For instance, in M-ary FSK with $M = 2^k$, the factor relating bit to symbol error probability yields to be $(2^{k-1}/2^k - 1)$. In more general cases, this factor may depend on the symbol being considered, or even the receiver structure employed.

In permutation FSK ($w > 1$), the signal correlations can be reflected by the distance properties of the permutation codes. It is found that if we are given a codeword, the distance distribution of other codewords is as follows:

$$\begin{array}{cc} \text{Hamming distance} & \text{number of codewords} \\ 2 & \binom{w}{1}\binom{v-w}{1} \\ 4 & \binom{w}{2}\binom{v-w}{2} \\ \vdots & \vdots \\ 2w & \binom{v-w}{w} \end{array} \tag{2.23}$$

where Hamming distance refers to the number of different positions between a pair of codewords. Expression (2.23) indicates that the remaining symbols have unequally correlated signals to the reference. Some symbols may have better distance features than others. The difficulty is that generally we can't make all the symbols follow the same rule, then finding bit error rate is a complicated task and it is related to the mapping between waveforms and symbols. But just as the examples given in Appendix B, on the average, we can assume that when a symbol error occurs, half of the bits are in error. Thus we have

$$P_b \simeq 0.5 P_s \tag{2.24}$$

In HPM, the same argument applies. We can use the above relation for coherent

HPM. In noncoherent HPM, we need to give detailed analysis since the receiver can be realized in two stages.

2.5 System Performance over an AWGN Channel

2.5.1 Performance Evaluation

To derive the symbol error probability of HPM in AWGN channel, we resort to the union upper bound. The error probability between a pair of symbols [25, page 243] is

$$P_2(m_1, m_2) = Q\left(\sqrt{k_s\gamma_b(1-\rho)}\right) \text{ for } m_1 \neq m_2, \tag{2.25}$$

where ρ is the correlation coefficient between the signals concerned and it is given by (2.15), $Q(x)$ is defined as

$$Q(x) = \frac{1}{\sqrt{2\pi}}\int_x^\infty e^{-t^2/2}dt,$$

and γ_b is the energy per bit to noise spectral density ratio.

The overall symbol error probability can be upper bounded by the sum of P_2 between any pair of the symbols and it is specified as

$$P_s \leq \frac{1}{M}\sum_{m_1=1}^{M}\sum_{m_1\neq m_2}^{M} P_2(m_1, m_2) \tag{2.26}$$

When the symbol error probability is not conditioned on any particular symbol, it becomes

$$P_s \leq \sum_{m_2=0, m_1\neq m_2}^{M-1} Q\left(\sqrt{k_s\gamma_b(1-\rho_{m_1m_2})}\right) \qquad \text{for any } m_1, \tag{2.27}$$

where

$$m_1 = i_1 wM_p + \sum_{r1=0}^{w-1}(w-1-r1)M_p j_{r1},$$

$$m_2 = i_2 wM_p + \sum_{r2=0}^{w-1}(w-1-r2)M_p j_{r2}.$$

In addition to giving the upper bound, we can also obtain the lower bound. From the results in [28, page 153], we have

$$P_s \geq \frac{2}{M} Q\left(\frac{d_{min}}{\sqrt{2N_0}}\right) = \frac{2}{M} Q\left(\sqrt{k_s\gamma_b(1-\rho_{max})}\right) \tag{2.28}$$

where ρ_{max} is the maximum value of correlation coefficients.

Once the symbol error probability is obtained, using the result given in section 2.4, the bit error probability is approximated as

$$P_b \leq \frac{1}{2} \sum_{m_2=0, m_1 \neq m_2}^{M-1} Q\left(\sqrt{k_s\gamma_b\left(1 - \frac{1}{w}\sum_{n=0}^{v-1} a_{i_1 n} a_{i_2 n} \cos(\theta_{nj_1} - \theta_{nj_2})\right)}\right)$$
$$\text{for any } m_1. \tag{2.29}$$

and

$$P_b \geq \frac{1}{M} Q\left(\sqrt{k_s\gamma_b(1-\rho_{max})}\right) \tag{2.30}$$

2.5.2 Numerical Results and Discussions

BER and the spectral efficiency η are two main measures to judge the performance of any modulation schemes. A major advantage of HPM is its bandwidth efficiency. Based on the previous analysis, expression (2.29) represents the bit error rate of HPM in AWGN channel and expression (2.20) or (2.21) refer to its spectral efficiency η. In the following we conduct the evaluation based on them and demonstrate the improvements achieved by this new scheme compared with other related schemes.

Bit error performances of HPM(5,2,2), (5,2,4) and (5,2,8) are illustrated in Figure 2.4. The performances of coherent PSK are used as reference. The lower bound for HPM(5,2,2) is also shown. The best error performance is given by HPM(5,2,4), while the worst one is HPM(5,2,8), but it still outperforms 8PSK in high signal to noise ratio conditions. There are crossovers between HPM curves and conventional PSK curves. The reason for these crossovers can be explained by analyzing the parameter $(k_s\gamma_b(1-\rho))$ in Q function, which is closely related to the error probability

of both schemes. As far as the maximum correlation coefficient is concerned, its value overwhelmingly determines the error probability, and under the comparable signal format, the former one yields a larger ρ. For instance, in HPM(5,2,8), ρ_{max} = 0.854, and in 8PSK ρ_{max} = 0.707. On the other hand, HPM scheme gives larger k_s. Consequently at low per bit energy to noise density ratio, the parameter in Q function exhibits smaller value in case of HPM, which leads to poor error performance. Nevertheless, at high per bit energy to noise density ratio, the big value of k_s in HPM makes the value of $k_s\gamma_b(1-\rho)$ increase fast, and this causes the BER curve of HPM to fall below that of M-ary PSK. Therefore, the crossovers may occur.

The performances of various HPM systems and conventional PSK systems in AWGN channels are tabulated in Table 2.3. The modulation schemes are indicated by a pair of numbers (frequency tones) in the brackets and a value representing the number of phases. The comparisons are made in terms of the normalized data rate $\eta = R_b/W$, and γ_b (i.e., required signal-to-noise ratio per bit to achieve a given bit error rate of 10^{-5}). Note that the minimum frequency separation for M-ary FSK and JFPM with M_p=2 is $1/2T_s$. Whereas it is $1/T_s$ in all other cases. Since each pair of the following signal set, HPM(2,1,4) and (4,1,2), (4,1,4) and (8,1,2), (8,1,4) and (16,1,2), has the same signal distance propertie respectively, we observe the same E_b/N_0 value under the same error condition. Their bandwidth efficiencies are also identical if the corresponding minimum frequency separations are achieved.

The bottom line of the table shows the performance of M_p-FPSK evaluated by [21]. It is a hybrid case with fixed $v = w = 2$. One symbol can be represented by any two phase combinations carried by two tones. Consequently for a given value M_p, a complete phase code gives rise to $M = M_p^2$ signals. Although the minimum frequency separation between adjacent tones are chosen to be $1/T_s$, the bandwidth used for transmission can be treated as the first null bandwidth which is $1.5/T_s$ rather than $2/T_s$. Therefore η yields to be $k_s/1.5$.

From the table, we observe that we have many alternatives to choose HPM param-

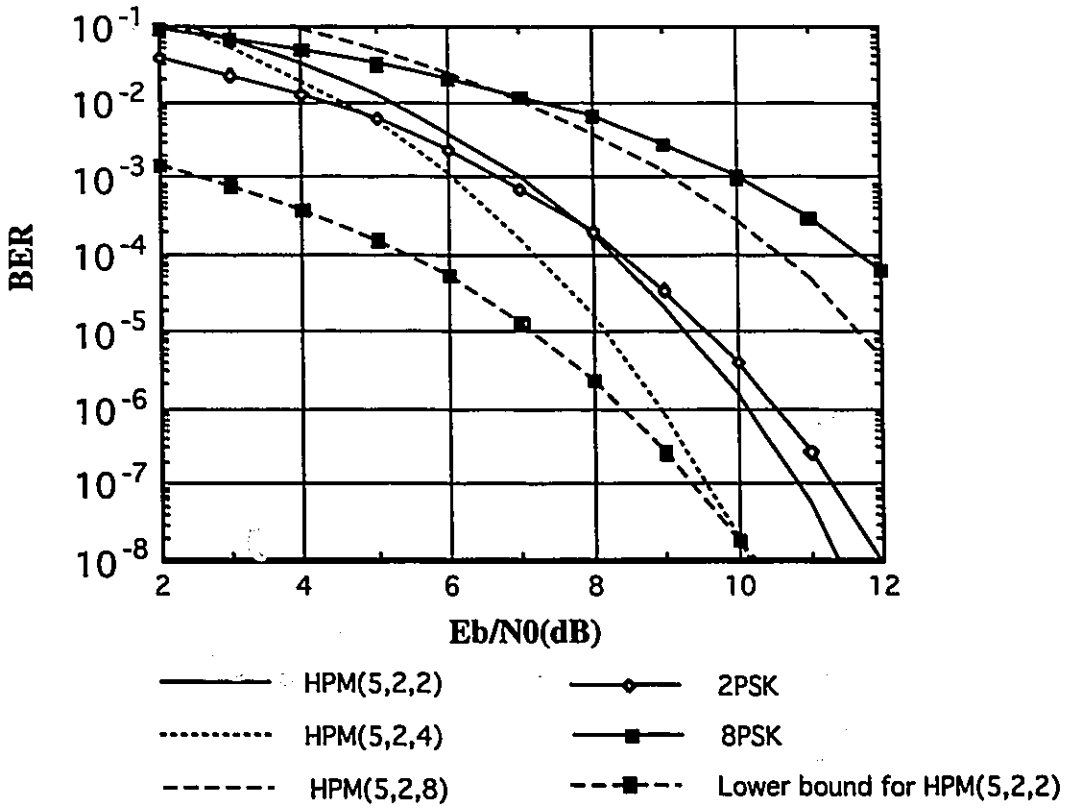

Figure 2.4: Bit error rate performance of coherent HPM(5,2,M_p) in AWGN channels when M_p=2,4,8.

eters to meet the given requirements. Two HPM systems having the same bandwidth efficiency may require different γ_b, and vice versa. As an example, for $\eta = 2.00$, we can choose either of HPM(2,1,2), (4,2,8), (4,2,2), (5,2,2) and approximately (16,5,2), but the required γ_b is 9.58 dB, 12.21 dB, 9.89 dB, 9.29 dB and 8.81 dB respectively. In this respect, when $M_p > 2$, the Δf has to be doubled to $1/T_s$ so that bandwidth efficiency substantially decreases. Therefore a good design involves proper selection of these parameters.

M_p (v,w)	1 (PFSK)	2	4	8
(1,1)(PSK)	-	9.58/1.00	9.58/2.00	12.97/3.00
(2,1)	12.60/1.00	9.58/2.00	8.30/1.50	11.91/2.00
(4,1)	9.89/1.00	8.30/1.50	7.38/1.00	10.94/1.25
(8,1)	8.41/0.75	7.38/1.00	6.70/0.625	10.15/0.75
(16,1)	7.43/0.50	6.70/0.625	6.16/0.375	9.48/0.438
(4,2)	12.78/1.00	9.89/2.00	8.57/1.50	12.21/2.00
(5,2)	11.31/1.20	9.29/2.00	8.16/1.40	11.70/1.80
(6,3)	11.98/1.33	9.82/2.33	8.58/1.667	-
(7,3)	11.13/1.43	9.34/2.286	8.25/1.571	-
(8,4)	11.69/1.50	9.73/2.50	8.54/1.75	-
(16,5)	10.09/1.50	8.81/2.126	7.92/1.375	-
FPSK	-	9.58/1.33	9.89/2.67	13.46/4.00

Table 2.3: Performance comparisons of various coherent HPM alphabets under different parameters(v, w, M_p). The entries in the table are $\gamma_b(dB)/\ \eta$(bps/Hz), i.e., energy per bit to noise power density ratio required to achieve bit error probability of 10^{-5} in AWGN channels versus bandwidth efficiency η.

In order to observe the relationships in a clearer manner, we draw a graph for the abscissa as the bandwidth efficiency η (bps/Hz), and the ordinate as the bit energy to noise-power spectral density $\gamma_b = E_b/N_0(dB)$. The comparative performance of a modulation scheme corresponds to a position in the graph, which is based on the bit error probability of 10^{-5}. The channel capacity boundary in AWGN channel is

depicted as a reference and it is stated [1] as

$$C = W \log_2 \left(1 + \frac{E_b}{N_0}\right).$$

where C is the channel capacity which represents the maximum number of bits that can be reliably transmitted per second over the channel. A communication system with the transmission rate R_b more than C can not operate reliably. A modulation scheme has a better performance when its position in the graph approaches the lower-right side of the figure. Generally for a modulation scheme, the closer its position is to this boundary, the more efficient it is. Figure 2.5 shows the comparative performances of some typical HPM alphabets with 4 phases and FPSK, MPSK and MFSK schemes as well. Figure 2.6 shows the comparisons of HPM and JFPM under different phase conditions. The following observations are drawn from these graphs:

(1) The best performance of HPM scheme is accomplished when M_p equals 4. This is true not only for achieving minimum γ_b, but also for reaching the minimum distance to the limit. In other words, if M_p takes other values, some conventional schemes such as MFSK or MDPSK could be closer to the limit.

(2) PSK and FPSK are more likely to achieve higher bandwidth efficiency. They have close values of γ_b under the same signal set. The larger η of FPSK is due to its efficient first null bandwidth.

(3) To achieve the minimum γ_b, some of JFPM systems may be the candidates. The most power efficient system in Table 2.3 is HPM(16,1,4) although it is not the scheme closest to the limit. Whereas conventional M-ary FSK lies in the area with lower spectral efficiency and medium γ_b. Therefore it is not a competitive modulation option as far as the efficiency is concerned.

(4) HPM systems lie in the region between that of M-ary FSK and PSK but possessing low γ_b. Some typical HPM systems can get closer to the channel capacity limit than conventional systems. But there is no big advantage of HPM with $w > 1$ over JFPM system in terms of the overall efficiency observed from the graph. That

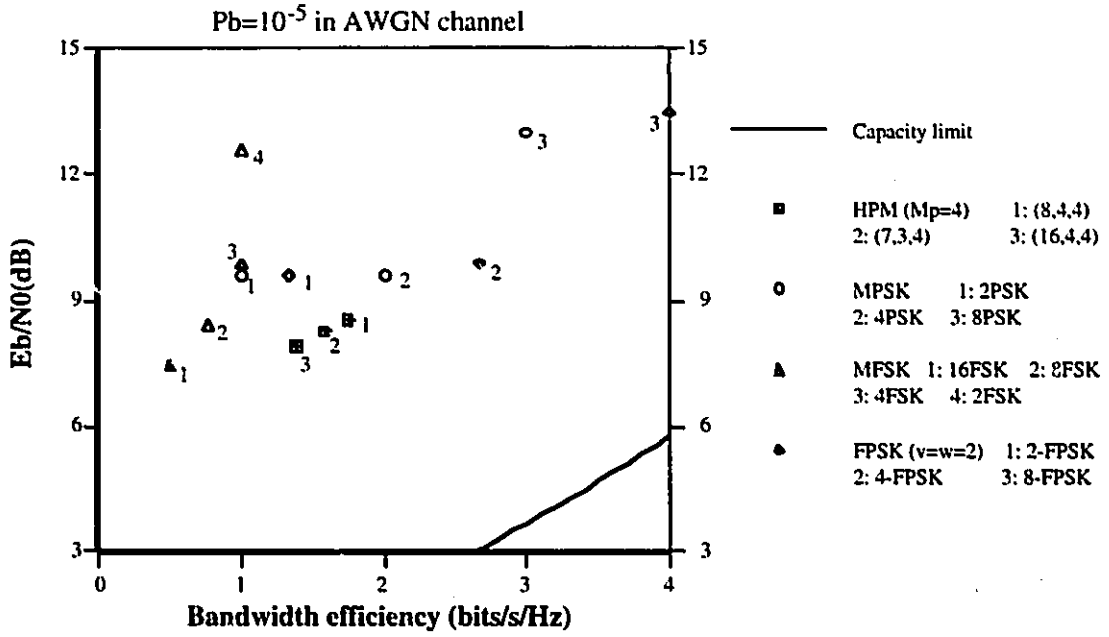

Figure 2.5: Performance(γ_b versus η) comparisons of coherent HPM(M_p=4) with various coherent detection modulation schemes under AWGN channels with bit error probability of 10^{-5}.

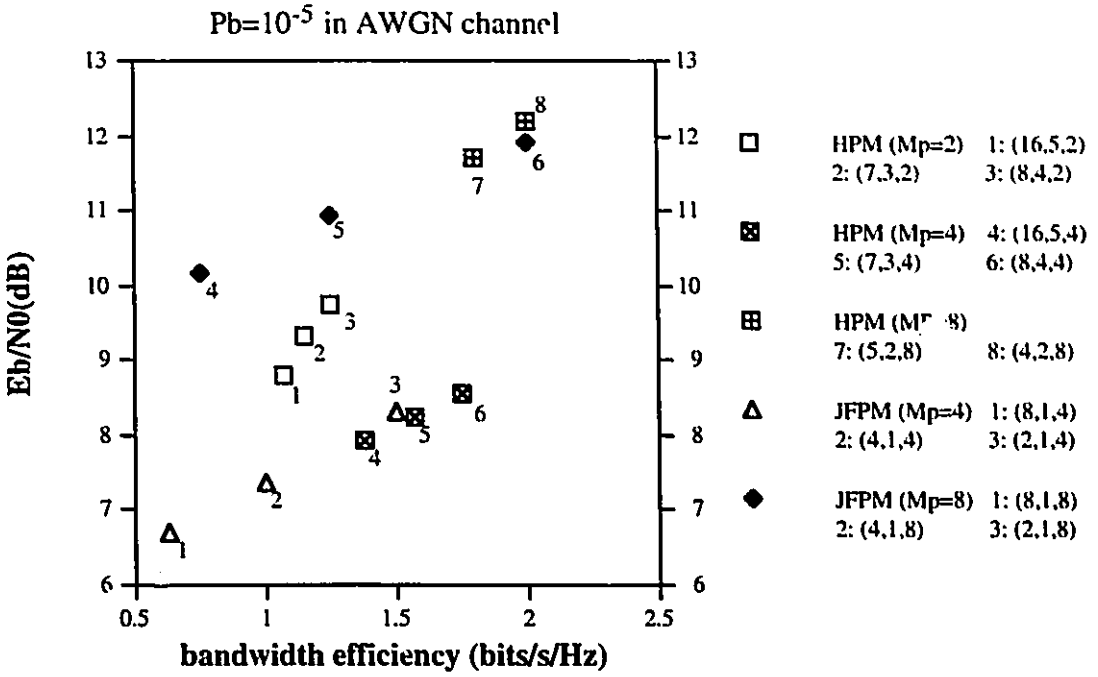

Figure 2.6: Performances(γ_b versus η) of coherent HPM and JFPM in AWGN channels with bit error probability of 10^{-5}.

we have to sacrifice the efficiency to set k_s as an integer may be the reason. But given the same transmission bandwidth, taking HPM(16,1,4) and (16,5,4) as an example, the latter scheme utilizes the available bandwidth more efficiently than the former one ($\eta = 1.375$ versus 0.375). On the other hand, HPM with $M_p = 2$ has good property since it is characterized by the minimum frequency separation of $1/2T_s$.

It also should be mentioned that the transmission bandwidth calculated so far is Nyquist minimum bandwidth with the use of Nyquist filtering. But such filters are not realizable so that the bandwidth efficiencies calculated are theoretical maximum values. For practical system, these theoretical values should be decreased by $(1 + \alpha)$ to account for realizable filters, with α standing for the roll-off factor $(0 < \alpha < 1)$.

2.6 HPM with Coherent Detection over Frequency Selective Fading Channels

In certain communication applications, such as mobile radio and land mobile satellite communications, the transmitted signals are passed through a time-variant multipath channel. The received signals appear as a set of delayed signals going through multiple paths due to diffusion, reflection and scattering. The overall effect results in signal fading. Furthermore, the nature of the physical medium changes as a function of time. In a typical metropolitan area, where there is no direct signal component at the receiver, the received signal is the sum of several random amplitude and random phase signals. Usually the impulse response of the channel can be modeled as a zero mean complex-valued Gaussian process, where the probability density function of the envelope of the faded signal has a Rayleigh distribution. In this thesis, consideration is given only to the Rayleigh fading channel.

In this section, we investigate the performance of coherent HPM over a frequency selective slowly fading channel. Results show that HPM offers limited performance improvements over conventional MPSK scheme. Further improvement can be ex-

pected if using a proper approach to take advantage of its intrinsic diversity.

2.6.1 Channel Model

The channel model we considered can be characterized by the impulse response [25]

$$\begin{aligned} h(\tau;t) &= \sum_i \alpha_i(t) e^{-j2\pi f_c \tau_i(t)} \delta(t-\tau_i(t)) \\ &= a_i(t)\delta(t-\tau_i(t)) \end{aligned} \tag{2.31}$$

where $\alpha_i(t)$ and $\tau_i(t)$ are respectively the attenuation factor and the propagation delay for the signal received on the i-th path, $a_i(t)$ represents a time-variant complex Gaussian random variable. Due to this assumption, the envelope of the impulse response $r = |h(\tau;t)|$ appears to be a Rayleigh-distributed random variable.

Usually the amplitude attenuation (or phase shift) in different subchannels are correlated with each other. But there are two extreme cases. If α_i (and ϕ_i) are identical for all $i = 1, 2, \ldots, v$, then the channel is called to be frequency nonselective or flat fading. On the contrary, if α_i and ϕ_i are independent with each other for all $i = 1, \ldots, v$, this is the simplest frequency selective channel model.

Furthermore, we suppose that the fading variations are slow enough, i.e., the channel attenuation and phase change slowly so that they can be treated as constant over at least one symbol duration.

In this thesis, our analysis focus on the frequency selective multipath fading channel model. In other words, the transmitted signal bandwidth $W = v/T_s$ is relatively larger than the coherence bandwidth of the channel. We also assume that each subcarrier with transmission bandwidth $1/T_s$ does not experience significant dispersion so that $1/T_s$ should be smaller than the coherence bandwidth of the channel. In this way, we see the channel as a multichannel model which consists of v independent subchannels. Each of the component signal undergoes independent attenuation and phase shift. In real situations, this assumption puts constraints on the selection of signal formats, i.e., we can not choose adjacent tones to represent a symbol. But for

easing the analysis, we make this assumption and also for simplicity, we assume that all the subchannels have identically distributed Rayleigh fading. More specifically, this multichannel model is characterized by three statistical vectors:

- amplitude attenuation $\alpha = (\alpha_1, \alpha_2, \ldots, \alpha_v)$.
- phase shift $\phi = (\phi_1, \phi_2, \ldots, \phi_v)$.
- propagation delay $\tau = (\tau_1, \tau_2, \ldots, \tau_v)$.

In our case, $\alpha_i (i = 1, \ldots, v)$ follows Rayleigh distribution and its probability density function is given by

$$p(\alpha_i) = \frac{\alpha_i}{\sigma_i^2} \exp\left(\frac{-\alpha_i^2}{2\sigma_i^2}\right) \qquad 0 < \alpha_i \tag{2.32}$$

where σ_i^2 represents the average scattered power in the i -th subchannel due to multipath. Under our assumption, all the subchannels have the identically distributed Rayleigh fading (i.e., σ_i^2 is identical for all i). $\phi_i (i = 1, \ldots, v)$ is uniformly distributed in $[0, 2\pi]$. In most cases, τ_i is smaller than a symbol duration. Without loss of generality, it is assumed that $\tau_i = 0$ for all i.

Beside fading, it is also assumed that all the subchannels contain independent additive white Gaussian noise with a flat power spectral density of $N_0/2$. Simply we can treat the fading as a multiplicative factor and the noise as an additive factor.

2.6.2 Performance Analysis

If the waveform $S_m(t)$ given by (2.6) is transmitted over the fading channel we have presented, the received signal during the k-th signaling interval can be expressed as

$$r(t) = B \sum_{n=0}^{v-1} \Big[\alpha_n a_{in} \cos(2\pi f_n t + \theta^{(k)} + \phi_n + \varphi_m) + z_n(t) \Big] \qquad kT_s \le t \le (k+1)T_s \tag{2.33}$$

where α_n and ϕ_n represent the attenuation and phase shift introduced by the n-th subchannel and $z_n(t)$ is a set of zero mean white Gaussian noise process with a two-sided power spectral density $N_0/2$.

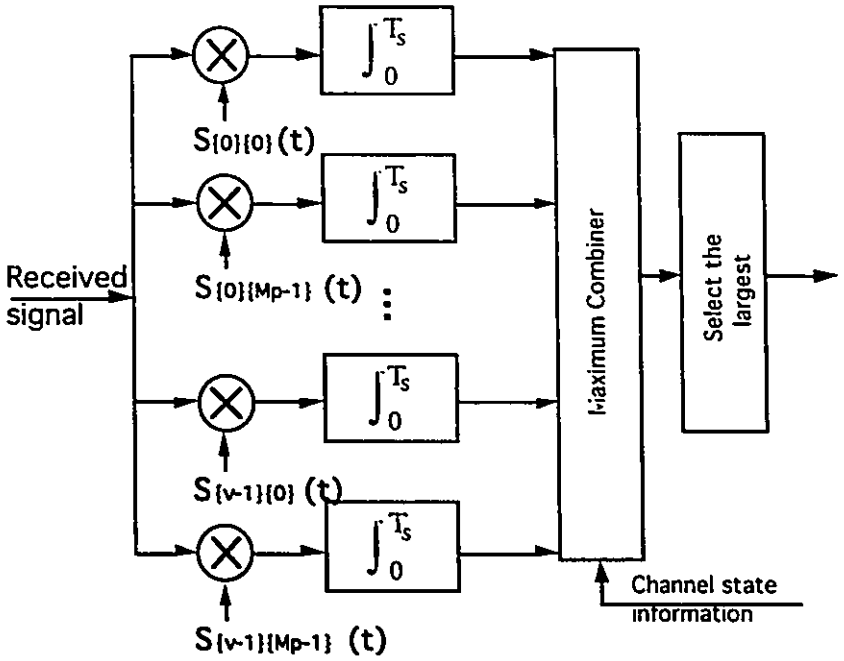

Figure 2.7: Coherent HPM receiver structure for fading channels.

Since it is assumed that all the subcarrier signals experience independent fading conditions, it is unlikely that all the component signals are struck by deep fades simultaneously. Hence HPM scheme has the nature of implicit diversity when applied to this specific channel. At the receiver, the information about the phases and frequencies for all the component signals is assumed to be extracted by the carrier tracking system. Thus the detector operates as a maximum likelihood detector. In order to exploit the implicit diversity of HPM scheme, a maximum combiner is required, which compensates for the amplitude gain and phase shift introduced by the channel. It combines the correlator outputs to form the decision variables for a specific symbol, i.e., multiplying all the corresponding correlator outputs by the fading factor $\alpha_n e^{-j\phi_n}$ in that subchannel and then adding them together. In the decision unit, the maximum output from the combiner is selected as decision. The block diagram for this maximum combining receiver is depicted in Figure 2.7.

Based on the analysis in Section 2.4, the HPM signal waveform of a given symbol differs in frequency and/or phase from the other signals in the signal set in at least one component signal. This reflects the basic property of permutation code, in which a codeword differs from the other codewords in 1 to w positions. In the sample HPM(4,2,2) system given in Table 2.1, each of the six waveforms, which represent S_1, S_2, S_4, S_6, S_8 and S_{10}, has only one identical subcarrier (frequency and phase) as the reference symbol S_0. All the other symbols use two totally different subcarriers compared with those of S_0, i.e. they have no similar component signals with those used by S_0. These distinct component signals possess the complete phase shifts from the reference waveform and undergo independent fading if transmitted. Therefore from the signal properties of HPM, we can observe that coherent HPM system applied to the fading channels is equivalent to a conventional MPSK system with L order diversity. The diversity order L is determined by the arrangement of waveforms and ranges from 1 to w. But it is fairly reasonable to consider that the error performance of HPM is determined by the error rate occurred when detecting those signals with the closest distance in signal space. This means that HPM scheme has only effective diversity of $L = 1$ if all the possible waveforms are used for transmission. Thus the symbol error probability of uncoded HPM can be approximated by the result of MPSK scheme without diversity.

In coherent detection, the error probability for conventional MPSK over fading channels with no diversity is given by [25, page 739]

$$P_s(M_p) = \frac{M_p - 1}{M_p} - \frac{\mu \sin(\pi/M_p)}{\pi\sqrt{1 - \mu^2 \cos^2(\pi/M_p)}} \cot^{-1} \frac{-\mu \cos(\pi/M_p)}{\sqrt{1 - \mu^2 \cos^2(\pi/M_p)}} \tag{2.34}$$

where

$$\mu = \sqrt{\bar{\gamma}_c/(1 + \bar{\gamma}_c)},$$

and $\bar{\gamma}_c = k_s \bar{\gamma}_b$, with $\bar{\gamma}_b$ representing the average bit energy to noise density ratio.

The bit error probability of HPM is approximated by

$$P_b \simeq \frac{1}{2} P_s(M_p) \tag{2.35}$$

2.6.3 Numerical Results

The error performance of HPM scheme is plotted in Figure 2.8. The bandwidth efficiency of each modulation scheme is enclosed in parenthesis in the figure. Table 2.4 tabulates some of the HPM performances under the condition of BER being 10^{-4} for the case of frequency selective fading.

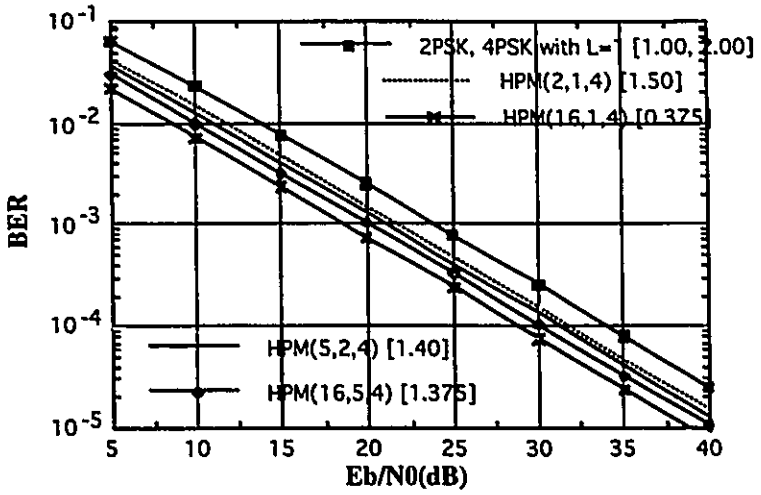

Figure 2.8: BER performances of coherent HPM over frequency selective fading channels.

Based on the observations from the table and figure, it seems that HPM with high value of w is not necessarily a suitable modulation candidate under this channel condition. This is because that less energy is allocated to each subcarrier when employing multiple carrier approach; and there is too close distance between adjacent signal waveforms. Therefore its implicit diversity is limited by 1, which offers no advantage to combat fading. Even though it can provide some improvements in power efficiency over the conventional MPSK scheme, it seems that JFPM is a better

M_p (v,w)	2	4	8
(1,1)(PSK)	33.9/1.00	33.5/2.00	35.7/3.00
(2,1)	27.9/2.00	31.8/1.50	36.2/2.00
(4,1)	26.2/1.50	30.5/1.00	35.3/1.25
(8,1)	24.9/1.00	29.6/0.625	34.5/0.75
(16,1)	24.0/0.625	28.8/0.375	33.8/0.438
(4,2)	27.9/1.00	31.8/1.50	36.2/2.00
(5,2)	27.0/1.00	31.1/1.40	35.7/1.80
(6,3)	27.3/1.167	31.3/1.667	35.9/2.167
(7,3)	26.7/1.143	30.9/1.571	35.6/2.00
(8,4)	27.0/1.25	31.1/1.75	35.7/2.25
(16,5)	25.6/1.063	30.1/1.375	34.9/1.688

Table 2.4: Performance comparisons of various coherent HPM alphabets over frequency selective fading channels. The results are based on $\gamma_b(dB)/\ \eta$(bps/Hz), i.e., energy per bit to noise density ratio required to achieve bit error probability of 10^{-4} versus bandwidth efficiency η.

option in this regard. But once an efficient measure is taken to enlarge the distance between HPM waveforms, its intrinsic diversity can be increased so that substantial performance improvements can be achieved.

2.7 The identical phase HPM version over Frequency Selective Fading Channels

The designing of HPM waveforms can vary from case to case. According to the channel model, the proper modification of transmitted waveforms indicates the flexibility of this scheme and the potential for improvement.

Under the specific condition of coherent detection and frequency selective fading channel model, by sacrificing the bandwidth efficiency, we are able to achieve the inherent diversity and thus the remarkable improvements compared to the HPM version

without implicit diversity. The designing of waveforms is described as follows: All the active tones have the identical phase, which is determined by the input symbol. The incoming symbol determines the combination of the active tones and the carried phase. The objective of the design is to eliminate the intersecting component signals as much as possible in all the waveforms. Since coherent detection is employed, the maximum inherent diversity which equals to w can be achieved at the receiver. An example of HPM(5,2,4), which is implemented in this manner, is given in Table 2.5.

symbol / Phase	f_0	f_1	f_2	f_3	f_4	waveform
$S_0 = 000$			0		0	$\cos f_2 t + \cos f_4 t$
$S_1 = 001$		$\pi/2$			$\pi/2$	$\cos(f_1 t + \frac{\pi}{2}) + \cos(f_4 t + \frac{\pi}{2})$
$S_2 = 010$	π				π	$\cos(f_0 t + \pi) + \cos(f_4 t + \pi)$
$S_3 = 011$			$\pi/2$	$\pi/2$		$\cos(f_2 t + \frac{\pi}{2}) + \cos(f_3 t + \frac{\pi}{2})$
$S_4 = 100$		$3\pi/2$		$3\pi/2$		$\cos(f_1 t + \frac{3\pi}{2}) + \cos(f_3 t + \frac{3\pi}{2})$
$S_5 = 101$	0			0		$\cos f_0 t + \cos f_3 t$
$S_6 = 110$		π	π			$\cos(f_1 t + \pi) + \cos(f_2 t + \pi)$
$S_7 = 111$	$3\pi/2$		$3\pi/2$			$\cos(f_0 t + \frac{3\pi}{2}) + \cos(f_2 t + \frac{3\pi}{2})$

Table 2.5: The identical phase version of HPM(5,2,4).

The scheme consists of selecting only 8 waveforms from the total possible 40 waveforms and hence $k_s = 3$. Each symbol is represented by an unique waveform which contains no shared components with any other waveforms. With the identical phase property, once the receiver signals are combined at the receiver, a equivalent diversity order of 2 can be obtained. The bandwidth efficiency of this example is $\eta = k_s/v = 0.6$ bps/Hz. And the power efficiency in each diversity branch is $\gamma_c = k_s/w = 1.5$.

There is another example HPM(6,3,4) with $k_s = 4$ and it is shown in Table 2.6. In this case, all the waveforms have only one common component signal shared with others. The effective diversity obtained is 2. While $\eta = 4/6 = 0.67$ bps/Hz and $\gamma_c = 4/3 = 1.33$.

symbol/ Phase	f_0	f_1	f_2	f_3	f_4	f_5
$S_0 = 0000$			0		0	0
$S_1 = 0001$	$\frac{\pi}{2}$				$\frac{\pi}{2}$	$\frac{\pi}{2}$
$S_2 = 0010$		$\frac{3\pi}{2}$			$\frac{3\pi}{2}$	$\frac{3\pi}{2}$
$S_3 = 0011$			π	π		π
$S_4 = 0100$		0		0		0
$S_5 = 0101$	$\frac{3\pi}{2}$			$\frac{3\pi}{2}$		$\frac{3\pi}{2}$
$S_6 = 0110$		$\frac{\pi}{2}$	$\frac{\pi}{2}$			$\frac{\pi}{2}$
$S_7 = 0111$	0		0			0
$S_8 = 1000$		$\frac{\pi}{2}$		$\frac{\pi}{2}$	$\frac{\pi}{2}$	
$S_9 = 1001$	π			π	π	
$S_{10} = 1010$		π	π		π	
$S_{11} = 1011$	$\frac{3\pi}{2}$		$\frac{3\pi}{2}$		$\frac{3\pi}{2}$	
$S_{12} = 1100$	0	0			0	
$S_{13} = 1101$		$\frac{3\pi}{2}$	$\frac{3\pi}{2}$	$\frac{3\pi}{2}$		
$S_{14} = 1110$	$\frac{\pi}{2}$		$\frac{\pi}{2}$	$\frac{\pi}{2}$		
$S_{15} = 1111$	π	π				π

Table 2.6: The identical phase version of HPM(6,3,4).

To make comparison, we consider the conventional 4PSK with diversity order of 2. The corresponding $\eta = k_s/L = 1$bps/Hz and $\gamma_c = k_s/L = 1$. From the value of η and γ_c, we can expect that HPM scheme achieves a certain power gain. However, since the mapping between symbol and phase signal can't be described by Gray code, the bit error rate is not clear and definite if the symbol error rate is known. We will not perform a detailed calculation. But we can expect that this modified HPM scheme has comparable performance with conventional PSK with diversity.

2.8 Conclusion

In this chapter, we first described the signal properties of HPM. An HPM waveform consists of several orthogonal component signals. A large size waveform set can be obtained by the arrangements of these component signals.

Then, based on coherent detection, the transmitter and receiver structure are presented. Note that uncoded HPM with coherent detection is not practical in real applications. Here we use it mainly as a reference. The error performance is first analyzed over AWGN channels. The comparisons are on the basis of energy per bit to noise density ratio required to achieve a given BER, and bandwidth efficiency. It is revealed that HPM is able to perform fairly well as far as power and bandwidth efficiency are concerned. The improvements over conventional M-ary DPSK and M-ary FSK are evident.

Another channel model which is characterized by frequency selective Rayleigh fading is introduced. Under this channel model, it is concluded that HPM using the maximum allowable number of waveforms has a poor performance due to too many shared component signals among HPM waveforms. On the other hand, HPM using some of the carefully selected waveforms can bring about remarkable improvement. Two HPM examples employing expurgated waveforms have been given. It is found that they have comparable performance with conventional M-ary PSK with diversity.

Chapter 3

Uncoded Noncoherent HPM Systems

3.1 Introduction

The coherent reception for HPM requires a bank of correlators and integrators, one for each possible frequency and phase signal. The correct estimates of all the phases and frequencies are required to be extracted and maintained by the receiver. However, in many dispersive channels, the channel spread factor which is the product of Doppler spread B_d and multipath spread T_m are so large that obtaining and maintaining these carrier and phase references is usually not feasible [31]. In order to avoid the difficulty in implementation, noncoherent reception is preferred. For the frequency detection part, noncoherent square-law FSK detector can operate without the information about the phase and provide fairly satisfactory performance. For the phase modulation part, we can employ differential phase shift keying for its relative simplicity, and also because it can resolve the phase ambiguity problem in the carrier tracking system for coherently detecting multiple phase signals [25]. Thus noncoherent HPM can be a realistic choice for some applications.

In this chapter, we first present the noncoherent HPM system structure. The demodulation process is based on noncoherent square law detection of HPM signal frequency components and differentially coherent demodulation of HPM signal phase

components. Since the receiver is implemented in two stages, the error probability can be developed by analyzing the performance of both stages. Bit error performance in AWGN and frequency selective fading channels are demonstrated. Although there are modifications in the transmitter and receiver models, most of the conclusions drawn from the performance of coherent HPM are still valid for noncoherent HPM. This is especially true in AWGN channels. Moreover, in fading channels many improvements can still be achieved by employing channel coding.

In the following sections, the transmitter and receiver models for a noncoherent system are presented in section 3.2. Based on the two-stage receiver structure, the bit error probability of HPM is derived in section 3.3. Assuming AWGN channel model, the system performances are analyzed and compared with other relevant schemes in section 3.4. In section 3.5, the uncoded HPM is applied to frequency selective Rayleigh fading (FSRF) channels. Finally the conclusions are made in section 3.6.

3.2 System Model

3.2.1 Transmitter Model and Bandwidth Efficiency

The uniqueness of noncoherent HPM transmitter resides in the modulation unit for HPM phase signals. A fraction of incoming bit stream is first differentially encoded in the encoder preceding the modulator. Consequently the information is contained in the phase difference between the two consecutive signaling intervals. For this purpose, we assume that the channel parameters remain constant over at least two successive signaling intervals so that differential demodulation can be employed at the receiver. But note that every information-bearing phase may be carried by a different subcarrier since there are frequency transitions at the end of every symbol duration.

The information-bearing phase of differential HPM signals in the k-th signaling interval can be represented as

$$\theta^{(k)} = \theta^{(k-1)} + \theta_j \quad \text{modulo } 2\pi \tag{3.1}$$

where

$$\theta_j = 2\pi j/M_p \quad j = 0, 1, \ldots, M_p - 1$$

is the phase difference between the two consecutive signaling intervals and is determined by a certain k_p bit in an incoming symbol. $\theta^{(k-1)}$ is the accumulated phase value for the previous signaling interval. The transmitted signal can still be expressed by (2.6).

The diagram of HPM transmitter is shown in Figure 3.1. The differential encoder can be realized by a simple logic circuit.

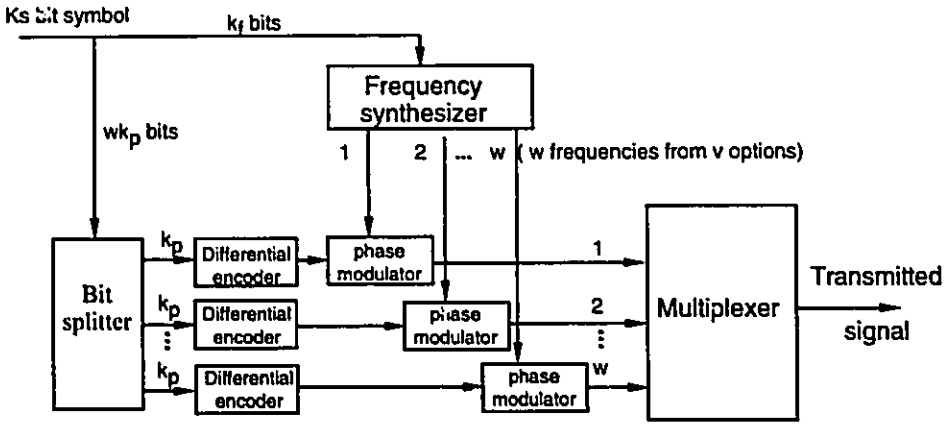

Figure 3.1: Transmitter model of HPM with differential encoding.

In noncoherent detection, the minimum frequency separation can be $1/T_s$ regardless of the number of phases. We obtain the bandwidth efficiency based on the minimum frequency separation as

$$\eta = \frac{k_s}{v} = \frac{k_f + wk_p}{v} \tag{3.2}$$

3.2.2 Receiver Model

HPM is a multi-frequency and multi-phase modulation technique. The signals in one polyphase subset are orthogonal to others. This property reminds us that the nonco-

herent detection can be accomplished in two-stages. First the transmitted frequencies are determined. This is the noncoherent PFSK detection part. And then the phases contained in the detected subcarriers are estimated and differentially decoded. This corresponds to the DPSK part.

For demodulating the multi-frequency signals without the knowledge of phase information, the square law detection is a good choice. At the first stage, a bank of matched filters and square-law detectors constitute the permutation FSK detector in which each frequency tone in the present symbol can be estimated. The signals can be seen as passing through v independent paths and the v matched filters are matched to each of the subcarrier frequency. At the front end, w of the paths contain signals plus noises and other paths contain only the noises. After the signals pass through the square law detectors, the comparisons are made at the decision unit. Due to large size of the signal set, we adopt simple configuration. The largest w outputs are selected and the corresponding codeword is identified. Since only part of codewords are used in binary systems, some redundancies are introduced. If the detected codeword is not in the signaling set, then the closest valid codeword is selected. In this respect, this structure can be considered as a hard decision decoder. Nevertheless, since more than half of the codes in complete code set are used, there is no big change in error correcting capability. Consequently only a slight improvement is expected compared with the system employing the complete codewords. The outcome from frequency detector is sent to the frequency synthesizer for generating the frequency reference. The phase demodulation requires this information. But the PFSK part can operate independently.

The treatment of demodulating the phase modulated signals requires a carrier reference. In DPSK, this reference is provided by the delayed version of present signals. For HPM signals, we can employ differentially coherent detection by extracting the carrier reference from the last stage. The second stage has a set of differential PSK detectors in which the phase difference between the present and previous symbol is

estimated. The frequency estimates are obtained by the synthesizer generated by the output from the PFSK detector. Since the processing duration for the PFSK detector to perform the integration is one symbol interval, we need to add a T_s delay to the signals fed into the DPSK part. The outputs from the DPSK detectors determine another part of the symbol. At the bit combiner, the bits coming from the outputs of the two stages form the complete symbol. The receiver structure for noncoherent HPM is illustrated in Figure 3.2. The one symbol delay is compensated before performing the bit combining for the detected bit stream by introducing another one-symbol delay following the PFSK detector.

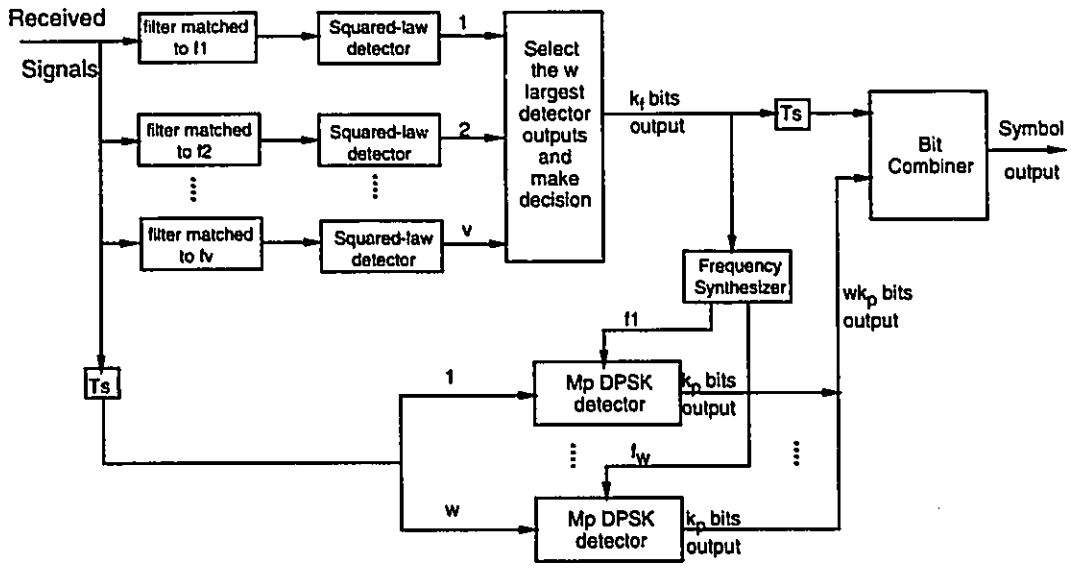

Figure 3.2: Receiver structure for noncoherent HPM.

Figure 3.3 gives the block diagram of matched filter FSK detector which is matched to frequency f_r, $r = 1, \ldots, v$. Each frequency detector is realized by a pair of correlators, followed by the integrate and dump filter to remove the dependence on the phase. And one possible block diagram of MDPSK detector is shown in Figure 3.4. The carrier references used for correlation come from the frequency detection stage.

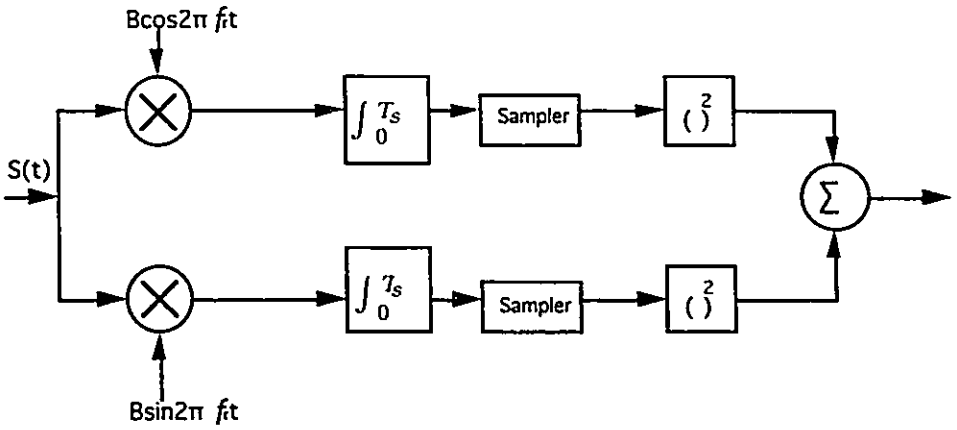

Figure 3.3: Matched filter square-law FSK receiver.

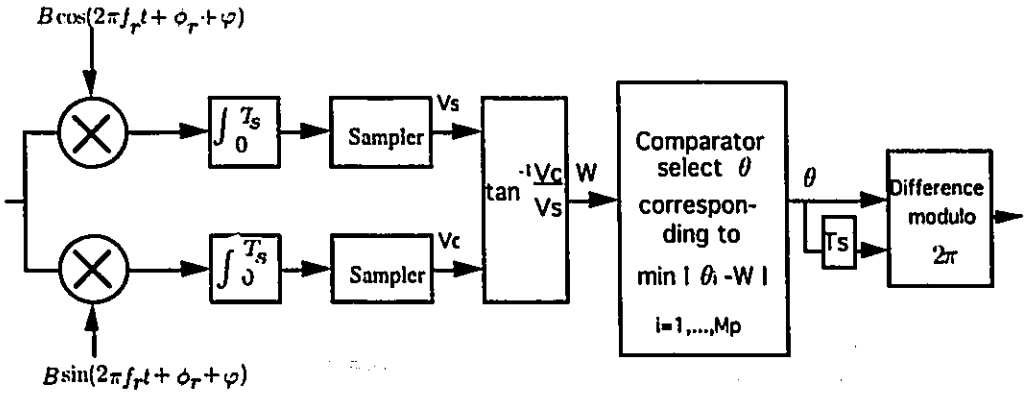

Figure 3.4: MDPSK part of an HPM receiver.

We introduce the notation V_s and V_c to represent the output values of matched filter from the in-phase and quadrature channel respectively. The detected value W is compared with all the possible phases θ_i $(i = 1, \ldots, M_p)$ in the comparator. The phase closest to the decision variable is selected and differential decoding is performed. In the final stage, the differential decoding is conducted to give the actual information.

3.3 Bit Error Probability

The receiver structure of noncoherent HPM consists of two stages, one permutation FSK part and one differential PSK part. The PFSK demodulator can operate without the knowledge about the phases, whereas the outputs of PFSK demodulator can be used to act as the carrier references for the differential demodulation in the next stage. Hence the erroneous decision made in the first stage has effects on the detection of the phase encoded signals since a wrong carrier estimation is provided. On the other hand, if a correct carrier reference is generated, an error can still be committed in the process of differential phase detection. From the above analysis, we find that the bit error probability of noncoherent HPM scheme is influenced by both the two stages and we need to analyze them separately.

First, the contribution of PFSK demodulator to the bit error probability P_{b1} is proportional to the value k_f. If an erroneous detection occurs in this stage (with the probability P_{PFSK}), according to the analysis in section 2.4, approximately half of the k_f bits in the k_s bits symbol would be in error. Therefore we obtain

$$P_{b1} = \frac{k_f}{2k_s} P_{PFSK} \tag{3.3}$$

Another contribution of the error bits comes from the DPSK part P_{b2}. The second stage is composed of w DPSK demodulators and each of them operates independently since we assume that the v subchannels are independent. In the first case, the carrier references provided by the PFSK stage are supposed to be correct. We suppose that the detection error probability in each of these DPSK demodulators is given

by $P_e(M_p)$. If Gray coding is employed for symbol to signal mapping, the bit error probability from one of these DPSK demodulators is well approximated by $P_e(M_p)/k_s$. Since w independent DPSK receivers exist, their overall effect has to be considered. It is apparent that the bit error probability for the whole DPSK part if given the correct frequency carriers is expressed as

$$P'_{b2} = \frac{(1-P_{PFSK})}{k_s}\left[P_e(1-P_e)^{w-1}C_w^1 + 2P_e^2(1-P_e)^{w-2}C_w^2 + \ldots + wP_e^w\right]$$
$$= \frac{1}{k_s}(1-P_{PFSK})\sum_{j=1}^{w} jP_e^j(1-P_e)^{w-j}\begin{pmatrix} w \\ j \end{pmatrix} \quad (3.4)$$

In another case, the frequency signals are incorrectly determined, hence one or more DPSK demodulators is provided with an incorrect carrier reference. The probability that the differentially detected bits are incorrectly detected is 1/2. Besides, the differentially decoded bits in the next signalling interval will also be affected since the present detected phase is needed in this detection. We attribute this to the requirement of two consecutive correct phase signals in the differential detection process. Therefore, the decoded bits in the next symbol duration also have the bit error probability 1/2.

As for the number of incorrectly detected frequency carriers, it ranges from 1 to w if an error occurs in the PFSK stage. We define the probability of having only i $(i = 1, \ldots, w)$ incorrectly detected frequency carriers as $P^{(i)}$. While its relationship to P_{PFSK} can be specified as

$$P_{PFSK} = \sum_{i=1}^{w} P^{(i)}$$

In fact, $P^{(1)}$ is the probability that at least one of the $(v-w)$ noise samples exceeds the value of the smallest w signal plus noise samples but none exceeds the second smallest value. While $P^{(w)}$ is the probability that at least w of the noise samples exceed the value of the largest w signal plus noise samples. To simplify the analysis, in this respect, we neglect the effect of redundancy introduced by the incomplete codes. The actual error performance is slightly better than the analysis.

After some substitutions, we obtain that the contribution from the DPSK part to the bit error probability is expressed by

$$P_{b2} = \frac{1}{k_s}\left[\sum_{i=1}^{w} iP^{(i)}k_p + (1 - P_{PFSK})\sum_{j=1}^{w} jP_e^j(1-P_e)^{w-j}\begin{pmatrix} w \\ j \end{pmatrix}\right] \tag{3.5}$$

However usually, especially for high signal to noise ratios, $P^{(1)}$ has the predominant effect in P_{PFSK}, i.e. the errors occur mainly due to a binary decision error. Therefore rather than deriving $P^{(i)}$, we approximate the first term in the square bracket in equation (3.5) by

$$\sum_{i=1}^{w} ik_pP^{(i)} \simeq k_pP_{PFSK}$$

For the same reason, it rarely happens that more than one of the w independent DPSK demodulators incorrectly detect the phase signals simultaneously. We can observe this by checking the second component ($j = 1$) in the second term in the square bracket in (3.5), which is $2P_e^2(1-P_e)^{w-2}\begin{pmatrix} w \\ 2 \end{pmatrix}$ and is negligible compared to the first component ($j = 1$). Thus the second term in the bracket in (3.5) is dominated by the error probability that only one DPSK detector makes an erroneous decision and it is given by $w(1 - P_{PFSK})P_e(1-P_e)^{w-1}$.

In summary, the expression (3.5) can be well approximated as

$$P_{b2} \simeq \frac{1}{k_s}\left(k_pP_{PFSK} + w(1 - P_{PFSK})P_e(1-P_e)^{w-1}\right) \tag{3.6}$$

The overall probability of bit error of noncoherent HPM is simplified as

$$P_b = P_{b1} + P_{b2} \simeq \frac{1}{k_s}\left(\frac{k_f}{2}P_{PFSK} + k_pP_{PFSK} + w(1 - P_{PFSK})P_e(1-P_e)^{w-1}\right) \tag{3.7}$$

In JFPM, the first stage is actually a M-ary FSK receiver. The orthogonality between signal waveforms simplifies the evaluation for P_{b1} and we can follow the same derivation method used in the case of M-ary FSK. Expression (3.7) can be modified as

$$P_b \simeq \frac{1}{k_s}\left(\frac{2^{k_f-1}}{2^{k_f}-1}k_fP_{MFSK} + k_pP_{MFSK} + P_e(1 - P_{MFSK})\right) \tag{3.8}$$

where P_{MFSK} is the error probability of noncoherent M-ary FSK scheme.

3.4 System Performance over an AWGN channel

In this section, we formulate both the symbol and bit error probability expressions for noncoherent HPM over AWGN channels. The performance is compared with some conventional modulation schemes.

3.4.1 Performance Evaluation

According to the receiver structure the probability of symbol error is related to the decision in two stages and it can be expressed by

$$P_s(v, w, M_p) = P_{PFSK} + (1 - P_{PFSK}) P_{DPSK|PFSK} \tag{3.9}$$

where P_{PFSK} is the error probability for PFSK part and $P_{DPSK|PFSK}$ is the error probability of DPSK part conditioned on the correct detection in the first stage.

The two stages can be treated separately. The first part is actually a noncoherent PFSK receiver and the error probability of PFSK detection [9] is given by

$$P_{PFSK}(v, w) = w \sum_{r=1}^{v-w} (-1)^{r+1} \binom{v-w}{r} \int_0^\infty [Q(\sqrt{2\gamma_c}, s)]^{w-1} \\ s I_0(s\sqrt{2\gamma_c}) \exp\left[-\frac{(r+1)s^2 + 2\gamma_c}{2}\right] ds \tag{3.10}$$

where $\gamma_c = \gamma_b k_s / w$ is the received SNR per subcarrier and $I_0()$ is the zero-order modified Bessel function. The function $Q(\alpha, \beta)$ is defined as

$$Q(\alpha, \beta) = \int_\beta^\infty t e^{-(t^2+\alpha^2)/2} I_0(\alpha t) dt$$

This expression involves multiple integrations and special functions. There is no closed form for the above expression when $M_p > 2$. A better alternative for evaluation is using an upper bound method. When the signal to noise density ratio is high, the asymptotic bound for the above expression [9] is

$$P_{PFSK}(v, w) \leq \frac{w}{v-w+1} \sum_{r=2}^{v-w+1} (-1)^r \binom{v-w+1}{r} \exp\left[-\gamma_c \left(1 - \frac{1}{r}\right)\right] \tag{3.11}$$

The equality holds when $w = 1$ and it is the well-known error probability expression for noncoherent detection of M-ary FSK.

There are w identical M_p-DPSK receivers in the second stage. For each M_p-DPSK receiver, the error probability is given [33] by

$$P_e(M_p) = \frac{\sin(\pi/M_p)}{2\pi} \int_{-\pi/2}^{\pi/2} \frac{\exp^{-\gamma_c[1-\cos(\pi/M_p)\cos t]}}{1-\cos(\pi/M_p)\cos t} dt \tag{3.12}$$

Since w receivers operate independently, the error probability for the whole second stage given that a correct decision is made in the first stage yields to be

$$P_{DPSK|PFSK} = 1 - (1 - P_e(M_p))^w \tag{3.13}$$

Putting (3.11) and (3.13) into (3.9), we obtain the symbol error probability for HPM.

To develop the expression of bit error probability, based on the analysis in Section 3.3, we substitute (3.11) and (3.12) into (3.7) and obtain

$$\begin{aligned} P_b = \frac{1}{k_s}\Bigg[\left(\frac{k_f}{2}+k_p\right)\frac{w}{v-w+1}\sum_{r=2}^{v-w+1}(-1)^r\binom{v-w+1}{r}\exp\left[-\gamma_c\left(1-\frac{1}{r}\right)\right]+ \\ w\left(1-\frac{w}{v-w+1}\sum_{r=2}^{v-w+1}(-1)^r\binom{v-w+1}{r}\exp\left[-\gamma_c\left(1-\frac{1}{r}\right)\right]\right) \\ \left(1-\frac{\sin(\pi/M_p)}{2\pi}\int_{-\pi/2}^{\pi/2}\frac{\exp^{-\gamma_c[1-\cos(\pi/M_p)\cos t]}}{1-\cos(\pi/M_p)\cos t}dt\right)^{w-1} \\ \frac{\sin(\pi/M_p)}{2\pi}\int_{-\pi/2}^{\pi/2}\frac{\exp^{-\gamma_c[1-\cos(\pi/M_p)\cos t]}}{1-\cos(\pi/M_p)\cos t}dt\Bigg] \end{aligned} \tag{3.14}$$

Similarly in the special case of JFPM, the bit error probability is expressed by (3.8). After making some substitutions, it becomes

$$\begin{aligned} P_b = \frac{1}{k_s}\Bigg[\left(\frac{2^{k_f-1}}{2^{k_f}-1}k_f+k_p\right)\frac{1}{v}\sum_{r=2}^{v}(-1)^r\binom{v}{r}\exp\left[-\gamma_c\left(1-\frac{1}{r}\right)\right] \\ \left(1-\frac{1}{v}\sum_{r=2}^{v}(-1)^r\binom{v}{r}\exp\left[-\gamma_c\left(1-\frac{1}{r}\right)\right]\right) \\ \frac{\sin(\pi/M_p)}{2\pi}\int_{-\pi/2}^{\pi/2}\frac{\exp^{-\gamma_c[1-\cos(\pi/M_p)\cos t]}}{1-\cos(\pi/M_p)\cos t}dt\Bigg] \end{aligned} \tag{3.15}$$

3.4.2 Numerical Results and Discussions

The bit error probability of HPM is given by (3.14) or (3.15), and its bandwidth efficiency is characterized by (3.2). The performance of a variety of HPM and conventional MDPSK systems, based on the bandwidth efficiency η versus γ_b to achieve 10^{-5} BER, are tabulated in Table 3.1 and Table 3.2. In each entry, the above value relates to the performance of a HPM which employs nonbinary transmission and can make full use of the HPM efficiency, while the entry below corresponds to the result of a HPM employing binary transmission. Thus there is a discrepancy between the theoretical system achieving the maximum efficiency and a practical system.

The BER performances of coherent and noncoherent HPM(5,2,M_p) are compared in Figure 3.5. The performance gap between coherent and noncoherent system becomes larger as γ_b increases. But the gap between noncoherent HPM(5,2,2) and (5,2,4) are smaller than the gap between their coherent counterparts.

The BER performance of HPM(8,4,M_p) when M_p=2,4 and 8 are plotted in Figure 3.6, where PFSK refers to permutation FSK. HPM(8,4,2) and (8,4,4) provide both power and bandwidth efficiency over PFSK(8,4), whereas HPM(8,4,8) has large η at the expense of γ_b. It is also true that the BER curves of PFSK (including MFSK) are steeper than those of MDPSK schemes. Since the bit error rate of HPM relates to both PFSK part and DPSK part. Thus some crossovers of the comparable schemes are observed from the figure, such as 8FSK and HPM(8,4,4), 2DPSK and HPM(8,4,2). In certain conditions, one part may have dominant effect over the other and the overall bit error rate is limited by either PFSK-part or DPSK-part (whichever one can provide the higher error rate). This explains the occurrence of the crossover between the curves of PFSK(8,4) and HPM(8,4,8). Due to the same reason, as shown in Figure 3.5, the curves of noncoherent HPM(5,2,2) and (5,2,4) are fairly close and they intersect in high γ_b region, while both of them are far away from the curve of (5,2,8).

As in the case of coherent HPM, the comparisons of HPM and the conventional

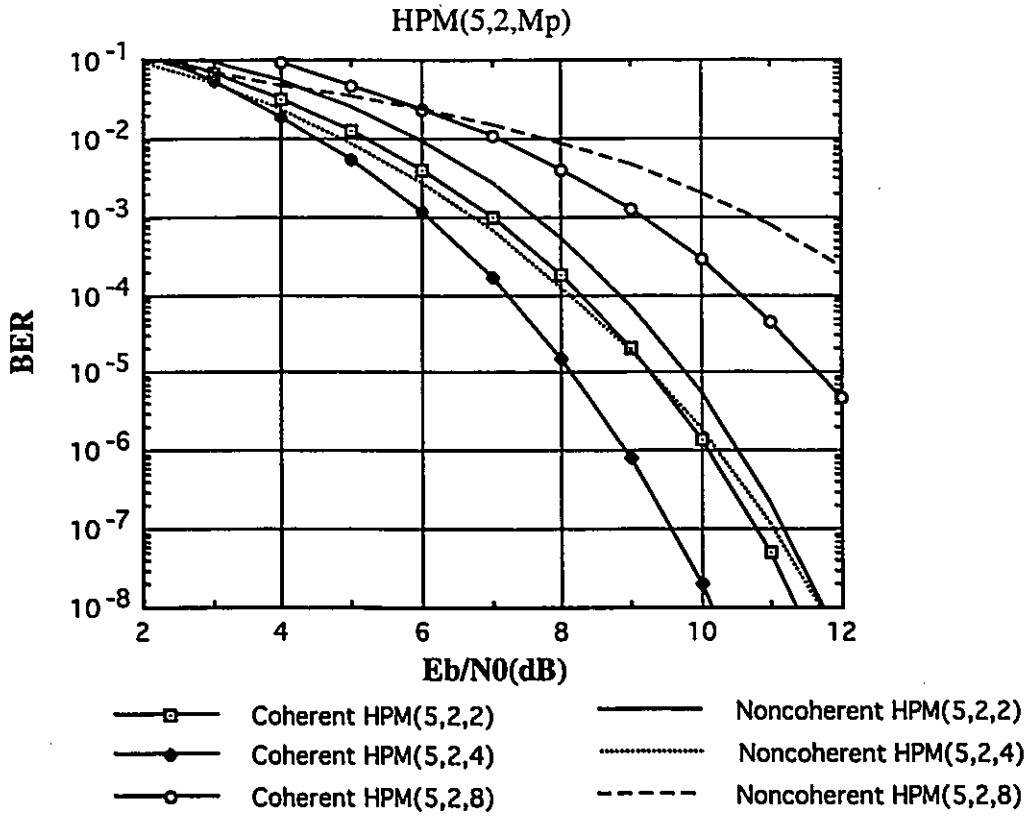

Figure 3.5: Bit error probability of coherent and noncoherent HPM(5,2,M_p) with M_p=2,4,8 in AWGN channels.

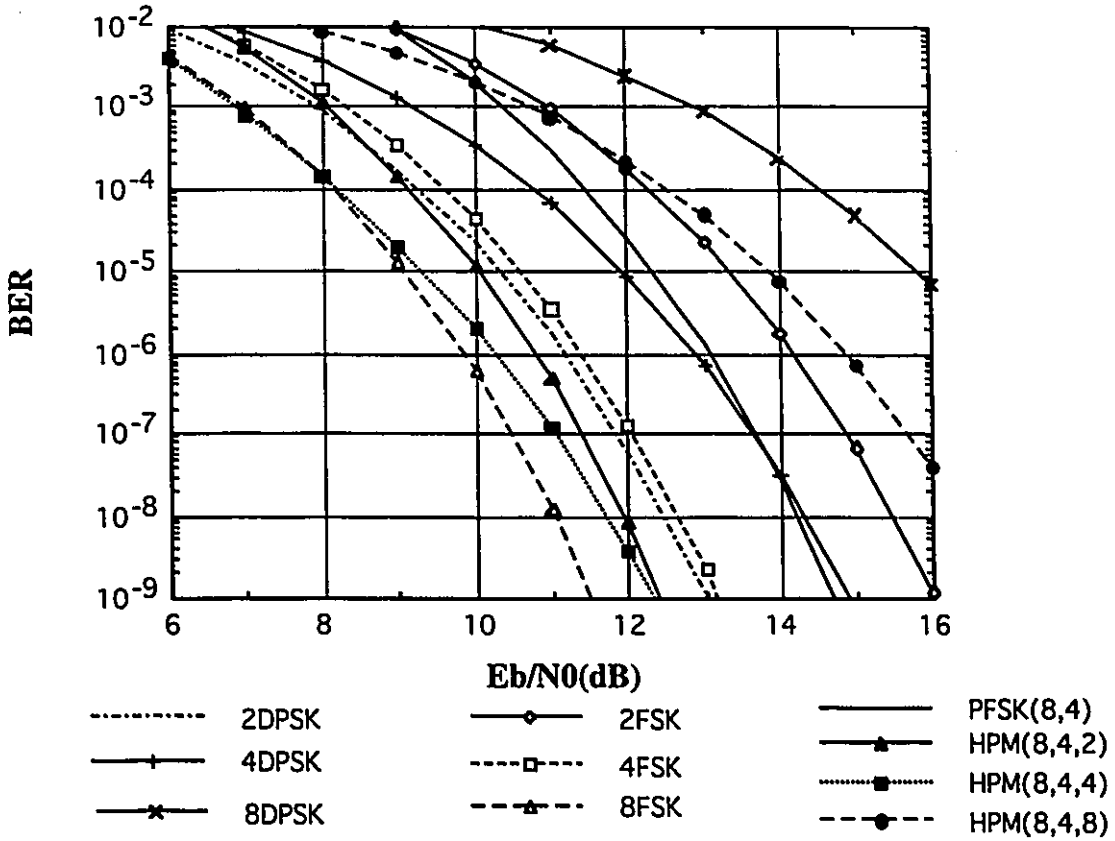

Figure 3.6: Bit error probability of noncoherent HPM(8,4,M_p) with M_p=2,4,8 and PFSK(8,4), M-ary FSK and MDPSK in AWGN channels.

Table 3.1: Performance comparisons of various HPM alphabets under different parameters(v, w, M_p). The entries in the table are the energy per bit to noise power density ratio $\gamma_b(dB)$ required to achieve bit error rate 10^{-5} in AWGN channels versus bandwidth efficiency R_b/W(bps/Hz).

$(v,w) \setminus M_p$	1 (PFSK)	2	4	8
(1,1)(MDPSK)	-	10.34/1.0	11.95/2.0	15.82/3.0
(2,1)	13.35/0.5	10.34/1.0	10.01/1.5	14.43/2.0
(4,1)	10.60/0.5	8.90/0.75	8.65/1.0	13.35/1.25
(8,1)	9.09/0.375	7.90/0.5	7.61/0.625	12.47/0.75
(16,1)	8.08/0.25	7.16/0.313	6.82/0.375	11.72/0.438
(4,2)	12.50/0.646	10.01/1.146	9.58/1.646	14.09/2.146
	13.62/0.500	10.61/1.000	10.02/1.500	14.44/2.000
(5,2)	11.56/0.664	9.52/1.064	9.08/1.464	13.70/1.864
	12.00/0.600	9.79/1.000	9.29/1.400	13.87/1.800
(6,2)	10.96/0.651	9.17/0.984	8.72/1.318	13.40/1.651
	12.11/0.500	9.89/0.833	9.30/1.167	13.87/1.500
(6,3)	12.33/0.72	9.99/1.22	9.38/1.72	13.93/2.22
	12.66/0.667	10.18/1.167	9.53/1.667	14.05/2.167
(7,2)	10.53/0.627	8.90/0.913	8.44/1.199	13.17/1.485
	10.94/0.571	9.18/0.857	8.67/1.143	13.36/1.429
(7,3)	11.68/0.733	9.64/1.161	9.03/1.590	13.65/2.018
	11.79/0.714	9.70/1.143	9.08/1.571	13.69/2.000
(8,2)	10.20/0.601	8.69/0.851	8.23/1.101	12.98/1.351
	11.00/0.500	9.24/0.750	8.68/1.000	13.36/1.250
(8,3)	11.22/0.726	9.37/1.101	8.76/1.476	13.42/1.851
	11.87/0.625	9.78/1.000	9.09/1.375	13.69/1.750
(8,4)	12.26/0.766	10.00/1.266	9.27/1.766	13.83/2.266
	12.35/0.750	10.06/1.250	9.31/1.750	13.87/2.250

Table 3.2: The continuation of Table 3.1

$(v, w) \setminus M_p$	1 (PFSK)	2	4	8
(10,2)	9.72/0.55	8.37/0.749	7.89/0.949	12.68/1.149
	10.12/0.500	8.67/0.700	8.14/0.900	12.89/1.100
(10,3)	10.58/0.691	8.98/0.991	8.36/1.291	13.07/1.971
	11.19/0.600	9.39/0.900	8.70/1.200	13.36/1.500
(10,4)	11.39/0.77	9.52/1.171	8.79/1.571	13.43/1.971
	11.81/0.700	9.78/1.100	9.01/1.500	13.60/1.900
(10,5)	12.23/0.798	10.03/1.298	9.20/1.798	13.76/2.298
	12.80/0.700	10.36/1.200	9.46/1.700	13.97/2.200
(16,2)	8.90/0.432	7.80/0.557	7.30/0.682	12.12/0.807
	9.51/0.375	8.27/0.500	7.70/0.625	12.47/0.750
(16,3)	9.56/0.571	8.30/0.758	7.68/0.946	12.44/1.133
	9.62/0.562	8.35/0.750	7.72/0.938	12.47/1.125
(16,4)	10.13/0.677	8.73/0.927	8.01/1.177	12.71/1.427
	10.48/0.625	8.97/0.875	8.22/1.125	12.89/1.375
(16,5)	10.67/0.756	9.11/1.068	8.31/1.381	12.97/1.693
	10.70/0.75	9.13/1.063	8.33/1.375	12.98/1.688

schemes are illustrated in Figure 3.7. The curve of the capacity limit is included as well. Similarly, HPM with $M_p = 4$ provides the best efficiency. In HPM, as mentioned above, either PFSK-part or DPSK-part may have dominant effect in some cases. When M_p takes on big values ($M_p \geq 8$), the error rate performance of HPM is mainly determined by its DPSK part. Therefore its performance resembles that of conventional DPSK system and it provides markable spectral efficiency as M_p increases. On the other hand, when M_p takes on small values, let's say $M_p = 2$, the performance of HPM resembles that of PFSK and it provides more power efficiency as v increases. In this aspect, there is a comprise between the two parts when $M_p = 4$. The comparisons of HPM with different M_p values are depicted in Figure 3.8. The points correspond to HPM schemes with $M_p = 4$ appear to be quite close to the capacity limit.

The advantage of HPM is notable. HPM(16,5,4) has almost the same power efficiency with its MFSK counterpart 16FSK (8.33 dB versus 8.08 dB), but it provides larger η (1.375 versus 0.25). HPM(8,4,4) has comparable η with its MDPSK counterpart 4DPSK (1.75 versus 2.0), but it requires much less power (9.31dB versus 11.95 dB), which yields a decrease of around 2.6 dB. The scheme achieving the minimum γ_b is JFPM. While a HPM with $w > 1$ falls into the region which lies in right to the region of JFPM in the figure. Thus slightly more power is required to tradeoff for spectral efficiency. This relationship is quite similar to that of permutation FSK and M-ary FSK. Hence based on the same available bandwidth, power efficiency is obtained by reducing the number of active tones w, and spectral efficiency is obtained by increasing M_p and w to proper values.

3.5 Noncoherent HPM over Frequency Selective Fading Channels

In this section, we consider the case of frequency selective fading channel defined in section 2.6.1. If noncoherent HPM is directly applied to this channel model, we

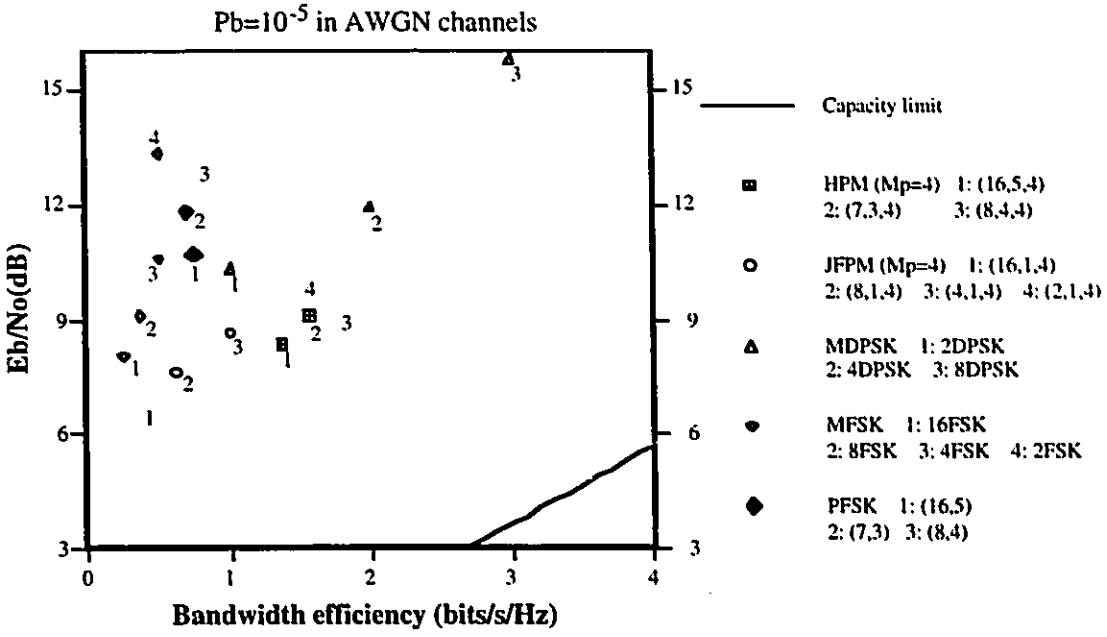

Figure 3.7: Performance(γ_b versus η) comparison of noncoherent HPM with various noncoherent detection modulation schemes under AWGN channels with bit error probability of 10^{-5}.

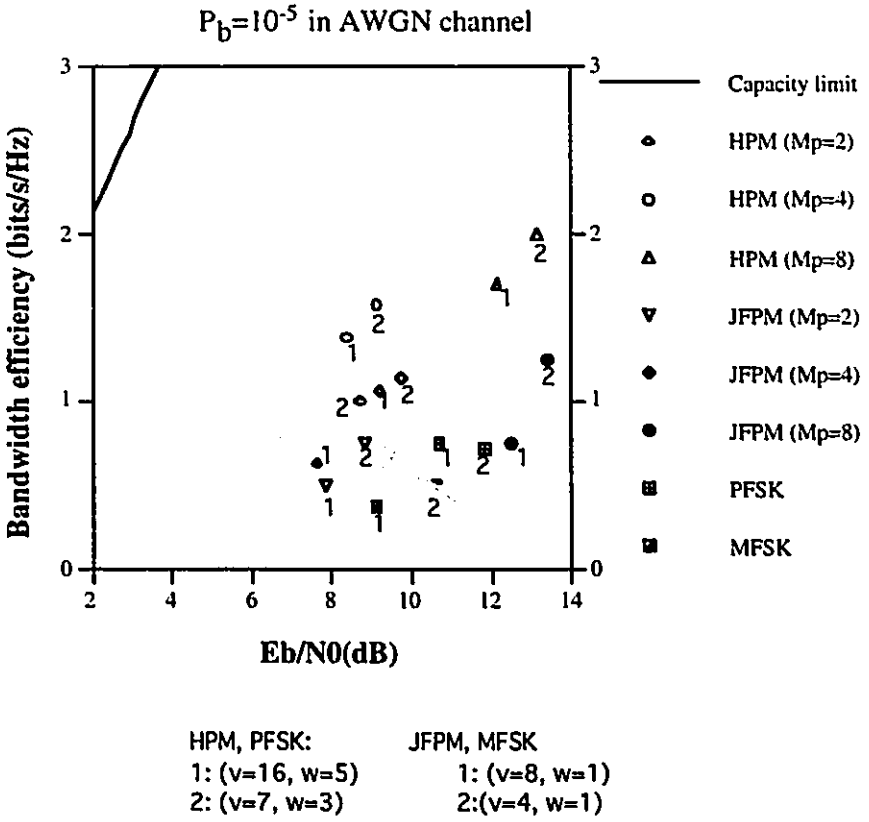

Figure 3.8: Performances(γ_b versus η) of noncoherent HPM, PFSK and JFPM in AWGN channels with bit error probability of 10^{-5}.

only need to reevaluate the error performance of PFSK and DPSK receiver in fading channel conditions.

The error probability of square law detection of permutation FSK modulation is developed in [10] and it yields to be

$$P_{PFSK}(v,w) = 1 - \frac{w}{1+\bar{\gamma}_c}\beta\left(\frac{w}{1+\bar{\gamma}_c}, v-w+1\right) \tag{3.16}$$

where $\bar{\gamma}_c = \bar{\gamma}_b k_s/w$ and $\beta(x,y)$ is beta function which is defined as

$$\beta(x,y) = \int_0^1 t^{x-1}(1-t)^{y-1}dt$$

For DPSK part, each of the DPSK receivers detects the multiple phase signals transmitted in a single Rayleigh fading subchannel. In this condition, the error probability for multiple phase detection [25] is

$$P_e(M_p) = \frac{M_p-1}{M_p} - \frac{\mu\sin(\pi/M_p)}{\pi\sqrt{1-\mu^2\cos^2(\pi/M_p)}}\cot^{-1}\frac{-\mu\cos(\pi/M_p)}{\sqrt{1-\mu^2\cos^2(\pi/M_p)}} \tag{3.17}$$

where $\mu = \bar{\gamma}_c/(1+\bar{\gamma}_c)$.

For HPM system, the overall bit error probability is obtained by putting (3.16) and (3.17) into (3.7)

$$\begin{aligned} P_b = \frac{1}{k_s}\Bigg[&\left(\frac{k_f}{2}+k_p\right)\left(1-\frac{w}{1+\bar{\gamma}_c}\beta\left(\frac{w}{1+\bar{\gamma}_c}, v-w+1\right)\right)+ \\ &w\left(\frac{w}{1+\bar{\gamma}_c}\beta\left(\frac{w}{1+\bar{\gamma}_c}, v-w+1\right)\right) \\ &\left(\frac{1}{M_p}+\frac{\mu\sin(\pi/M_p)}{\pi\sqrt{1-\mu^2\cos^2(\pi/M_p)}}\cot^{-1}\frac{-\mu\cos(\pi/M_p)}{\sqrt{1-\mu^2\cos^2(\pi/M_p)}}\right)^{w-1} \\ &\left(\frac{M_p-1}{M_p}-\frac{\mu\sin(\pi/M_p)}{\pi\sqrt{1-\mu^2\cos^2(\pi/M_p)}}\cot^{-1}\frac{-\mu\cos(\pi/M_p)}{\sqrt{1-\mu^2\cos^2(\pi/M_p)}}\right)\Bigg] \end{aligned} \tag{3.18}$$

The BER performances of HPM(2,1,4) and (7,3,4) are shown in Figure 3.9. Unlike the case in AWGN channels, conventional 4DPSK offers both the power and bandwidth efficiency and seems to be the best option. But HPM scheme still outperforms permutation FSK scheme.

The performance of HPM, permutation FSK and DPSK scheme are also tabulated in Table 3.3. The table indicates that the power efficiency decreases substantially as w increases. For instance, HPM(16,2,4) and (16,5,4) require 38.56 dB and 41.24 dB respectively to meet the error rate demand in fading channels. Whereas they require 7.70 dB and 8.33 dB respectively in AWGN channels. More signal energy in transmission is needed to combat fading. In addition, HPM with $M_p = 8$ has comparable power efficiency compared to HPM with $M_p = 4$.

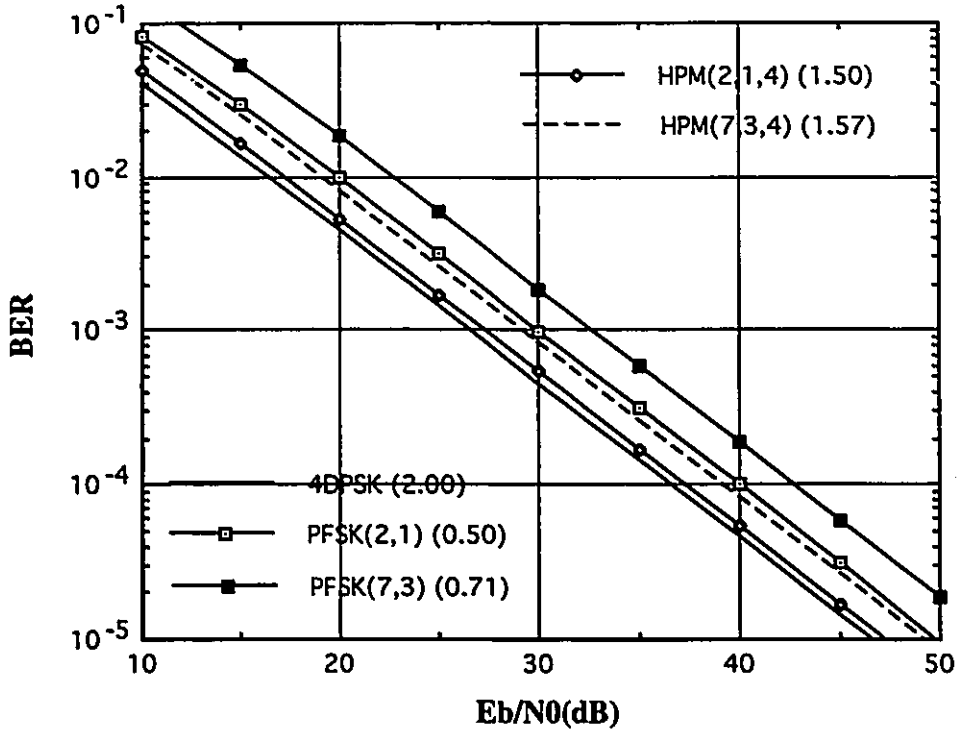

Figure 3.9: Bit error probability of noncoherent HPM(2,1,4) and (7,3,4) over frequency selective fading channels.

$(v,w) \setminus M_p$	1 (PFSK)	2	4	8
(1,1)(MDPSK)	-	36.97	36.56	38.73
(2,1)	40.00	37.95	37.27	38.26
(4,1)	37.84	37.20	36.92	37.65
(8,1)	36.90	36.67	36.54	37.18
(16,1)	36.34	36.31	36.30	36.84
(4,2)	41.73	39.38	38.43	38.99
(5,2)	40.84	39.08	38.25	38.67
(6,2)	41.40	39.57	38.69	38.99
(6,3)	43.11	40.39	39.13	39.25
(7,2)	40.56	39.09	38.32	38.59
(7,3)	42.71	40.37	39.17	39.20
(8,2)	40.85	39.36	38.58	38.78
(8,3)	43.11	40.74	39.50	39.45
(8,4)	44.41	41.48	39.97	39.75
(10,2)	40.33	39.11	38.39	38.53
(10,3)	42.86	40.79	39.61	39.45
(10,4)	44.44	41.80	40.35	39.99
(10,5)	46.09	42.69	40.92	40.45
(16,2)	40.29	39.18	38.56	38.58
(16,3)	41.94	40.42	39.44	39.24
(16,4)	43.89	41.89	40.62	40.15
(16,5)	44.91	42.67	41.24	40.65

Table 3.3: Performance comparisons of various HPM alphabets under different parameters(v, w, M_p). The entries in the table are energy per bit to noise power density ratio $\gamma_b(dB)$ required to achieve bit error rate 10^{-4} in frequency selective Rayleigh fading channels.

3.6 Conclusion

For the purpose of giving a practical system, we presented a noncoherent HPM system model. Noncoherent FSK detection and differential PSK detection are employed. The HPM signals are detected in a two-stage manner.

The expression of bit error probability has been developed. The performance has been shown by BER versus energy per bit to noise power density ratio.

In the plot with power efficiency as the ordinate and bandwidth efficiency as the abscissa, it can be concluded that HPM scheme lies in a region closer to the channel capacity than other schemes considered, including JFPM, MDPSK, M-ary FSK and permutation FSK. This indicates that HPM has both power and bandwidth efficiency in AWGN channel. Besides, HPM can provide a huge selection of alphabets to achieve a comparable performance. This is another aspect exhibiting the flexibility of HPM scheme.

Chapter 4

Coded Noncoherent HPM Systems

4.1 Introduction

In permutation modulation, the codewords corresponding to different input sequences can be chosen from all the possible permuting arrangements. In this respect, permutation FSK outperforms conventional M-ary FSK in both the bandwidth and power efficiency. This is true not only in AWGN channels but also in frequency selective fading channels. HPM possesses the properties of permutation modulation as well and embodies both its advantages and disadvantages. In fading channels, HPM does not perform as well as conventional multiple phase modulation. The reason is that in the signaling set, some symbols have as many as $w-1$ component signals in common. In other words, one codeword differs from another codeword in only one position so that the pairwise error probability is greatly reduced. For instance in HPM(4,2,2), out of total 16 symbols, 7 of them differ only in 1 component signal. The bandwidth efficiency of HPM is based on the fact that the codewords are assigned as close as possible to achieve maximum number of codewords. But this reduces the power gain and causes inefficiency in fading channel conditions.

We have mentioned that system performance is quite related with channel characteristics. The techniques developed for communications over AWGN channels may

not be effective in fading conditions. This leads us to search for a modified version of HPM.

Improvements can be achieved by selecting only a portion of the total possible waveforms. More specifically, in mapping the frequency tones to represent the symbols, we expurgate the complete permutation codes and thus reduce the alphabet size of codewords. By properly performing the expurgating, we are able to obtain a set of codewords with good properties, i.e., large Hamming distance and constant weight w and length v. In HPM(4,2,2), we may only use 2 of the total 6 codewords in performing the mapping from frequency tones to symbols. By employing these codewords to design the waveforms, the distance between waveforms is enlarged and the effective diversity increases in fading channels. Therefore considerable gains can be accomplished at the expense of bandwidth efficiency. In fact, the use of this technique is a kind of modulation scheme employing channel coding, and it can be treated as coded modulation in a sense that coding and modulation techniques are optimally integrated.

One of the problems arising is how to select codes which define the signaling set. The codes used for this purpose must meet the following conditions:

- good distance properties,
- constant weight and length,
- symmetric, i.e., the properties are independent of all the codewords which in turn determines that the symbol error probability is independent of the signal chosen.

Constant weight indicates fixed number of active carriers in any signaling interval, and therefore the signals with equal energy in any carrier, which greatly simplifies the receiver. For the same reason, the property of symmetry is attractive in implementation. Some constant weight block codes may be the candidates. We will also resort to the design theory in mathematics to provide some solutions. A design is a combinatorial structure satisfying certain regular properties. Multi-tone FSK modulation employing the balanced incomplete block design (BIBD) is proposed and studied in

[13]. In fact, BIB design is a subclass of a more general design family: t-designs. In this thesis, we apply the theory of t-designs to the designing of HPM waveforms. Two typical families in t-designs: Steiner and Hadamard codes will be investigated and the performances are compared with the uncoded system. Thus the scheme can be referred to as coded HPM scheme. Note that the term "coded" here does not indicate FEC coding, i.e., the coding process preceding the modulation, it actually means that the selection of modulated signals obeys a rule which can be described by a set of codewords.

In section 4.2, a basic description on t-designs is given. The design of HPM waveforms is specified in section 4.3 and some of the relations among codewords are also reviewed. The system performance over AWGN channels are evaluated in section 4.4 in which the Steiner HPM and Hadamard HPM are analyzed. In the same way, we will study the system performance over FSRF channels in section 4.5. Then we give the simulation results of coded HPM in section 4.6. Finally the conclusion is reached in section 4.7.

4.2 Principles of t-designs

The subject of design theory has grown out of several branches of mathematics and it has close connections with coding theory. Designs, or more precisely t-designs, are combinatorial structures with certain properties. The literature covering this topic include [37]-[44].

A t-design is a collection of b blocks, formed by the arrangement of w elements chosen from v elements, and it is identified by t-(v, w, λ) with $v \geq w \geq t$, where $\lambda > 0$ and it is the total number of blocks containing a certain t-subset of elements in a t-design. In t-designs, only a small fraction of the w combinations out of v are selected so that the total number of blocks in a design $b < \begin{pmatrix} v \\ w \end{pmatrix}$. In addition, the following conditions must be satisfied:

•Each block or codeword contains w elements.

•Each element appears in exactly r blocks.

•Each t-subset of elements appears together in λ blocks.

Let us give a picturesque example. Suppose we want to organize a total of b sport teams. Each team has a constant w male and $v - w$ female members and is engaged in a distinct sport. But the total number of male athletes is limited and every male athlete has to take part in exactly r teams. At the same time, any t-combination of male athletes can be present in the same team in exactly λ teams. The way of forming these b teams basically is the subset of a t-design.

One of the key problems in t-designs is the question of their existence. Therefore the parameters in a design are not independent and must satisfy various arithmetical conditions. An elementary relation among the parameters is:

$$bw = rv \tag{4.1}$$

This equation counts the total number of single element occurrence in two ways. Each block contains w points and the total number of points in the collection of blocks is bw. On the other hand, each of the v points appears r times in the collection. Another relation is given by

$$b = \lambda \binom{v}{t} / \binom{w}{t} \tag{4.2}$$

The famous Hadamard code $H(n,k)$ is a 2-$(n-1, \frac{1}{2}n-1, \frac{1}{4}n-1)$ design. If conventional M-ary FSK can be seen as a sort of coded modulation, the waveform is actually selected according to a 1-$(M,1,1)$ design. Until recently t-designs were known only for $t \leq 5$, but in fact it is shown now that t-designs exist for all t [39].

The designs with $\lambda = 1$ are usually called Steiner systems and represented by $S(t,w,v)$. Hence each t-subset of elements appears together in only one block. This implies that any one of the combinations with t elements can determine a codeword. Steiner design has the definite properties between codewords, which make it easier for analysis. In fact, a t-design can also be called generalized Steiner system. Thus

we use it as a starting point.

Some examples of typical $S(t, w, v)$ systems are listed in Table 4.1. From the block code point of view, the intersecting positions between any two constant weight blocks are at most $t-1$. the minimum Hamming distance of all blocks in the system is $d_{min} = 2(w - t + 1)$. Hence the Hamming distance d between any two codewords is specified as

$$2(w - t + 1) \leq d \leq 2w.$$

4.3 Design of Coded HPM waveforms

When a design acts as a set of codewords for choosing waveforms, the number of k_f-bit symbols can be represented is limited by b and it satisfies

$$k_f = \lfloor \log_2 b \rfloor \tag{4.3}$$

so that only $M_f = 2^{k_f}$ codewords out of b are needed to represent k_f bits of information.

Table 4.1: Some of the Steiner systems

$S(t, w, v)$	k_f	M_f	b	r	$d_{min} = 2(w - t + 1)$
S(1,1,2)	1	2	2	1	2
S(2,3,7)	2	4	7	3	4
S(2,3,9)	3	8	12	4	4
S(2,4,16)	4	16	20	5	6
S(2,5,21)	4	16	21	5	8
S(3,4,8)	3	8	14	7	4
S(3,5,17)	6	64	68	20	6
S(3,6,22)	6	64	77	21	8
S(4,5,11)	6	64	66	30	4
S(5,6,12)	7	128	132	66	4

In this thesis, the designs are applied to selecting the active tones in forming the HPM signals. In this case, we refer to the frequency modulation part as multiple-

tone FSK (MT-FSK) rather than PFSK since the corresponding codewords are no longer a set of permutation codes. In designing the waveforms for MT-FSK signals, we express a t-design in a way with a set of codewords having element 0 or 1. An example of $S(2,3,9)$ is given in Table 4.2. Note this is only one of the ways to realize $S(2,3,9)$. There are other arrangements satisfying the conditions. Usually t-designs can be extracted from codes, and the existing designs can be found in literature.

Table 4.2: $S(2,3,9)$ design and the corresponding waveforms

codeword	waveform
111000000	$\cos\pi f_0 t + \cos\pi f_1 t + \cos\pi f_2 t$
100100100	$\cos\pi f_0 t + \cos\pi f_3 t + \cos\pi f_6 t$
100010001	$\cos\pi f_0 t + \cos\pi f_4 t + \cos f_8 t$
100001010	$\cos\pi f_0 t + \cos\pi f_5 t + \cos\pi f_7 t$
010100001	$\cos\pi f_1 t + \cos\pi f_3 t + \cos f_8 t$
010010010	$\cos\pi f_1 t + \cos\pi f_4 t + \cos\pi f_7 t$
010001100	$\cos\pi f_1 t + \cos\pi f_5 t + \cos\pi f_6 t$
001100010	$\cos\pi f_2 t + \cos\pi f_3 t + \cos\pi f_7 t$
001010100	$\cos\pi f_2 t + \cos\pi f_4 t + \cos\pi f_6 t$
001001001	$\cos\pi f_2 t + \cos\pi f_5 t + \cos f_8 t$
000111000	$\cos\pi f_3 t + \cos\pi f_4 t + \cos\pi f_5 t$
000000111	$\cos\pi f_6 t + \cos\pi f_7 t + \cos f_8 t$

Each codeword corresponds to a waveform and can be used to represent a symbol. Each position in the codeword indicates the corresponding frequency. "1" means that the specific frequency tone is present in the waveform while "0" indicates that the frequency tone is unused. If the first position represents f_0, the second one represents f_1 etc., we obtain the 12 corresponding waveforms given in the table. For binary communications, $M_f = 8$ waveforms are necessary to represent 3 bits symbol. Hence 4 waveforms need to be further eliminated. In this specific example, by eliminating the 4 waveforms containing f_8, we actually make use of only 8 different frequency tones and we rename it as $S(2,3,8)$.

Based on the same rule, each active tone carries a distinct phase determined by

other part of k_s-bit symbol. The obtained HPM waveforms are shown in Table 4.3. We can see that we actually combine MT-FSK with multiple phase modulation and we denote the scheme as HPM(v, w, t, M_p). The bandwidth efficiency of coded HPM can still be expressed by (3.2), but we note that k_f is greatly reduced and is given by (4.3) when employing channel coding.

Table 4.3: Coded HPM(8,3,2,2) waveforms with $M_p = 2$, based on $S(2, 3, 8)$ expurgated from $S(2, 3, 9)$

symbol	codeword	phase	waveform
S_0=0000	11100000	0	$\cos \pi f_0 t + \cos \pi f_1 t + \cos \pi f_2 t$
S_1=0001	11100000	π	$\cos(\pi f_0 t + \pi) + \cos(\pi f_1 t + \pi) + \cos(\pi f_2 t + \pi)$
S_2=0010	10010010	0	$\cos \pi f_0 t + \cos \pi f_3 t + \cos \pi f_6 t$
S_3=0011	10010010	π	$\cos(\pi f_0 t + \pi) + \cos(\pi f_3 t + \pi) + \cos(\pi f_6 t + \pi)$
$S_4 = 0100$	10000101	0	$\cos \pi f_0 t + \cos \pi f_5 t + \cos \pi f_7 t$
$S_5 = 0101$	10000101	π	$\cos(\pi f_0 t + \pi) + \cos(\pi f_5 t + \pi) + \cos(\pi f_7 t + \pi)$
$S_6 = 0110$	01001001	0	$\cos \pi f_1 t + \cos \pi f_4 t + \cos \pi f_7 t$
$S_7 = 0011$	01001001	π	$\cos(\pi f_1 t + \pi) + \cos(\pi f_4 t + \pi) + \cos(\pi f_7 t + \pi)$
$S_8 = 1000$	01000110	0	$\cos \pi f_1 t + \cos \pi f_5 t + \cos \pi f_6 t$
$S_9 = 1001$	01000110	π	$\cos(\pi f_1 t + \pi) + \cos(\pi f_5 t + \pi) + \cos(\pi f_6 t + \pi)$
$S_{10} = 1010$	00110001	0	$\cos \pi f_2 t + \cos \pi f_3 t + \cos \pi f_7 t$
$S_{11} = 1011$	00110001	π	$\cos(\pi f_2 t + \pi) + \cos(\pi f_3 t + \pi) + \cos(\pi f_7 t + \pi)$
$S_{12} = 1100$	00101010	0	$\cos \pi f_2 t + \cos \pi f_4 t + \cos \pi f_6 t$
$S_{13} = 1101$	00101010	π	$\cos(\pi f_2 t + \pi) + \cos(\pi f_4 t + \pi) + \cos(\pi f_6 t + \pi)$
$S_{14} = 1110$	00011100	0	$\cos \pi f_3 t + \cos \pi f_4 t + \cos \pi f_5 t$
$S_{15} = 1111$	00011100	π	$\cos(\pi f_3 t + \pi) + \cos(\pi f_4 t + \pi) + \cos(\pi f_5 t + \pi)$

In general cases, we have to use all of the v tones even though $(b - M_f)$ extra waveforms may be eliminated to convey $\log_2 M_f$ bits of information. For the efficiency purpose, it is desirable to choose a t-design with b close to M_f so that most of the available codewords can be used. For instance, both $S(2, 3, 15)$ and $S(2, 3, 19)$ can accommodate 32 codewords to represent 5 bits information. But their b is 35 and 57 respectively. Obviously the system based on former alphabet using only 15 tones will give rise to better bandwidth efficiency.

In order to evaluate the error performance of HPM employing t-designs, we must

first determine the distance distribution between codewords, which affects the error correction capability of a design. If we take one of the codewords C from a t-(v, w, λ) design, all the remaining codewords can be partitioned into w parts. They are

- $X_{w-1}(C)$ containing codewords intersecting with C on $w-1$ points.

$\vdots$

- $X_1(C)$ containing codewords intersecting with C on single point.
- $X_0(C)$ containing codewords orthogonal to C (no common elements).

We define by $x_{w-1}, \ldots, x_1, x_0$ the number of codewords for each of the above parts respectively. They are also called block intersection numbers [37]. In a $S(t, w, v)$ system, we have

$$x_w = x_{w-1} = \ldots x_t \equiv 0 \tag{4.4}$$

and

$$\begin{aligned} x_{t-1} &= \lambda_{w,(t-1)} C_w^{t-1} \\ &\vdots \\ x_1 &= \lambda_{w1} C_w^1 \\ x_0 &= \lambda_{w0} \end{aligned} \tag{4.5}$$

where $\lambda_{w0}, \lambda_{w1}, \ldots, \lambda_{w,(t-1)}$ are the elements of the bottom row from the *Pascal triangle* [37] and they have definite values only in Steiner systems. How to calculate them if a specific Steiner system is given is described in Appendix D. The basic relation among these numbers is

$$x_0 + x_1 + \ldots + x_{t-1} = b - 1 \tag{4.6}$$

4.4 Performance Evaluation over an AWGN channel

4.4.1 Receiver Model

By decreasing the total number of waveforms in the signaling set, a redundancy is introduced and in fact the codewords are capable of correcting errors. Employing channel coding decreases the actual information bit rate since fewer information bits are conveyed per symbol, which would reduce the bandwidth efficiency, but some power gain can be obtained by increasing the distances between symbols. In AWGN channels, we do not need to reduce the efficiency further by transmitting the identical phase signals in multiple active carriers. Thus each carrier still carries an independent phase. Therefore the signal properties of HPM signals are unchanged when t-designs are employed in selecting the active frequency tones.

As for the receiver, if we still use the receiver structure described in Section 3.2.2, we only need to add a decoder following the comparator unit in the frequency detector part. In this case, we call it MT-FSK part. After the comparator selects the w largest variables, a corresponding codeword is determined and fed into the decoder. Only the valid codeword closest to the input of the decoder is chosen as the decision. Therefore we can consider the MT-FSK receiver as a frequency demodulator employing hard-decision decoding. An error occurs if more than a certain number of frequencies are incorrectly detected. Certainly the error correction capability is determined by the parameters of t-designs. In this condition, the larger the minimum Hamming distance between valid codewords, the larger the error correction capability.

In order to achieve a better performance, we modify the MT-FSK part by employing optimum soft-decision decoding technique. This can be realized by adding a set of b combiners (in binary systems, M_f combiners are enough) which combine the corresponding w values from the square law detectors. Each combiner corresponds to a unique valid codeword and a symbol. All these b outputs from the combiner are

passed to the decoder and only the largest one is selected. The receiver block diagram for the MT-FSK part is illustrated in Figure 4.1.

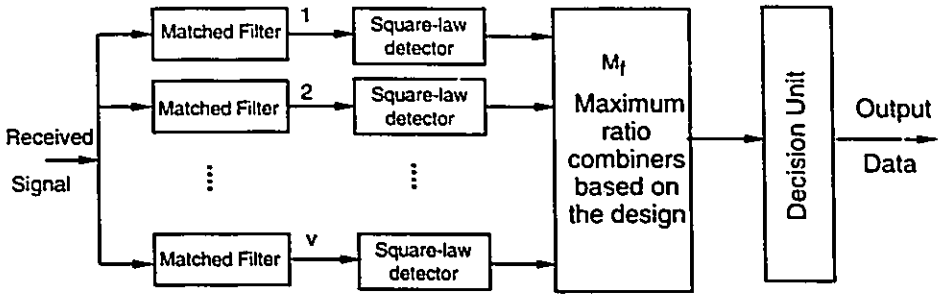

Figure 4.1: Receiver block diagram for the MT-FSK part of coded HPM.

4.4.2 Steiner HPM

In this section, Steiner systems are applied to selecting the active tones. To evaluate the error performance in the specified condition, we still perform the analysis in two stages. There is no change in the second stage and the evaluation given in section 3.4.1 is still true for DPSK part. The first stage is a noncoherent MT-FSK demodulator with optimum soft-decision decoding. The pairwise probability of error with the Hamming distance d between any two codewords is given [25, page 407] by

$$P_2(\gamma_b, d) = \frac{e^{-k\gamma_b/2}}{2^{2d-1}} \sum_{n=0}^{d-1} \frac{1}{n!} \left(\frac{k\gamma_b}{2}\right) \sum_{r=0}^{d-1-n} \binom{2d-1}{r} \qquad d = w - t + 1, \ldots, w \quad (4.7)$$

where $k = k_s d/w$ so that $k\gamma_b$ is actually the effective symbol to noise ratio between two symbols. This is because two codewords may have intersections and the corresponding waveforms share the component signals. In making the decisions, only the components which uniquely belong to a symbol in the decision variables have the actual effect.

We know that the pairwise error probability is also dependent on d. Using the union upper bound method, we obtain the symbol error probability for MT-FSK part

$$P_{MTFSK}(\gamma_b, w) \leq x_0 P_2(\gamma_b, w) + x_1 P_2(\gamma_b, w-1) \\ \ldots + x_{t-1} P_2(\gamma_b, w-t+1) \tag{4.8}$$

where x_i, $i = 0, \ldots, t-1$ is given by (4.5).

In determining the bit error probability, we find that the only difference lies in the MT-FSK part compared to the uncoded HPM discussed in section 3.4.1 and we need only to make the modifications related to this part. Even though the codewords in a design have regular patterns, they are still not codes with equal distance. The parameters of a design determine its distance distribution between codewords. For instance, in $S(3, 5, 17)$, out of 67 codewords other than a given reference codeword, 40 differ with the reference in 6 positions, 15 differ in 8 positions and 12 are orthogonal to the reference. A different scenario occurs under another alphabet. But generally, we can still use $P_b \approx 0.5 P_s$ as the approximation.

If a detection error occurs in the MT-FSK stage, a codeword is incorrectly detected as another codeword in the same set. But it is highly probable that the wrong decision is made to the nearest x_{t-1} neighbor codewords in which a codeword has $(w-t+1)$ erroneous elements. This implies that most probably $(w-t+1)$ tones are mistaken and sent to the second stage for carrier reference. While in PFSK detector, only one tone is more easily mistaken when a character error occurs. Any one of the DPSK detectors provided with wrong carrier information has 1/2 of bit error probability. Recall from section 3.3, the overall bit error probability for Steiner HPM can be modified as

$$P_b \simeq \frac{1}{k_s}\left(\frac{k_f}{2} P_{MTFSK} + (w-t+1) k_p P_{MTFSK} + w(1-P_{MTFSK}) P_e (1-P_e)^{w-1}\right) \tag{4.9}$$

where P_e is given by (3.12).

4.4.3 Hadamard HPM

We have mentioned earlier that Hadamard code can be classified as a t-design. A Hadamard code can be extracted from the Hadamard matrix, which is a $n \times n$ matrix. Each row has constant weight $n/2$ out of n elements, while only one row consists of all zeros. The number of intersecting elements to a given codeword is $n/4$. If considering the complement of these codewords and excluding the all zero and all one codeword, we obtain a total $2(n-1)$ codewords for a given n. Therefore a Hadamard code can be denoted by $H(n,k)$ with $k = 1 + \lfloor \log_2(n-1) \rfloor$, which is the maximum number of bits that can be represented by this set of codewords. For example, if $n = 4$, the Hadamard matrix is

$$M_4 = \begin{pmatrix} 0 & 0 & 0 & 0 \\ 0 & 1 & 0 & 1 \\ 0 & 0 & 1 & 1 \\ 0 & 1 & 1 & 0 \end{pmatrix}$$

The complement of M_4 is

$$\bar{M}_4 = \begin{pmatrix} 1 & 1 & 1 & 1 \\ 1 & 0 & 1 & 0 \\ 1 & 1 & 0 & 0 \\ 1 & 0 & 0 & 1 \end{pmatrix}$$

Combining the two matrixes, we obtain $2(n-1) = 6$ constant weight codewords (0101, 0011, 0110, 1010, 1100, 1001).

The Hadamard code is a powerful code in terms of its large minimum distance. It is also observed that in the total of $2(n-1)$ codewords, $2(n-2)$ codewords have $n/4$ elements, and 1 codeword is orthogonal, to a given codeword. In fact, the simplest Hadamard code is given by the permutation set 2 out of 4. Three codewords are actually the complement of the other three. The corresponding design of waveforms are shown by Table 2.1.

In determining the bit error probability of Hadamard HPM, we follow the same approach used before. When an error occurs in the MT-FSK stage, it is highly likely that $n/4$ detected carriers are incorrect and the remaining $n/4$ ones are correct. Another different point is that we can use $2^{k-1}/(2^k - 1)$ as the conversion factor

between BER and SER since most of codewords have the same distance $n/4$ to a given codeword. Hence the bit error probability can be specified by

$$P_b \simeq \frac{1}{k_s}\left(\frac{2^{k_f-1}}{2^{k_f}-1}P_{MTFSK} + \frac{n}{4}k_p P_{MTFSK} + \frac{n}{2}(1-P_{MTFSK})P_e(1-P_e)^{w-1}\right) \quad (4.10)$$

$$P_{MTFSK}(\gamma_b, n) \leq (M_f - 1)P_2(\gamma_b, n/4), \quad (4.11)$$

where $P_2(\gamma_b, n)$ is given by (4.7).

4.4.4 Numerical Results

The performances of some Steiner HPM systems are tabulated in Table 4.4 while Table 4.5 gives the results for Hadamard HPM, and it requires more than 8 dB to achieve BER of 10^{-5} in any sets. But Steiner HPM needs 1 to 2 dB less than that value. In this condition, Steiner HPM outperforms Hadamard HPM. This is because of the signal to noise density ratio in each subchannel being too small in Hadamard HPM.

Based on the observations from Table 4.6 and Table 3.1, we find that MT-FSK has some power gains at the expense of bandwidth efficiency. But since the number of bits conveyed per symbol also reduces as expurgating part of the codewords, this power gain is limited. Increasing the Hamming distance may not result in remarkable power gain even though there is a large coding gain. For instance, MT-FSK(21,3,2) outperforms MT-FSK(21,5,2) by almost 1.4 dB (8.73 dB versus 10.12 dB) and has larger bandwidth efficiency as well (0.286 versus 0.190) while their d_{min} is $w-t+1 = 4$ and 8 respectively. Less energy is allocated to each carrier as w increases, which would deteriorate the condition of signal to noise ratio. This drawback can be overcome by combining the phase modulation to get larger power gain.

In the case of HPM, when M_p takes on large values, the error performance is mainly determined by DPSK part and the coding gain inherent in coded HPM disappears. Anyway, in terms of power efficiency, Steiner HPM with $M_p = 2$ still demonstrates

(v,w,t)	M_f	b	$M_p=1$ (MT-FSK)	$M_p=2$	$M_p=4$	$M_p=8$
(8,3,2)	8	8	11.36/0.375	8.37/0.75	10.01/1.125	14.43/1.50
(15,3,2)	32	35	9.41/0.333	7.41/0.533	9.04/0.733	13.69/0.933
(21,3,2)	64	70	8.74/0.286	7.02/0.429	8.62/0.571	13.35/0.714
(16,4,2)	16	20	10.14/0.25	7.38/0.50	10.01/0.75	14.43/1.00
(40,4,2)	128	130	8.05/0.175	6.19/0.275	8.93/0.375	13.60/0.475
(21,5,2)	16	21	10.12/0.190	7.56/0.429	10.34/0.667	14.68/0.905
(64,8,2)	64	72	8.92/0.094	7.68/0.219	10.42/0.344	14.75/0.469
(14.4.3)	64	91	10.03/0.429	7.81/0.714	9.26/1.00	13.86/1.286
(16,4,3)	128	140	9.41/0.438	7.45/0.688	8.93/0.938	13.60/1.188
(20,4,3)	256	285	8.92/0.40	7.16/0.60	8.62/0.80	13.35/1.00
(38,4,3)	2096	2109	7.75/0.289	6.40/0.395	7.79/0.50	12.68/0.605
(17,5,3)	64	68	9.64/0.353	7.12/0.647	9.70/0.941	14.20/1.235
(22,6,3)	64	77	9.55/0.273	7.10/0.545	10.01/0.819	14.43/1.091
(26,6,3)	128	130	8.94/0.269	6.74/0.50	9.75/0.731	14.24/0.962
(65,9,3)	512	520	8.05/0.138	7.04/0.277	10.01/0.415	14.43/0.554
(11,5,4)	64	66	10.99/0.545	8.34/1.00	9.70/1.455	14.20/1.909
(12,6,5)	128	132	11.24/0.583	8.50/1.083	9.75/1.583	14.24/2.083
(28,7,5)	4096	4680	8.58/0.429	6.59/0.679	8.98/0.929	13.64/1.179
(24,8,5)	512	759	9.44/0.375	6.93/0.708	9.81/1.042	14.29/1.375

Table 4.4: Performance of some Steiner HPM alphabets. The entries in the table are energy per bit to noise density ratio $\gamma_b(dB)$ required to achieve bit error rate 10^{-5} in AWGN channels versus bandwidth efficiency R_b/W(bps/Hz).

(n,k_f)	$M_p=1$	$M_p=2$	$M_p=4$
(12,4)	11.92/0.333	8.16/0.833	10.57/1.33
(16,4)	12.18/0.250	8.42/0.75	10.88/1.25
(20,5)	11.62/0.250	8.42/0.75	10.88/1.25
(24,5)	11.80/0.208	8.69/0.708	11.05/1.208
(28,5)	11.96/0.179	8.89/0.679	11.17/1.179
(32,5)	12.10/0.156	9.05/0.656	11.26/1.156
(36,6)	11.62/0.167	8.98/0.667	11.22/1.167
(40,6)	11.74/0.150	9.10/0.65	11.28/1.15

Table 4.5: γ_b/η performance of Hadamard HPM over AWGN channels at the bit error rate of 10^{-5}.

its attraction. In that table, the HPM(40,4,2,2) scheme requires γ_b =6.19 dB and $\eta = 0.275$ at a BER of 10^{-5}, compared to conventional 64-FSK with γ_b =6.56 dB and $\eta = 0.094$. In this case, increasing w has the effect of increasing the value k_s as well. we can observe that HPM(21,3,2,2) outperforms (21,5,2,2) by only 0.5 dB (7.02 dB versus 7.56 dB) with the same bandwidth efficiency 0.429.

With the same available bandwidth $v = 16$ and active tones $w = 4$, we compare the BER performance of MT-FSK, Steiner and uncoded HPM(16,4,2) in Figure 4.2. The advantage of coded system is evident. Steiner HPM(16,4,2,2) and (16,4,3,2) have the comparable BER performance even though they possess different coding gains. In addition, the same bandwidth efficiency can be achieved by using different HPM alphabets. Figure 4.3 gives the Steiner and uncoded HPM under this condition. Their corresponding bandwidth efficiency η is listed in the square bracket following the notation.

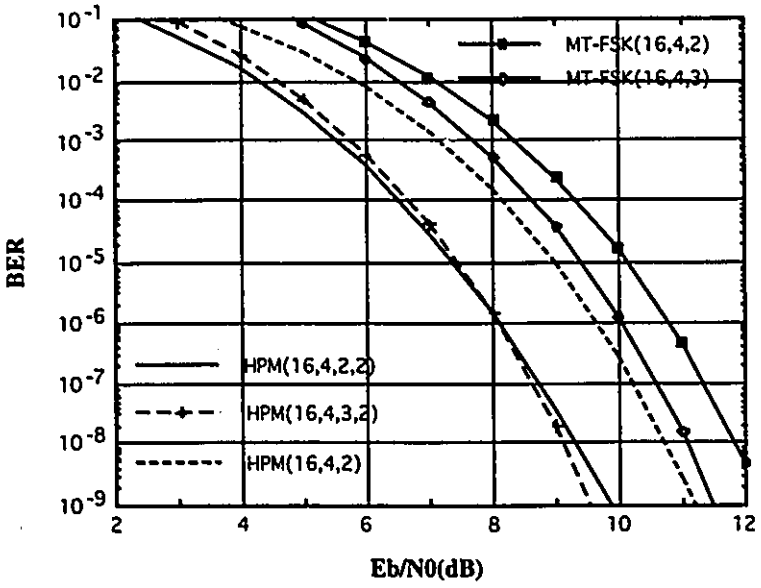

Figure 4.2: Bit error probability of coded and uncoded HPM with $v = 16$ and $w = 4$ in AWGN channels.

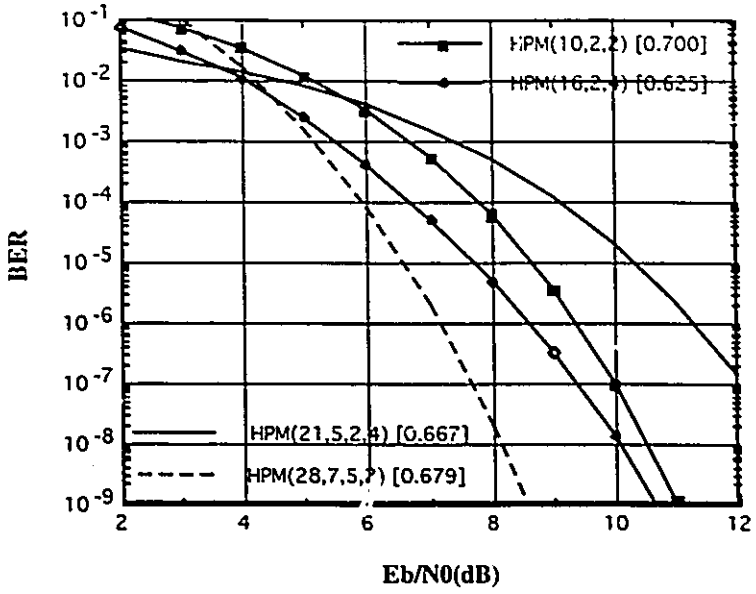

Figure 4.3: Bit error probability of coded and uncoded HPM with comparable bandwidth efficiency in AWGN channels.

4.5 Performance Evaluation over Frequency Selective Fading Channels

4.5.1 Receiver Model

From the previous section, we observe that HPM has advantages due to its large size of signal sets based on the available resources, which provides both power and spectral efficiency. When employing channel coding, the scheme is capable of correcting errors in AWGN channels in a sense that an error occurring in one subchannel does not necessarily lead to a symbol error. In multipath fading channel, even though there are other approaches, the most effective method against fading is diversity. Usually diversity can be realized by means of frequency, time or space diversity.

HPM has inherent diversity under certain conditions. In frequency selective fading channels, if all the active frequencies carry the identical information-bearing phases, the implicit diversity can be fully exploited by employing coherent detection. In the

case of noncoherent detection using square law FSK detection, only the amplitude of the received signals has the effect on FSK demodulation. Thus other measures have to be taken to make use of the inherent diversity. We observe that just like MT-FSK scheme, coded HPM can solve this problem. The distance between codewords is an indication of intrinsic diversity under this channel condition rather than an indication of error correction capability in AWGN channels. Furthermore, MT-FSK combined with phase modulation can compensate for the bandwidth efficiency losses introduced by coding.

The existence of common carriers has the side effect of reducing the distance of two waveforms in signal space. Since w carriers are active per symbol duration, the maximum diversity that can be obtained is limited by w at the MT-FSK receiver. The effective diversity depends on the number of shared carriers and thus is related to the property of codewords. The DPSK part also has significant effect on the overall performance. In order to keep a balance between MT-FSK and DPSK parts, it is necessary to obtain certain order of diversity in DPSK detection. This can be achieved by transmitting the identical phases in all the active carriers. The phase is also determined by the incoming symbol. Consequently we can expect w order of diversity at the DPSK receiver, which is equal to the number of active tones. In this way, any individual part will not have the dominant effect on the overall performance and a substantial power gain is obtained and the advantage of multiple carrier transmission is still maintained.

According to the modulation process, the bandwidth efficiency based on minimum frequency separation is expressed by

$$\eta = \frac{k_s}{v} = \frac{k_f + k_p}{v} \tag{4.12}$$

The receiver structure is depicted in Figure 4.4. The second stage is composed of w DPSK detectors to demodulate signals transmitted in independent and identically distributed subchannels. The outputs of these different diversity paths are added together at the combiner. The largest result corresponding to an existing phase is

selected as the decision.

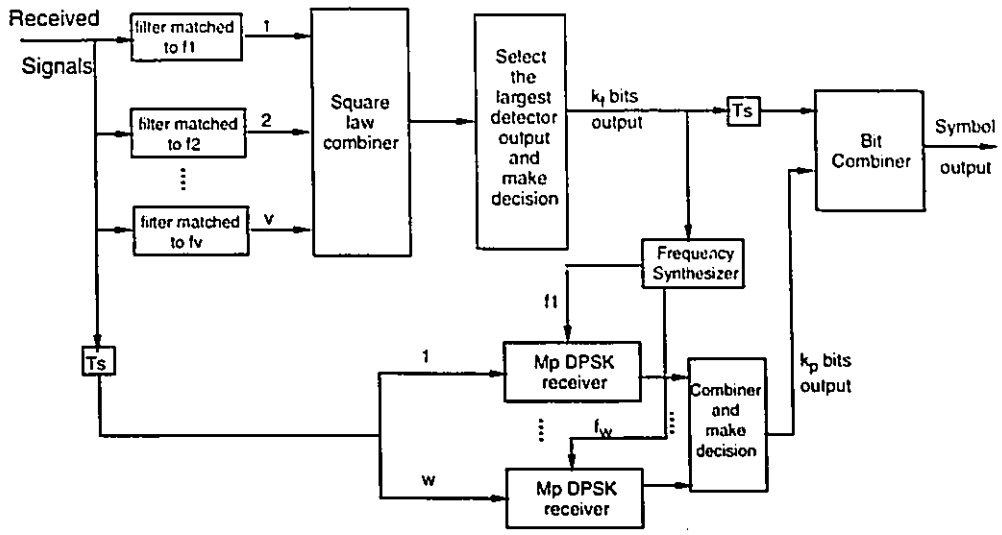

Figure 4.4: Receiver diagram for coded HPM in frequency selective fading channels

In the following, we will focus on HPM employing two families in t-designs: Steiner system and Hadamard code. The selection of parameters would be based on the performance improvement versus complexity tradeoff.

4.5.2 Steiner HPM

The receiver of coded HPM consists of the MT-FSK and DPSK stages. As for the MT-FSK part, since the integration of waveform is determined by the codeword in a t-design, the distance between codewords is closely related to the performance. If two codewords separated by a Hamming distance $2d$, the corresponding HPM waveforms can be seen as having d diversity branches since only the signals in these d branches can be combined and have the effect to make a difference with other signals. Therefore, the pairwise error probability with Hamming distance separation of $2d$ [25] at the MT-FSK stage is

$$P_2(\bar{\gamma}_c, d) = \left(\frac{1}{2+\bar{\gamma}_c}\right)^d \sum_{r=0}^{d-1} \binom{d-1+r}{r} \left(\frac{1+\bar{\gamma}_c}{2+\bar{\gamma}_c}\right)^r \quad d = w-t+1, \ldots, w \quad (4.13)$$

where $\bar{\gamma}_c = \gamma_b k_s / w$ is the signal to noise ratio in each diversity branch.

The error probability conditioned on all possible symbols is upper bounded by

$$P_{MTFSK}(\bar{\gamma}_c, w) \leq x_0 P_2(\bar{\gamma}_c, w) + x_1 P_2(\bar{\gamma}_c, w-1) \\ \ldots + x_{t-1} P_2(\bar{\gamma}_c, w-t+1) \tag{4.14}$$

In the second stage, the error probability of differential phase modulation with diversity order L over Rayleigh fading channels is given [25] by

$$P_2(M_p, L) = \frac{(-1)^{L-1}(1-\mu^2)^L}{\pi(L-1)!} \left(\frac{\partial^{L-1}}{\partial b^{L-1}} \left\{ \frac{1}{b-\mu^2} \left[\frac{\pi}{M_p}(M_p - 1) \right. \right. \right. \\ \left. \left. \left. - \frac{\mu \sin(\pi/M_p)}{\sqrt{b-\mu^2\cos^2(\pi/M_p)}} \cot^{-1} \frac{-\mu\cos(\pi/M_p)}{\sqrt{b-\mu^2\cos^2(\pi/M_p)}} \right] \right\} \right)_{b=1} \tag{4.15}$$

where $\mu = \frac{\gamma_c}{1+\gamma_c}$.

For simplicity purpose, we consider the cases of BPSK and QPSK only. The performance of multiple phase systems degrades as $M_p > 4$. The bit error rate for DPSK with diversity order L in Rayleigh fading channel when employing Gray code mapping [30] is

$$P_{b2}(L) = \frac{1}{2}\left[1 - \mu \sum_{k=0}^{L-1} \binom{2k}{k} \left(\frac{1-\mu^2}{4} \right)^k \right] \tag{4.16}$$

where

$$\mu = \frac{\bar{\gamma}_c}{1+\bar{\gamma}_c}$$

for DBPSK and

$$\mu = \frac{\bar{\gamma}_c}{\sqrt{2+4\bar{\gamma}_c+\bar{\gamma}_c^2}}$$

for DQPSK.

Based on the same arguments specified in section 4.4, it is highly probable that a codeword is mistakenly detected as one of the x_{t-1} closest codewords if a detection error occurs. If this happens, at least $w-t+1$ carriers are incorrect. But it is well approximated that $t-1$ carriers, which are the common carriers between the transmitted waveform and the incorrectly detected waveform, can be correctly selected

and act as carrier references for further detection. In this case, the demodulation of differential phase signals is in fact performed with $t-1$ correct carrier references and $w-t+1$ wrong ones. Certainly wrong carrier reference will not make any contribution to the detection of phase signals. Therefore we may see the signals transmitted through $t-1$ diversity branches. If an error occurs, i.e., the DPSK receiver makes an erroneous decision conditioned on an incorrect detection at the MT-FSK stage, there is 1/2 probability that a bit error occurs in the present and the following symbol interval. Thus we may express the bit error probability of Steiner HPM as

$$P_b \simeq \frac{1}{k_s}\left(\frac{k_f}{2}P_{MTFSK} + k_p P_{MTFSK} P_{b2}(L=t-1)\right) + \frac{k_p}{k_s}(1-P_{MTFSK})P_{b2}(L=w), \tag{4.17}$$

where $P_{b2}(L)$ is given by (4.16) and P_{MTFSK} is given by (4.14). In expression (4.17), the term in the big bracket represents the error contribution caused by the MT-FSK stage, and the second term represents the contribution made by the DPSK stage under the condition of entirely correct detection of carrier frequencies.

4.5.3 Hadamard HPM

Following the same process as used before, we obtain the bit error probability for Hadamard HPM as

$$P_b \simeq \frac{1}{k_s}\left(\frac{2^{k_f-1}}{2^{k_f}-1}P_{MTFSK} + k_p P_{MTFSK} P_{b2}(L=n/4)\right) + \frac{k_p}{k_s}(1-P_{MTFSK})P_{b2}(L=n/2), \tag{4.18}$$

where P_{MTFSK} is given by

$$P_{MTFSK}(\bar{\gamma}_c, n) \leq (M_f-1)P_2(\bar{\gamma}_c, n/4), \tag{4.19}$$

where $P_2(\bar{\gamma}_c, n)$ is given by (4.13).

4.5.4 Numerical Results of Coded HPM

In Steiner HPM, we know that the implicit diversity is determined by the value of $(w - t + 1)$, which is the minimum distance of codewords. This can be illustrated by Figure 4.5. The BER performances of Steiner HPM(v, w, t) with $M_p = 4$ are compared with conventional M-ary FSK with comparable diversity order and the same k_s value (5,6 and 6 respectively). Each notation is followed by the value of bandwidth efficiency. We observe that HPM schemes have comparable error performance with very attractive bandwidth efficiency.

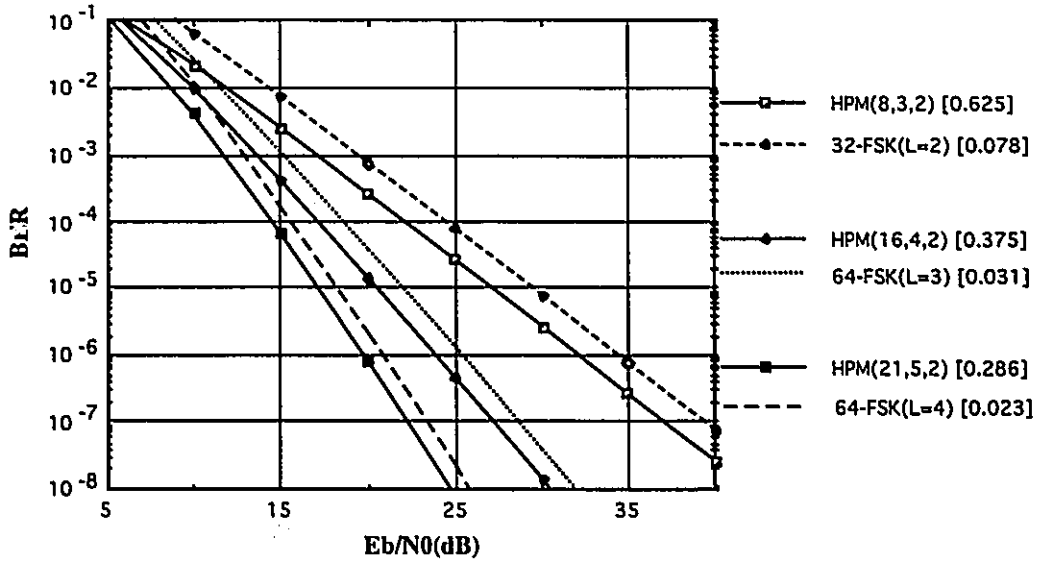

Figure 4.5: BER performance of Steiner HPM(v, w, t) with $M_p = 4$, compared with conventional M-ary FSK with comparable value of k_s and diversity order.

The performances of some typical Steiner HPM are compared in Table 4.6. The most notable improvement can be achieved by means of increasing the implicit diversity. We observe the big difference between the alphabet (21,3,2) and (22,6,3), which has equivalent diversity of 2 and 4 respectively. The same implicit diversity

can be obtained through different alphabets. For instance, both (15,3,2) and (11,5,4) can achieve the second order effective diversity, and both of them have 64 codewords. But there are more shared carriers in (11,5,4) than (15,3,2) to accommodate more codewords using fewer orthogonal tones. Therefore much more power is allocated to the shared carriers and this will result in power losses in each individual active carrier. In addition, the improvement achieved by power gains is limited. This is shown by comparing the alphabet (22,6,3) and (26,6,3).

(v,w,t)	M_f	b	$M_p=1$ (MT-FSK)	$M_p=2$	$M_p=4$
(8,3,2)	8	8	25.36/0.375	23.48/0.50	22.04/0.625
(15,3,2)	32	35	24.92/0.333	23.73/0.40	22.73/0.467
(21,3,2)	64	70	25.02/0.286	24.01/0.333	23.15/0.381
(16,4,2)	16	20	19.45/0.250	18.16/0.312	17.11/0.375
(40,4,2)	128	130	18.81/0.175	18.04/0.20	17.36/0.225
(21,5,2)	16	21	16.72/0.190	15.50/0.238	14.53/0.286
(64,8,2)	64	72	12.98/0.094	12.20/0.109	11.55/0.125
(14,4,3)	64	91	26.49/0.429	25.49/0.50	24.62/0.571
(16,4,3)	128	140	26.23/0.438	25.36/0.50	24.59/0.562
(17,5,3)	64	68	20.14/0.289	19.24/0.412	18.46/0.471
(22,6,3)	64	77	17.35/0.273	16.50/0.318	15.77/0.364
(26,6,3)	128	130	16.95/0.269	16.22/0.308	15.58/0.346
(65,9,3)	512	520	12.87/0.138	12.33/0.154	11.85/0.169
(11,5,4)	64	66	27.46/0.545	26.45/0.636	25.58/0.727
(12,6,5)	128	132	28.46/0.583	27.59/0.667	26.83/0.75
(28,7,5)	4096	4680	21.30/0.429	20.84/0.464	20.41/0.50
(24,8,5)	512	759	18.57/0.375	18.00/0.417	17.48/0.458

Table 4.6: Performance of some Steiner HPM alphabets. The entries in the table are energy per bit to noise power density ratio $\gamma_b(dB)$ required to achieve bit error rate 10^{-4} in frequency selective fading channels versus bandwidth efficiency R_b/W(bps/Hz).

From the table, the best performance is still given by HPM with $M_p = 4$, which provides spectral efficiency not exceeding 1.0b/s/Hz. In terms of selecting the design parameters, (24,8,5), (22,6,3) and (21,5,2) exhibit satisfactory results. Thus carefully

selecting the alphabet is essential to achieve best result. This can be shown by comparing the difference between (22,6,3) and (21,3,2), even though they possess similar η. In general, under the same effective diversity, the alphabet with larger t gives more spectral efficiency, but the degradation becomes obvious. Considering all the factors, selecting t with moderate value is appropriate.

Table 4.7 lists the results of Hadamard HPM. Comparing it with Table 4.6, we observe that, under the same bandwidth efficiency, HPM employing Steiner system and Hadamard codes demonstrate comparable performances. In the cases of S(17,5,3) and H(12,4), S(26,6,3) and H(20,5), they require the similar γ_b (18.46 versus 18.95 dB and 15.77 versus 15.41 dB) in the same condition.

(n, k_f)	$M_p = 1$	$M_p = 2$	$M_p = 4$
(12,4)	21.31/0.333	20.01/0.417	18.95/0.50
(16,4)	18.84/0.250	17.61/0.312	16.61/0.375
(20,5)	17.19/0.250	16.23/0.30	15.41/0.35
(24,5)	16.29/0.208	15.35/0.25	14.55/0.292
(28,5)	15.70/0.179	14.77/0.214	13.98/0.25
(32,5)	15.28/0.156	14.37/0.188	13.59/0.219
(36,6)	14.64/0.167	13.87/0.194	13.21/0.222
(40,6)	14.39/0.150	13.63/0.175	12.97/0.20

Table 4.7: γ_b/η performance of Hadamard HPM over fading channels at the bit error rate of 10^{-4}.

Table 4.8 gives the performance of conventional M-ary FSK and MDPSK with diversity. It is apparent that coded HPM is much more efficient than MFSK scheme, and its performance is also close to that of MDPSK, if the comparisons are made under the fair criterion. But other factors have to be taken into account. MDPSK employing diversity techniques has to use a set of receivers to capture the signals in separate branches, whereas coded HPM has the inherent feature of diversity and only one receiver is needed.

	MDPSK			MFSK		
	2	4	8	2	4	8
L=1	36.9/1.0	36.6/2.0	38.8/3.0	40.0/0.5	37.9/0.5	36.9/0.375
L=2	22.3/0.5	22.2/1.0	25.0/1.5	25.3/0.25	23.1/0.25	22.0/0.188
L=4	16.4/0.25	16.3/0.5	19.2/0.75	19.4/0.125	17.2/0.125	16.0/0.094

Table 4.8: γ_b/η performance of noncoherent FSK and DPSK with diversity over fading channels at BER of 10^{-4}.

4.6 Simulation Results and Comparisons

In this section, the simulation of HPM scheme in the condition of fading channel is performed to verify the theoretical analysis in previous section.

We consider only noncoherent detection. To avoid the complexity, we choose the simplest HPM based on S(2,3,6) and $M_p = 2$. Due to the orthogonality of the the frequency carriers, there is no interference between adjacent tones. This permits us using two set of index values to represent the transmitted signals: v integers indicating the sequence of the signals in the signal set; another v float values representing the signal energy which is $\gamma_c = \gamma_b k_s/w$ and constant for all symbols.

For an incoming symbol, the first k_f bits determine the combination of active tones. The corresponding positions are preset by a given value γ_c. The other positions representing the unused tones in the current symbol interval remain as zero. In dealing with the phase, the incoming k_p bits have to be differentially encoded. Since we consider only 2 phases case, the phase can be represented by the sign of energy value which is positive or negative, depending on the input symbol and the phase in previous symbol duration.

The signals are passed through fading channels which contain fading and AWGN. In frequency selective case, each component signal undergoes independent fading. Therefore, the transmission process can be seen as the w energy values multiplied by

fading factors and added by additive white Gaussian noise. While other subchannels contain only the noise components.

At the decision unit, the absolute values of the received signals are combined and compared, the phase of two consecutive symbol interval are compared and the symbol is determined. Finally, the number of bit errors is counted. In Figure 4.6, the model for simulating the BER performance is shown.

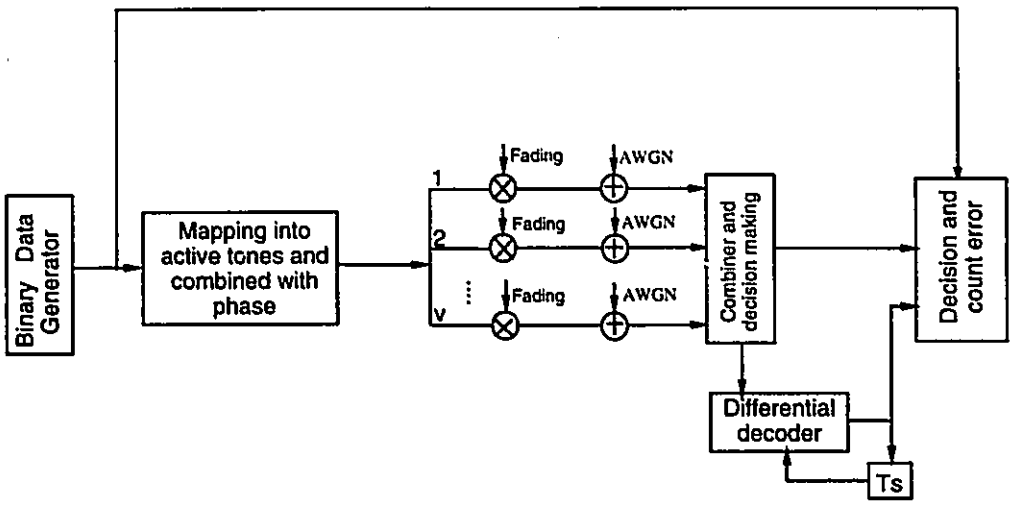

Figure 4.6: The block diagram of the simulation model for coded HPM

In each given γ_b, 1000 errors are generated before the next γ_b value is used. The fading and AWGN are statistically independent. The simulation result of HPM(6,3,2,2) is depicted in Figure 4.7. The curve of theoretical analysis is also added. It reveals that the two curves agree well.

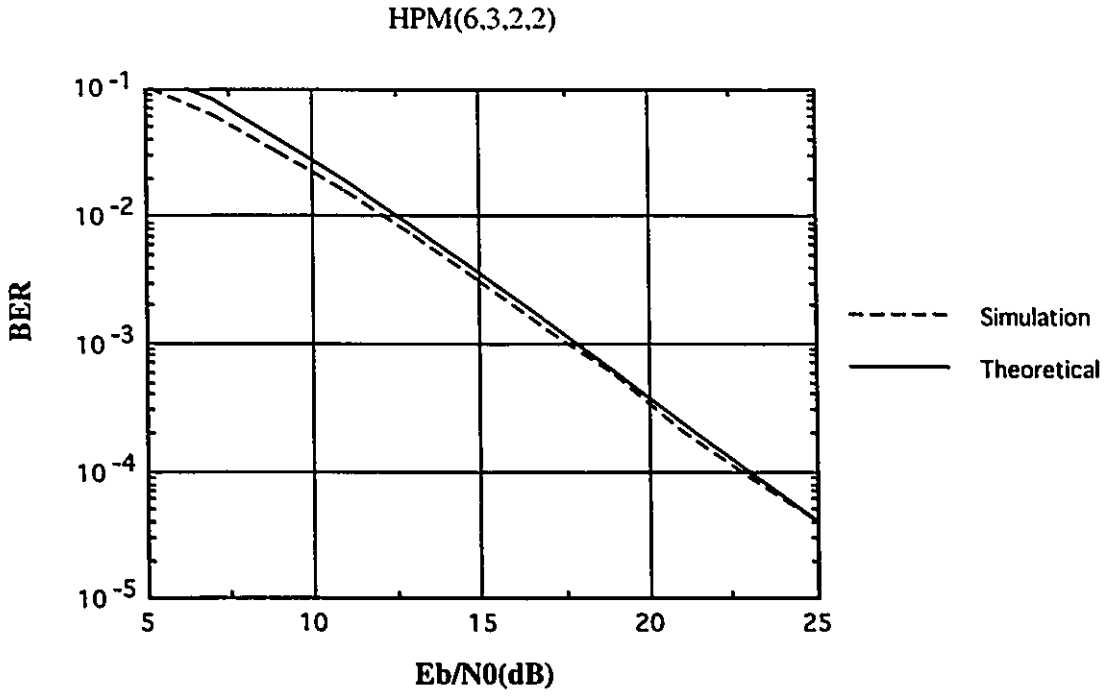

Figure 4.7: The simulation results of coded HPM(6,3,2,2) over frequency selective fading channels.

4.7 Conclusion

In this chapter, we conducted studies on the performance of coded HPM. The coding in fact refers to selecting the active tones. In fact, our objective is to present a systematic way of selecting waveforms from all the possible ones, i.e., expurgating part of codewords from a complete permutation code. Our studies are based on t-designs and their properties are briefly discussed. Two families from t-designs, Steiner and Hadamard code, are investigated.

In AWGN channels, coded HPM demonstrates its coding gain and the best performance is obtained when M_p=2. Steiner HPM is superior to Hadamard HPM. But the multicarrier feature of HPM imposes restriction on the overall power gain.

In FSRF channels, the coding gain inherent in coded HPM turns into intrinsic diversity which can be exploited by employing appropriate receiver. This has contributed to the dramatic performance improvements. The effective diversity is not proportional to the parameter w, which is the number of active carriers, but determined by the Hamming distance of the code employed. Steiner HPM has comparable performance to Hadamard HPM. While in these code families for concern, some alphabets are superior to others and indicate themselves to be good candidates for coded HPM.

Chapter 5

Conclusions and Suggestions

5.1 Thesis Summary

In applications of mobile and satellite communications, the growing need for digital communications has led to seek highly efficient and low error rate modulation systems. For this purpose this thesis studied a power and bandwidth efficient modulation scheme abbreviated as HPM. A mathematical expression for HPM signals has been presented. A HPM waveform consists of a few orthogonal component signals which may experience different fading and noise conditions. The minimum frequency separation to meet the orthogonal carrier condition has been derived. From this point, the required transmission bandwidth can be determined and we give the expression for bandwidth efficiency.

The performance of HPM has been studied in AWGN and frequency selective Rayleigh fading channels. Coherent and noncoherent detection strategies have been considered. Regarding the system performance, our main focus is on the BER performance and bandwidth efficiency. For uncoded HPM, the upper bound method has been used for the analytical evaluation of the error performance. A differential noncoherent receiver structure was introduced for practical applications. The probability of error was analyzed and an approximation for bit error rate expression was obtained. It is concluded that in AWGN channels, uncoded HPM is a quite efficient

and powerful scheme. Under a given v, more bandwidth efficiency can be obtained by increasing the number of phases M_p or the number of active tones w, while more power efficiency can be obtained by decreasing w and putting M_p at a small value (2 or 4). Therefore the parameters has to be carefully selected for a specific application. There is much more freedom for a designer to make the selection.

However, the error performance of uncoded HPM is very poor in fading channels. Coded HPM was proposed as a solution. In fact, uncoded HPM employs a complete permutation code, whereas coded HPM is associated with only a subset of complete code. Spectral efficiency is sacrificed to achieve significant coding gain. In FSRF channels, this coding gain is transformed into diversity gain.

Two powerful codes, namely Steiner system and Hadamard code were discussed. We modified noncoherent receiver structure to fully exploit the potential provided by coding. Bit error probability expression was developed by using the union bound. In AWGN channels, the effect of coding gain can be shown in Table 5.1, which list some typical uncoded and coded systems. The effective diversity gain, which is determined by Hamming distance of the code employed, has contributed to the dramatic improvement in FSRF channels. Table 5.2 gives the comparison in this condition. It is shown that Steiner HPM has comparable performance with Hadamard HPM. A Monte Carlo simulation was performed to validate the analytical results.

γ_b/η (dB)/(bps/s/Hz)	M_p=2	M_p=4	M_p=8
$(v=8, w=3)$	9.78/1.00	9.09/1.375	13.69/1.75
$(v=8, w=3, t=2)$	8.37/0.75	10.01/1.125	14.43/1.50
$(v=16, w=4)$	8.97/0.875	8.22/1.125	12.89/1.375
$(v=16, w=4, t=2)$	7.38/0.50	10.01/0.75	14.43/1.00
$(v=16, w=4, t=3)$	7.45/0.688	8.93/0.938	13.60/1.188

Table 5.1: Performance of uncoded and Steiner HPM in AWGN channels at BER of 10^{-5}.

In conclusion, HPM can be a power and bandwidth efficient modulation scheme. Given a HPM alphabet, the selection of waveforms to form a signal is quite flexible.

γ_b/η (dB)/(bps/s/Hz)	M_p=2	M_p=4
$(v = 8, w = 3)$	40.74/1.00	39.50/1.375
$(v = 8, w = 3, t = 2)$	23.48/0.50/0.75	22.04/0.625
$(v = 16, w = 4)$	41.89/0.875	40.62/1.12
$(v = 16, w = 4, t = 2)$	18.16/0.312	17.11/0.375
$(v = 16, w = 4, t = 3)$	25.36/0.50	24.59/0.562

Table 5.2: Performance of uncoded and Steiner HPM in FSRF channels at BER of 10^{-4}.

Coded HPM is quite robust in frequency selective fading channels. Secondly, there are many combinations of signal formats available, and the same bandwidth or power efficiency can be achieved by using different HPM sets, and this will give more freedom to the system designer to make a selection.

5.2 Suggestions for Future Research

With respect to permutation modulation and its derivative HPM, there are other issues and areas which could be further studied. We feel that efforts can be focused on the following suggestions.

1. It is expected that HPM can be applied to practical systems, such as CDMA systems. The frequency hopped HPM is relatively easy to implement and its performance needs to be studied. The system is expected to be quite robust against fading and partial band noise.

2. Using error correcting codes and coded HPM, a form of concatenated coding/diversing effect can be achieved. This is expected to provide additional improvements.

Appendix A

Selection of HPM parameters

The input to many communication systems is binary data. A certain number of information bits can be easily mapped into one symbol and the information transmitted can be directly measured by the number of bits per symbol. But we may observe that given the parameters w and v, the value of $\begin{pmatrix} v \\ w \end{pmatrix}$ is usually not a power of 2. For example using $v = 8$ and $w = 3$, the total number of permutations is 56, which is not a power of 2. This means that the maximum number of information bits that could be conveyed by HPM may be a noninteger value. To make HPM with a selected alphabet applicable in practical situation, we can choose k_f as $\left\lfloor \log_2 \begin{pmatrix} v \\ w \end{pmatrix} \right\rfloor$, which is the largest integer less than or equal to $\log_2 \begin{pmatrix} v \\ w \end{pmatrix}$. While k_p usually takes an integer value. There are some remaining blocks which are not used to represent any symbols. These unused blocks may be utilized for error correction purpose and this may enhance the error performance a little bit. But the overall effect of doing this would be a reduction of both the bandwidth and power efficiency because fewer bits are transmitted in one symbol. In other words, when HPM is applied to a binary data transmission system, its maximum potential may not be utilized. On the other hand, if HPM is applied to a specific nonbinary transmission system, i.e., the original data to be transmitted is not a binary bit stream and the parameters of HPM are properly selected, that the maximum transmission capability can be approached or achieved. But note that this is a rare case. In this condition each transmitted symbol is a

nonbinary character and it is still measured in bits with a real value. Each character has a corresponding signaling frame and almost all the available signaling frames are used.

Appendix B

Examples to calculate the bit error conversion factor in the case of permutation FSK

In this appendix we give a specific example to show that bit error probability P_b is approximately half of the symbol error rate P_s in permutation FSK. Let us use PFSK($v = 5, w = 2$) as an example.

PFSK(5,2) yields 10 waveforms and can be used to represent 8 symbols in binary transmission. We only need to select 8 waveforms. The selected waveforms can be represented by 8 codewords and this has been shown in Table B.1. There are many ways of assigning waveforms to represent symbols. In this table, two possible ways are given. Since the 8 codewords are not all equally apart from each other, the symbol error rate, and also bit error rate, is related to the symbol considered. To find bit error probability of the whole system conditioned on the symbol error rate is obtained, we first calculate the bit error rate for each symbol, and then find the average for all symbols.

The calculation process is explained as follows. Assuming the symbol 000 is transmitted, the corresponding codeword is 00101. We suppose that an error occurs after receiving, but the erroneous decision is more likely made with equal probability to the closest 5 waveforms (in this case, they are 01001, 10001, 00110,01100,10100), which

codeword	symbol	P_b	symbol	P_b
00101	000	$7/15P_s$	000	$7/15P_s$
01001	001	$6/12P_s$	001	$5/12P_s$
10001	010	$5/12P_s$	010	$6/12P_s$
00110	101	$8/15P_s$	100	$8/15P_s$
01010	011	$7/12P_s$	101	$5/12P_s$
10010	111	$5/12P_s$	111	$6/12P_s$
01100	100	$8/15P_s$	011	$10/15P_s$
10100	110	$7/15P_s$	110	$7/15P_s$

Table B.1: Two ways to realize PFSK(5,2) and the corresponding P_b.

have 1 common tone with 00101. The corresponding symbols are 001, 010, 101, 100, 110. Summing the number of 1's in these symbols and averaged over 5×3, we obtain the conversion factor between P_b and P_s if the symbol 000 is transmitted. It is

$$(1+1+2+1+2)/15 = 7/15$$

In the same way, we obtain the results for each symbol and list them in the middle of Table B.1. Then we find the average for all the considered symbols and obtain

$$\left(\frac{7}{15}+\frac{6}{12}+\frac{5}{12}+\frac{8}{15}+\frac{7}{12}+\frac{5}{12}+\frac{8}{15}+\frac{7}{15}\right)/8 = 0.490$$

Therefore on the average, P_b=0.49P_s in this case.

Another way to realize the signal mapping is also given in the right part of Table B.1. The corresponding results are given and thus

$$P_b = \left(\frac{7}{15}+\frac{5}{12}+\frac{6}{12}+\frac{8}{15}+\frac{5}{12}+\frac{6}{12}+\frac{10}{15}+\frac{7}{15}\right)/8 = 0.496P_s$$

From the two examples, we can say that $P_b \simeq 0.5P_s$ is fairly accurate in the case of PFSK.

Appendix C

Correlation Coefficients of Some HPM Signal Sets

In this section, we give the correlation coefficients (ρ) of some HPM alphabets. These data are used when calculating the error probability of coherent uncoded HPM. Any one of symbols can be selected as the reference and the $M-1$ correlation coefficients are listed in sequence in the brackets.

HPM(4,2,2):

{0, 0, -1, 0.5, -0.5, 0.5, -0.5, 0.5, -0.5, 0.5, -0.5, 0, 0, 0, 0}

HPM(4,2,4):

{0.5, 0, 0.5, 0.5, 0, -0.5, 0, 0, -0.5, -1, -0.5, 0.5, 0, -0.5, 0, 0.5, 0, -0.5, 0, 0.5, 0, -0.5, 0, 0.5, 0, -0.5, 0, 0.5, 0, -0.5, 0, 0.5, 0, -0.5, 0, 0.5, 0, -0.5, 0, 0.5, 0, -0.5, 0, 0.5, 0, -0.5, 0, 0.5, 0, -0.5, 0, 0, 0, 0, 0, 0, 0, 0, 0, 0, 0, 0, 0, 0, 0, 0, 0, 0, 0}

HPM(4,2,8):

{ 0.854, 0.5, 0.147, 0, 0.147, 0.5, 0.854, 0.854, 0.707, 0.354, 0, -0.147, 0, 0.354, 0.707, 0.5, 0.354, 0, -0.354, -0.5, -0.354, 0, 0.354, 0.147, 0, -0.354, -0.707, -0.854, -0.707, -0.354, 0, 0, -0.147, -0.5, -0.854, -1, -0.854, -0.5, -0.147, 0.147, 0, -0.354, -0.707, -0.854, -0.707, -0.354, 0, 0.5, 0.354, 0, -0.354, -0.5, -0.354, 0, 0.354, 0.854, 0.707, 0.354, 0, -0.147,0, 0.354, 0.707, 0.5, 0.354, 0, -0.354, -0.5, -0.354, 0, 0.354, 0.5, 0.354, 0, -0.354, -0.5, -0.354, 0, 0.354, 0.5, 0.354, 0, -0.354, -0.5, -0.354, 0, 0.354, 0.5, 0.354, 0, -0.354,

-0.5, -0.354, 0, 0.354, 0.5, 0.354, 0, -0.354, -0.5, -0.354, 0, 0.354, 0.5, 0.354, 0, -0.354,
-0.5, -0.354, 0, 0.354, 0.5, 0.354, 0, -0.354, -0.5, -0.354, 0, 0.354, 0.5, 0.354, 0, -0.354,
-0.5, -0.354, 0, 0.354, 0.5, 0.354, 0, -0.354, -0.5, -0.354, 0, 0.354, 0.5, 0.354, 0, -0.354,
-0.5, -0.354, 0, 0.354, 0.5, 0.354, 0, -0.354, -0.5, -0.354, 0, 0.354, 0.5, 0.354, 0, -0.354,
-0.5, -0.354, 0, 0.354, 0.5, 0.354, 0, -0.354, -0.5, -0.354, 0, 0.354, 0.5, 0.354, 0, -0.354,
-0.5, -0.354, 0, 0.354, 0.5, 0.354, 0, -0.354, -0.5, -0.354, 0, 0.354, 0.5, 0.354, 0, -0.354,
-0.5, -0.354, 0, 0.354, 0, 0, 0, 0, 0, 0, 0, 0, 0, 0, 0, 0, 0, 0, 0, 0, 0, 0, 0, 0, 0, 0, 0, 0, 0,
0, 0, 0, 0, 0, 0, 0, 0, 0, 0, 0, 0, 0, 0, 0, 0, 0, 0, 0, 0, 0, 0, 0, 0, 0, 0, 0, 0, 0, 0, 0, 0, 0,
0, 0, 0, 0, 0, 0 }

HPM(5,2,2):

{0, 0, -1, 0.5, -0.5, 0.5, -0.5, 0.5, -0.5, 0.5, -0.5, 0.5, -0.5, 0.5, -0.5, 0.5, -0.5, 0.5, -0.5,
0.5, -0.5, 0.5, -0.5, 0, 0, 0, 0, 0, 0, 0, 0 }

HPM(5,2,4):

{0.5, 0, 0.5, 0.5, 0, -0.5, 0, 0, -0.5, -1, -0.5, 0.5, 0, -0.5, 0, 0.5, 0, -0.5, 0, 0.5, 0, -0.5,
0, 0.5, 0, -0.5, 0, 0.5, 0, -0.5, 0, 0.5, 0, -0.5, 0, 0.5, 0, -0.5, 0, 0.5, 0, -0.5, 0, 0.5, 0,
-0.5, 0, 0.5, 0, -0.5, 0, 0.5, 0, -0.5, 0, 0.5, 0, -0.5, 0, 0.5, 0, -0.5, 0, 0.5, 0, -0.5, 0, 0.5,
0, -0.5, 0, 0.5, 0, -0.5, 0, 0.5, 0, -0.5, 0, 0.5, 0, -0.5, 0, 0.5, 0, -0.5, 0, 0.5, 0, -0.5, 0,
0.5, 0, -0.5, 0, 0, 0, 0, 0, 0, 0, 0, 0, 0, 0, 0, 0, 0, 0, 0, 0, 0, 0, 0, 0, 0, 0, 0, 0, 0, 0, 0, 0,
0, 0, 0, 0 }

Appendix D

Elements of t-designs

D.1 Introduction

The subject of design theory has grown out of several branches of mathematics and it has close connections with coding theory. Designs, or more precisely t-designs, are combinatorial structures with certain properties. They originated in the design of agricultural experiments.

The definition of t-designs is given in [37]: Let $\mathbf{X}$ be a v-set (a set with v elements), whose elements are called *points*. A t-design is a collection of distinct w-subsets (called *blocks*) of $\mathbf{X}$ with the property that any t-subset of $\mathbf{X}$ is contained in exactly λ blocks. We call this a t-(v, w, λ) design and $v \geq w \geq t$, where λ is the total number of blocks containing a certain t-subset of elements in a t-design. Thus a t-design is the arrangements of w elements chosen from a v-set while satisfying the appropriate conditions constrained by the parameters t and λ. It consists of a set of blocks and each block has a set of points.

A t-design with λ=1 is called *Steiner system* and usually denoted by $S(t, w, v)$. Alternatively, a t-design can also be called generalized Steiner system. A 2-design is often called *block design* or *balanced incomplete block design*, abbreviated to BIBD. Until recently t-designs were known only for $t \leq 5$, but in fact it is shown now that t-designs exist for all t.

D.2 Properties of t-designs

The total number of combinations of w elements chosen from v-sets is $\begin{pmatrix} v \\ w \end{pmatrix}$. In t-designs only a small fraction of these combinations are selected so that the total number of blocks of a t-design is denoted by b, where b is smaller than $\begin{pmatrix} v \\ w \end{pmatrix}$. Therefore the parameters of a t-design are not independent and there exist elementary relations among them. In the following section, we will give a brief review of these relations or constraints and other special properties of t-designs.

One of the key problem in t-designs is the question of their existence. In order for a t-(v, w, λ) design to exist, the parameters must satisfy various arithmetical conditions.

In a t-(v, w, λ)design, let $P_1, \ldots, P_t$ be any t distinct points, λ_i be the number of blocks containing $P_1, \ldots, P_t$, for $1 \leq i \leq t$. Let $\lambda_0 = b$ be the total number of blocks. Each point belongs to exactly $r = \lambda_1$ blocks. Then λ_i is independent of the choice of $P_1, \ldots, P_t$, and

$$\lambda_i = \lambda \begin{pmatrix} v-i \\ t-i \end{pmatrix} / \begin{pmatrix} w-i \\ t-i \end{pmatrix} \tag{D.1}$$

and

$$b = \lambda_0 = \lambda \begin{pmatrix} v \\ t \end{pmatrix} / \begin{pmatrix} w \\ t \end{pmatrix} \tag{D.2}$$

Equation (D.1) implies that a t-(v, w, λ) design is also an i- (v, w, λ_i) design for $1 \leq i \leq t$. Thus a $S(3, 4, 8)$ design is also a 2-(8,4,3) or a 1-(8,4,7) design.
The parameters of a t-design satisfy the equation

$$bw = rv \tag{D.3}$$

This equation counts the total number of single element occurrences in two ways. Each of the block contains w points and the total number of points in the collection of blocks is bw. On the other hand, each of the v points appears r times in the collection.

From equation (D.1), it can be deducted

$$\lambda_2(v-1) = r(w-1) \qquad \text{for} \quad t \geq 2. \tag{D.4}$$

When $b = v$ and hence $r = w$, the design is a *symmetric design.*

A necessary condition for a t-(v, w, λ) design to exist is that the solutions for (D.1) and (D.2) are integers. In some cases, e.g., for Steiner systems $S(2,3,v)$, $S(2,4,v)$, $S(2,5,v)$ and $S(3,4,v)$, this condition is also sufficient, but not always true for general cases. For example, an $S(2, 7, 43)$ design does not exist even though the condition is satisfied. Generally the precise conditions under which t-designs exist are still unknown.

A t-design can be expressed by a collection of binary codes of length v and constant weight w. Each element of the code is represented by "1" if the element belongs to a block of design and the other elements represented by "0". If we put these codes in a matrix manner, it is called the *incidence matrix* for the design and usually a $v \times b$ matrix with each row being one of the blocks of the design. Take the $S(2, 3, 7)$ for example. It can also be identified by (b, v, r, w, λ) =(7,7,3,3,1).

$$\begin{pmatrix} 1 & 1 & 0 & 1 & 0 & 0 & 0 \\ 0 & 1 & 1 & 0 & 1 & 0 & 0 \\ 0 & 0 & 1 & 1 & 0 & 1 & 0 \\ 0 & 0 & 0 & 1 & 1 & 0 & 1 \\ 1 & 0 & 0 & 0 & 1 & 1 & 0 \\ 0 & 1 & 0 & 0 & 0 & 1 & 1 \\ 1 & 0 & 1 & 0 & 0 & 0 & 1 \end{pmatrix}$$

This is a set of codes with length 7 and constant Hamming weight 3. We observe that there are 7 blocks with 7 points in each block. Each point appears in 3 blocks and each pair appears only in one block.

Finally, the existence of a t-(v, w, λ) implies the existence of $(t-i)$-$(v-i, w-i, \lambda-i)$ for $0 < i < t$. This means if a $S(5, 6, 12)$ exists, the designs of $S(4,5,11)$, $S(3,4,10)$, $S(2,3,9)$ and $S(1,2,8)$ also exist.

D.3 The block intersection number

The definition of *block intersection numbers* of a t-design is given in [37]:
In a t-(v, w, λ) design, let $P_1, \ldots, P_w$ be the points belonging to one of the blocks. Consider the blocks which contain $P_1, \ldots, P_j$ but do not contain $P_{j+1}, \ldots, P_i$, for $0 \leq j \leq i$ (for $j = 0$ we consider the blocks which do not contain $P_1, \ldots, P_i$, and for $j = i$ we consider the blocks which contain $P_1, \ldots, P_j$). If the number is well defined, i.e. it is a constant and independent of the choice of $P_1, \ldots, P_i$, we denote it by λ_{ij}. It gives the number of blocks containing a certain subset of the chosen block $P_1, \ldots, P_w$. The λ_{ij} are called *block intersection numbers.*

It is obvious that λ_{ij} are well defined for $i \leq t$. In fact $\lambda_{ii} = \lambda_i$ for $i \leq t$, with $\lambda_{tt} = \lambda$. Also the λ_{ij} satisfy the *Pascal property* [37]

$$\lambda_{ij} = \lambda_{i+1,j} + \lambda_{i+1,j+1} \tag{D.5}$$

whenever they are well defined. For any t-design, we can obtain the *Pascal triangle* of its block intersection numbers and put them into following way:

$$\begin{array}{ccccccccc}
 & & & \lambda_{00} & = & \lambda_0 & & & \\
 & & \lambda_{10} & & \lambda_{11} & = & \lambda_1 & & \\
 & \lambda_{20} & & \lambda_{21} & & \lambda_{22} & = & \lambda_2 & \\
 & & & \cdots & & & & & \\
\lambda_{t0} & & \lambda_{t1} & & \cdots & & \lambda_{tt} & = & \lambda
\end{array}$$

The triangle at least has $t + 1$ rows and every element in the triangle is the summation of the two elements directly below it in the triangle. Using this property, for a given t-design, $\lambda_{00}, \lambda_{11}, \ldots, \lambda$ can be calculated according to (D.1) so that all the components in the triangle can be obtained.

In the special case if the design is a Steiner system so that $\lambda = 1$, then $\lambda_{tt} = \lambda_{t+1,t+1} = \ldots = \lambda_{ww} = 1$ and the λ_{ij} are well defined for all $0 \leq j \leq i \leq w$. Therefore the Pascal triangle for the Steiner system has altogether $w+1$ rows and can be shown as

$$\begin{array}{ccccccc}
 & & & \lambda_{00} & & & \\
 & & \lambda_{10} & & \lambda_{11} & & \\
 & \lambda_{20} & & \lambda_{21} & & \lambda_{22} & \\
 & & & \cdots & & & \\
\lambda_{w0} & \lambda_{w1} & & \cdots & & \lambda_{w,w-1} & \lambda_{ww}
\end{array}$$

If we take one of the blocks C from a t-(v, w, λ) design, all the remaining blocks can be partitioned into w parts(any blocks appear in the design only once, i.e. there is no repeated block). They are

$\bullet X_{w-1}(C)$ containing blocks intersecting with C on $w-1$ points.

$\vdots$

$\bullet X_1(C)$ containing blocks intersecting with C on single point.

$\bullet X_0(C)$ containing blocks orthogonal to C (no common elements).

We define $x_{w-1}, \ldots, x_1, x_0$ the number of blocks for each of the above parts respectively. They are also called *block intersection numbers* and provide the block intersection distribution which is worth of studying when t-designs are applied to coding and modulation in communication systems.

If the design is a Steiner system, $x_{w-1}, \ldots, x_1, x_0$ are well defined, i.e. they are constants and independent of the choice C. Otherwise they are indefinite because in this case ($\lambda > 1$)they are not constants and dependent upon the choice of C. If C changes, their values may also change. Thus their analysis is quite complicated in t-design with $\lambda > 1$.

In a $S(t, w, v)$ system, it is also a $(t-1)$-(v, w, λ_{t-1}) design. Any t-subsets of one block appear in exactly one block and any $(t-1)$-subsets of one block appear in exactly λ_{t-1} block. Thus

$$x_w = x_{w-1} = \ldots x_t \equiv 0. \tag{D.6}$$

and

$$x_{t-1} = \lambda_{w,(t-1)} C_w^{t-1}$$

$\vdots$

$$x_1 = \lambda_{w1} C_w^1$$

$$x_0 = \lambda_{w0} \tag{D.7}$$

where $\lambda_{w0}, \lambda_{w1}, \ldots, \lambda_{w,(t-1)}$ are the elements of the bottom row from the Pascal triangle. Certainly,

$$x_0 + x_1 + \ldots + x_{t-1} = b - 1 \tag{D.8}$$

From the block code point of view, the intersecting positions between any two constant weight blocks are at most $t-1$, the minimum Hamming distance of all blocks in the system is $d_{min} = 2(w - t + 1)$. Therefore the distance between any two blocks is $d \geq 2(w - t + 1)$.

Take $S(3, 4, 8)$ for example. Its Pascal triangle is:

```
                14
            7       7
        3       4       3
    1       2       2       1
1       0       2       0       1
```

This design is also a 2-(8,4,3)design. In this case,

$$x_2 = \lambda_{42} C_4^2 = 2 \times 6 = 12$$

$$x_1 = \lambda_{41} C_4^1 = 0$$

$$x_0 = \lambda_{40} = 1$$

This design ($b = 14$) contain 12 blocks intersecting with the chosen block C on 2 points and one block orthogonal to C. The $d_{min} = 4$.

D.4 Some families of t-designs

Although t-designs exist for large t, they are much harder to construct. In fact, there are much rare families of designs for $t > 2$. Most designs come from BIBD ($t = 2$) and Steiner system ($\lambda = 1$). Some well-known families are listed below:

1. The simplest case is that $t = 1$ and $\lambda = 1$. This design is actually that all the blocks are orthogonal with each other and the number of blocks equal to v/w.

This will limit the number of blocks and reduce the bandwidth efficiency when the designs are employed in multitone transmission. Especially when $w = 1$, this leads to the well known M-ary FSK with $M = b$.

2. In Steiner BIBD, the basic relations among the parameters are given by

$$b = \frac{v(v-1)}{w(w-1)} \tag{D.9}$$

$$r = \frac{v-1}{w-1} \tag{D.10}$$

To obtain integer solutions for these equations, v$\equiv$ 1 or w mod $w(w-1)$.
And equation (D.4) becomes

$$\lambda(v-1) = r(w-1) \tag{D.11}$$

This equation counts the occurrences of pairs containing a certain point q. A pair containing q appears in r blocks and in each of these r blocks, the choice of another point forming the pair is $w-1$. While q is paired λ times with each of the remaining $v-1$ elements. This shows that (D.11) holds. The block intersection numbers of this design are simply given by

$$x_1 = w(r-1) = \tfrac{w}{w-1}(v-w)$$
$$x_0 = b - x_1 - 1$$

The well known families under this condition ($t = 2$ and λ=1) are

- Steiner triple systems $S(2,3,v)$, which exist for all $v \equiv$1 or 3 mod 6.
- Hanani systems $S(2,4,v)$, which exist for all $v \equiv$1 or 4 mod 12.
- Hanani systems $S(2,5,v)$, which exist for all $v \equiv$1 or 5,mod 20.
- Projective and Euclidean systems, which exist for $n > 1$ and q a prime power.

(i)$S(2,q,q^n)$ with $n \geq 2$. It is also called affine plane.
(ii)$S(2,q+1,(q^n-1)/(q-1))$ with $n \geq 3$.

- Hyperbolic systems $S(2,2^n,2^{2n+1}-2^n)$ for n an integer >1.
- Hermitian systems $S(2,q+1,q^3+1)$, which exist for q a prime power.

3. For $t = 3$ the following Steiner systems are known:

   • Quadruple systems $S(3, 4, v)$ exist for all $v \equiv 2$ or 4 mod 6. It is an extension of Steiner triple system.

   • Inversive systems $S(3, q + 1, q^2 + 1)$ exist for q a prime power.

4. For $t = 4$ and $t = 5$ the only known Steiner systems are the Mathieu systems, $S(5,8,24)$, $S(5,6,12)$, $S(4,7,23)$, $S(4,5,11)$.

5. Another important family of design is Hadamard designs. We will discuss it later. One example of Hadamard designs is *Paley design*. It has parameters 2-$(q, \frac{1}{2}(q-1), \frac{1}{4}(q-3))$ with $q = n - 1$ is a prime power ($q \equiv 3$ mod 4).

D.5 Codes and designs

Here we come to the issue on how to generate a t-design. There is an interesting connection between t-designs and codes. This leads to the construction of new designs using knowledge about codes. We can start with a binary block code and select from it a subset consisting of all words of a certain fixed weight. This method of constructing code is also called *expurgation*. We say that vectors of a fixed weight w in a binary code of length n hold a t-design if the blocks determined by these vectors are the blocks of a t-design on n points. But it is not necessarily that vectors of weight w in an arbitrary code hold a design. Usually the codes holding a design are *perfect codes* or *nearly perfect codes*.

Two notable conclusions of this idea are as follows.

• If a perfect code C on a set of over GF(q) and of minimum distance $d = 2e + 1$ and contains the zero chain, then the set D of weight d domains of C is a $(q-1)^e - (e + 1, 2e + 1, n)$ design, where e is the error-correcting ability of the code.

The famous Hamming code and Golay code are perfect codes and some conclusions are known:

1. The codewords of weight 3 in any Hamming code H_n, $n = 2^m - 1$, form an

$S(2,3,2^m-1)$ and the codewords of weight 4 in any extended Hamming code of length 2^m form an $S(3,4,2^m)$. As the following, we extract all the codes with constant weight of 3 from

$$H_7 = \begin{pmatrix} 0&0&0&0&0&0&0 \\ 0&0&0&1&1&0&1 \\ 0&0&1&1&0&1&0 \\ 0&0&1&0&1&1&1 \\ 0&1&1&0&1&0&0 \\ 0&1&1&1&0&0&1 \\ 0&1&0&1&1&1&0 \\ 0&1&0&0&0&1&1 \\ 1&1&0&1&0&0&0 \\ 1&1&0&0&1&0&1 \\ 1&1&1&0&0&1&0 \\ 1&1&1&1&1&1&1 \\ 1&0&1&1&1&0&0 \\ 1&0&1&0&0&0&1 \\ 1&0&0&0&1&1&0 \\ 1&0&0&1&0&1&1 \end{pmatrix},$$

we obtain the $S(2,3,7)$ with 7 codewords illustrated in Page 105.

2. The supports (the positions of the nonzero elements of nonbinary codes) of the codewords of weight 5 in the ternary Golay code G_{11} form an $S(4,5,11)$ and the supports of the codewords of weight 6 in G_{12} form an $S(5,6,12)$.

3. The codewords of weight 7 in the binary Golay code G_{23} form an $S(4,7,23)$ and the codewords of weight 8 in the extended Golay code G_{24} form an $S(5,8,24)$.

• In any nearly perfect e-error-correcting code C of length n, the code vectors at distance $d = 2e+1$ from a given code vector determine a t-design with parameters $[(n-e)/(e+1)]$-(e,d,n).

Many t-designs can be constructed in this way and many more examples can be found in literature [45]-[47].

The Hadamard code is a constant weight code which can be extracted from the Hadamard matrix. A Hadamard matrix is an $n \times n$ matrix (n is an even integer) of

"1"s and "0"s with the property that any row differs from any other row in exactly $n/2$ positions. One row of the matrix contains all zeros. The other rows are half zeros and half ones. The Hadamard code is obtained by selecting these latter $n-1$ rows and their complements. The total number of blocks is $2(n-1)$ and the code is denoted by $H(n,k)$ with $k = 1+\lfloor \log_2(n-1) \rfloor$. The minimum Hamming distance of the set is $n/2$ which indicates it may have larger distance compared with other families mentioned above. If $n \geq 8$, actually the Hadamard code is a symmetric 2-$(n-1, \frac{1}{2}n-1, \frac{1}{4}n-1)$ design. Thus the $H(20,5)$ code is a 2-(19, 9, 4)design with a minimum Hamming distance 10. The extension of a Hadamard 2-design is a 3-$(n, \frac{1}{2}n, \frac{1}{4}n-1)$ design called Hadamard 3-design.

Bibliography

[1] B. Sklar, "Defining, designing, and evaluating digital communication systems," IEEE Commun. Mag., vol. 29, pp. 92-101, Nov. 1993.

[2] J.A.C. Bingham, "Multicarrier modulation for data transmission: an idea whose time has come," IEEE Commun.Magazine, pp. 5-14, May 1990.

[3] M. Okada, S. Hara and N. Morinaga, "Bit error rate performances of orthogonal multicarrier modulation radio transmission systems," IEICE Trans. on Commun. vol. E76-B, pp. 113-119, Feb. 1993.

[4] A. Chini, M. S. El-Tanany and S. A. Mahmoud, "Multi Carrier Modulation for Indoor Wireless Communications, ICUPC Conference, pp. 674-678, 1993.

[5] P. Okrah and J. M. Cioffi, "Multichannel modulation as a technique for transmission in radio channels," 1993 IEEE VTC, pp. 29-33.

[6] L. Vandendorpe, "Multitone spread spectrum multiple access communications system in a multipath rician fading channel," 1994 IEEE ICC, Vol. 3, pp. 1638-1642.

[7] A. Chouly, A. Brajal and S. Jourdan, "Orthogonal multicarrier techniques applied to direct sequence spread spectrum CDMA systems,"1993 IEEE GLOBECOM, Vol. 3, pp. 1723-1728.

[8] D. Slepian,"Permutation Modulation," Proc. IEEE, vol.53, pp. 228-236, Mar. 1965.

[9] H. L. Schneider,"Data transmission with FSK Permutation Modulation." BSTJ., vol.47, pp. 1131-1138, July-Aug. 1969.

[10] E. Brookner,"The performance of FSK permutation modulations in fading channels and their comparison based on a general method for the comparison of M-ary modulations," IEEE Trans. Comm.Tech., vol.com-17 , No.6, pp. 616-639, Dec. 1969.

[11] E. Biglieri,V. Castellani and M. Pent,"Waveform transmission with permutation modulation," Electron. Lett., vol. 5, pp. 149-151, April 3, 1969.

[12] W. Roehr, D. Cameron,"Permutation modulation for advance radio paging," Proc. of the IEEE Southeastcon '93.

[13] G.E. Atkin and H.P. Corrales,"An efficient modulation/coding scheme for MFSK systems on bandwidth constrained channel,"IEEE JSAC, vol.SAC-7, No.9, pp. 1396-1401, Dec. 1989.

[14] A. Yongacoglu, J. Wang, "Spread- spectrum system employing permutation modulation," Proc. the 3rd European Confer. on Satellite Commun., pp. 409-413, 1993.

[15] T.M.P. Percival,R. Boreli, R.A.Z. Simington,D.K. Kwan and S. Reisenfeld, "A new combined modulation and multiple access scheme for VSATS," The 9th Internal. Confer. Digital Satellite Comm., Copenhagen, Denmark, pp. 399-406, May 18-22, 1992.

[16] J. B. Anderson and C. W. Sundberg, "Advances in constant envelope coded modulation," IEEE Commun. Mag., vol. 29, pp. 36-45, Dec. 1991.

[17] R. Petrovic,"Multicarrier permutation modulation for narrowband PCS" Wireless 93, Edmonton, July 1993.

[18] I.S. Reed and R.A. Scholtz, "N-orthogonal phase-modulated codes," IEEE Trans on Info. Theory, IT-12, pp. 388-395, 1966.

[19] W. Lindsey and M. Simon, "L-orthogonal signal transmission and detection," IEEE Trans on Comm., Vol. COM-20, pp. 953-960, 1972.

[20] I. Ghareeb, A. Yongacoglu, "Performance of joint frequency phase modulation over Rayleigh fading channels," IEE Proc.-Commun., Vol. 141, No.4, pp. 241-247, Aug. 1994

[21] R. A. Khalona, G. E. Atkin and L. LoCicero, "On the performance of a hybrid frequency and phase shift keying modulation technique," IEEE Trans. on Commun., Vol. 41, No.5, pp. 655-659, May 1993

[22] R. Padovani and J.K. Wolf, "Coded phase/frequency modulation," IEEE Trans. Commun., Vol. COM -34, pp. 446-453, May 1986.

[23] J. Wang and A. Yongacoglu, "Direct sequence CDMA employing combined modulation schemes," 1993 IEEE GLOBECOM, Vol. 3, pp. 1729-1733.

[24] A. P. Watson and T. J. Stevenson, "Multitone M-ary frequency shift keying - multiple access (MTMFSK-MA) with coding,"Proc. of the IEEE 1993 Pacific Rim Confer. on Commun., Computer and Signal Processing, pp. 455-458.

[25] J.G. Proakis, *"Digital Communication,"* 2nd Edition, New York: McGraw-Hill, 1989.

[26] J. M. Wozencraft and I. M. Jacobs, *"Principles of Communication Engineering."* John Wiley and Sons, Inc., New York, 1965.

[27] William C. Y. Lee, *"Mobile Communications Engineering,"* New York, McGraw-Hill, 1982.

[28] S. Benedetto, E. Biglieri and V. Castellani, *"Digital Transmission Theory,"* Englewood Cliffs, NJ: Prentice-Hall Public. Co., 1987.

[29] Y.C. Chow, J.P. McGeehan and A.R. Nix. "Simplified error bound analysis for M-DPSK in fading channels with diversity reception." IEE Proc. Commun., Vol. 141, No.5, pp. 341-350, October 1994.

[30] J. Proakis, "Probabilities of error for adaptive reception of M-phase signals." IEEE Trans. on Commun., vol. COM-16, pp. 71-81, Feb. 1968.

[31] S. Stein, "Fading Channel Issues in System Engineering, IEEE Journal on Selec. Areas in Commun., Vol. SAc-5, No. 2, pp. 68-89, Feb. 1987.

[32] D.L. Noneaker and M.B. Pursley, "Error probability bounds for M-PSK and M-DPSK and selective fading diversity channels," IEEE Trans. on Vehic. Tech., Vol. 43, No. 4, pp. 997-1004, Nov. 1994.

[33] R.F. Pawula, S.O. Rice and J.H. Roberts, "Distribution of the phase angle between two vectors perturbed by Gaussian noise," IEEE Trans., COM-30, pp. 1828-1841, 1982.

[34] J. Karlof,"Permutation codes for Gaussian channel," IEEE Trans. Inform. Theory, vol. IT-35, pp. 726-732, July 1989.

[35] I. Ingemarsson,"Optimized permutation modulation," IEEE Trans. Inform. Theory, vol. 36, No.5,1098-1100, Sep. 1990.

[36] G.E. Atkin, B.Patel and J. Rahhal,"Combined source coding and modulation for fading channel," IEEE VTC, pp. 491-494, 1993.

[37] F.J. MacWilliams and N.J. Sloane, *"The Theory of Error-Correcting Codes"*, Amsterdam:North-Holland Publishing, 1977.

[38] I.F. Blake and R.C. Mullin, *"The Mathematical Theory of Coding"*, New York: Academic Press, 1975.

[39] J.H. Conway and N.J. Slone, *"Sphere Packings,Lattices and Groups"*, New York: Springer-Verlag, 1993.

[40] E.F. Assmus,JR. and J.D. KEY, *"Designs and Their Codes"*, Cambridge Univ. Press, 1992.

[41] P.J. Cameron and J.H. van Lint, *"Graphs, Codes and Designs"*, London:Cambridge Univ. Press, 1980.

[42] E.S. Lander, *"Symmetric Designs: An Algebraic Approach"*, Cambridge Univ. Press, 1983.

[43] Vera Pless, *"Introduction to The Theory of Error-Correcting Codes"*, John Wiley and Sons, 1989.

[44] D.R. Hughes and F.C. Piper, *"Design Theory"*, Cambridge Univ. Press, 1985.

[45] A. E. Brouwer, J. B. Shearer and N. J. A. Sloane, "A New Table of Constant Weight Codes", IEEE Trans. on Info. Theory, Vol. 36, No. 6, pp. 1334-1380, Nov. 1990.

[46] C. C. Lindner and A. Rosa, Eds., *"Topics on Steiner systems"*, Annals of Discrete Mathmatics, vol. 7. Amsterdam: North-Holland, 1980.

[47] A. Rosa, R. A. Mathon, and K. T. Phelps, "Small Steiner triple systems and their properties", Ars. Combin., vol. 15, pp. 3-110, 1983.

[48] M. C. Jeruchim, P. Balaban and K. S. Shanmugan, *"Simulation of Communication Systems"*, Plenum Press, New York, 1992.